

NORTHWESTERN UNIVERSITY

Tissue Engineering Scaffolds for Protein and DNA Delivery:
A Platform for Islet Transplantation

A DISSERTATION

SUBMITTED TO THE GRADUATE SCHOOL
IN PARTIAL FULFILLMENT OF THE REQUIREMENTS

for the degree

DOCTOR OF PHILOSOPHY

Field of Chemical Engineering

By

Christopher B. Rives

EVANSTON, ILLINOIS

DECEMBER 2008

Abstract

Tissue Engineering Scaffolds for Protein and DNA Delivery: A Platform for Islet Transplantation

Christopher B. Rives

Tissue engineering offers a promising approach for the replacement of diseased or injured tissues, and is based upon the premise that cells can be induced to form new tissues when presented with the appropriate set of environmental cues. Polymer scaffolds play a central role in most tissue engineering strategies by providing a three-dimensional structure to support cell adhesion and organize tissue formation. However, the creation of controllable microenvironments capable of directing cellular behavior and coordinating the formation of complex tissues represents a significant challenge in the field of tissue engineering. To this end, controlled delivery of proteins and DNA from scaffolds can be used to manipulate soluble signals (e.g. growth factors) present within the local tissue microenvironment, and thereby regulate a variety of cellular processes such as migration, proliferation, and apoptosis. The primary objective of this dissertation was to develop scaffolds for DNA and protein delivery, in order to create an effective platform for islet transplantation, which is a cell-replacement therapy for the treatment of type I diabetes. DNA-releasing scaffolds were evaluated for their ability to provide localized and sustained transgene expression *in vivo* at different anatomical locations. Both the implant site and DNA dose were important factors that regulated the extent and duration of transgene expression. A critical limitation in the initial scaffold design was discovered in that the DNA incorporation efficiency was dependent on the scaffold structure. To eliminate this constraint, an alternative layered scaffold design was developed. Microcomputed tomography analysis demonstrated the ability of scaffolds delivering angiogenic proteins or

DNA encoding angiogenic proteins to locally enhance vascularization, which will likely be important for promoting islet survival and function. Scaffolds were also developed for sustained delivery of exendin-4, a peptide that exhibits several therapeutic effects on islet cells. Initial studies have demonstrated that islets transplanted on exendin-4-releasing scaffolds exhibit enhanced function relative to those transplanted on control scaffolds. The continued development of scaffolds for controlled delivery of DNA and additional therapeutic proteins will likely lead to novel strategies for improving the outcome of islet transplantation.

Table of Contents

1. CHAPTER 1	14
1.1. Introduction and Research Objectives	14
1.2. Background	17
<i>1.2.1. Tissue engineering scaffolds</i>	<i>17</i>
<i>1.2.2. Gene delivery from scaffolds</i>	<i>18</i>
<i>1.2.3. Islet transplantation</i>	<i>20</i>
<i>1.2.3. Angiogenesis</i>	<i>23</i>
2. CHAPTER 2: PLG Scaffolds for Plasmid Delivery: <i>In Vivo</i> Transgene Expression at a Subcutaneous Site	26
2.1. Introduction	26
2.2. Materials and methods	27
<i>2.2.1 Materials</i>	<i>27</i>
<i>2.2.2 Fabrication of DNA-loaded scaffolds</i>	<i>28</i>
<i>2.2.3 Characterization of in vitro release kinetics and incorporation efficiency</i>	<i>29</i>
<i>2.2.4 Measuring in vivo transgene expression with bioluminescence imaging</i>	<i>29</i>
<i>2.2.5 Histological analysis and immunohistochemistry</i>	<i>30</i>
2.3. Results	31
<i>2.3.1 Scaffold fabrication</i>	<i>31</i>
<i>2.3.2 Plasmid incorporation efficiency and in vitro release kinetics</i>	<i>35</i>
<i>2.3.3 In vivo transgene expression</i>	<i>37</i>
2.4. Discussion	46

	5
3. CHAPTER 3: Layered PLG Scaffolds for Plasmid Delivery and Cell Transplantation: <i>In Vivo</i> Transgene Expression at an Intraperitoneal Fat Site	51
3.1. Introduction	51
3.2. Materials and Methods	53
3.2.1. <i>DNA sources</i>	53
3.2.2. <i>Scaffold fabrication</i>	53
3.2.3. <i>Scanning electron microscopy (SEM)</i>	54
3.2.4. <i>Characterization of DNA incorporation and in vitro release kinetics</i>	54
3.2.5. <i>Measuring in vivo transgene expression</i>	55
3.2.6. <i>Histological analysis and immunohistochemistry</i>	56
3.2.7. <i>Evaluation of angiogenesis using microcomputed tomography</i>	57
3.2.8. <i>Islet transplantation</i>	58
3.2.9. <i>Statistical Analysis</i>	59
3.3. Results	59
3.3.1. <i>Layered scaffold design</i>	59
3.3.2. <i>DNA incorporation and in vitro release kinetics</i>	60
3.3.3. <i>In vivo transgene expression</i>	65
3.3.4. <i>Histological analysis and immunohistochemistry</i>	67
3.3.5. <i>Angiogenesis</i>	71
3.3.6. <i>Islet transplantation</i>	74
3.4. Discussion	75
4. CHAPTER 4: Exendin-4 Releasing Scaffolds for Islet Transplantation	79
4.1. Introduction	79

4.2. Materials and Methods	82
4.2.1. <i>Materials</i>	82
4.2.2. <i>Encapsulation of exendin-4 inside PLG microspheres</i>	82
4.2.3. <i>Fabrication of exendin-4 loaded scaffolds</i>	83
4.2.4. <i>Characterization of release kinetics</i>	83
4.2.5. <i>Islet transplantation</i>	84
4.3. Results	85
4.3.1. <i>In vitro release kinetics</i>	85
4.3.2. <i>Islet transplantation</i>	92
4.4. Discussion	94
5. CONCLUSIONS AND RECOMMENDATIONS	97
5.1. Perspective	97
5.2. Chapter 2: PLG Scaffolds for Plasmid Delivery: <i>In Vivo</i> Transgene Expression at a Subcutaneous Site	100
5.2.1. <i>Conclusions</i>	100
5.2.2. <i>Recommendations</i>	101
5.3. Chapter 3: Layered PLG Scaffolds for Plasmid Delivery and Cell Transplantation: <i>In Vivo</i> Transgene Expression at an Intraperitoneal Fat Site	102
5.3.1. <i>Conclusions</i>	102
5.3.2. <i>Recommendations</i>	103
5.4. Chapter 4: Exendin-4 Releasing Scaffolds for Islet Transplantation	105
5.4.1. <i>Conclusions</i>	105
5.4.2. <i>Recommendations</i>	106

6. APPENDIX	107
6.1. Lyophilization of DNA with PLG microspheres	107
6.2. <i>In vivo</i> transgene expression obtained by drying DNA onto the surface of scaffolds	110
6.3. Fabrication of cationic PLG microspheres for DNA adsorption	113
6.4. Flow cytometric analysis to determine the cellular composition of tissue forming within scaffolds at the intraperitoneal fat site	121
6.5. VEGF-releasing scaffolds: evaluation of angiogenesis by microcomputed tomography	125
6.6. <i>In vitro</i> plasmid release kinetics from layered scaffolds: increasing the amount of polymer in the center layer	133
6.7. <i>In vivo</i> transgene expression at the interaperitoneal fat site for traditional scaffolds	136
7. References	137

List of Figures and Tables

- Figure 1-1.** Drug delivery strategies from tissue engineering scaffolds. **15**
- Figure 2-1.** H&E staining of scaffold cross-sections at 14 days post-implantation to evaluate structural integrity and the extent of cellular infiltration. (A) A scaffold fabricated with the high/low molecular weight polymer blend exhibited a collapsed pore structure and supported only minimal cellular infiltration at the scaffold periphery (indicated by arrows). “P” indicates polymer. Note that the center of the scaffold tore out during sectioning due to the lack of cellular infiltration and weak mechanical strength of the polymer. Image was taken at 50x magnification, scale bar equals 0.5 mm. (B) A scaffold fabricated with the high molecular weight polymer maintained an intact pore structure, but supported only minimal cellular infiltration at the scaffold periphery (indicated by arrows). Image was taken at 25x magnification, scale bar equals 1 mm. **32**
- Figure 2-2.** Microsphere size increases with increasing concentration of the PLG solution. Images of microspheres made with a (A) 2% PLG solution, (B) 6% PLG solution, and (C) 10% PLG solution. All images were taken at the same magnification, 400x. Scale bars equal 20 μm . **33**
- Figure 2-3.** H&E-stained cross-section of a scaffold fabricated from microspheres made with a 6% PLG solution. Hematoxylin stains cell nuclei a blue/purple color, and thereby indicates the distribution of cells within the scaffold. Complete cellular infiltration throughout the scaffold interior was observed by 2 weeks post-implantation. Images were taken at (A) 10x or (B) 40x magnification. **34**
- Figure 2-4.** Characterization of plasmid incorporation and *in vitro* release kinetics. (A) DNA incorporation efficiency with standard mixing and wet granulation. *Significance at $P < 0.001$. (B) *In vitro* cumulative DNA release from scaffolds fabricated by wet granulation and subsequent gas foaming process. **36**
- Figure 2-5.** Bioluminescence imaging of firefly luciferase expression for scaffolds loaded with 500 μg of pLuc. Scaffolds were made with the high/low molecular weight blend. (A) Images showing light emission for a single mouse at different time points. (B) Emitted light intensity (photons/s) in region of interest over the implant sites (n=8) for scaffolds incorporating pLuc (circles), scaffolds without DNA (squares), and background (x). *Statistical significance at $P < 0.05$ relative to control. **39**
- Figure 2-6.** Bioluminescence imaging of firefly luciferase expression for scaffolds loaded with 800 μg of pLuc. Scaffolds were made with the high/low molecular weight blend. (A) Images showing a single mouse at different time points. (B) *In vivo* CCD signal intensity (photons/s) in region of interest over implant sites (n=6) for

scaffolds with pLuc (circles), scaffolds without DNA (squares), scaffolds with empty vector (diamonds), and background (x). *Statistical significance at $P < 0.05$ between pLuc and all other conditions for all time points. **40**

- Figure 2-7.** Bioluminescence imaging of firefly luciferase expression for scaffolds fabricated with different DNA doses. All scaffolds were made with the high/low molecular weight blend. (A) Emitted light intensity (photons/s) in region of interest over the implant sites ($n = 5$) for scaffolds loaded with 600 μg of pLuc (blue squares), 400 μg of pLuc (red circles), or 300 μg of pLuc (black triangles). Background is indicated by green diamonds. (B) Images showing a single mouse for each condition at different time points. **41**
- Figure 2-8.** Immunohistochemical staining with luciferase antibodies to determine the distribution of transfected cells. Images were taken from scaffolds loaded with 800 μg of pLuc that were retrieved at 17 days post-implantation. The scaffold was made with the high/low molecular weight blend, but unlike most of the other samples made with this formulation, it supported cellular infiltration. Transfected cells were found immediately adjacent to the polymer surface, as shown in (A) 200x and (B) 400x magnification. Scale bars equal 100 μm . Labels indicate polymer (P), surrounding tissue (T), and luciferase staining (arrows). **43**
- Figure 2-9.** Bioluminescence imaging of firefly luciferase expression for scaffolds fabricated with different molecular weight polymers. All scaffolds were loaded with 600 μg of pLuc. (A) Emitted light intensity (photons/s) in region of interest over the implant sites ($n = 5$) for scaffolds made with the high/low molecular weight polymer blend (blue squares) or only the high molecular weight polymer (red circles). Background is indicated by green diamonds. (B) Images showing a single mouse for each condition at different time points. **44**
- Figure 2-10.** Bioluminescence imaging of firefly luciferase expression for scaffolds fabricated with different pore sizes. All scaffolds were loaded with 600 μg of pLuc and made with the high/low molecular weight polymer blend. (A) Emitted light intensity (photons/s) in region of interest over the implant sites ($n = 5$) for scaffolds with 250-425 μm pore sizes (blue squares) or 106-250 μm pore sizes (red circles). Background is indicated by green diamonds. (B) Images showing a single mouse for each condition at different time points. **45**
- Table 2-1.** Summary of results. **49**
- Figure 2-11.** Image showing the presence of muscle fibers in tissue immediately adjacent to the scaffold. H&E stained cross-section of a high molecular weight scaffold at 62 days post-implantation (arrows indicate location of longitudinal and transverse muscle fibers). **50**

- Figure 3-1.** Scanning electron micrographs of a layered PLG scaffold. (A) Side view of the composite scaffold. Scale bar equals 1 mm. (B) Magnified view of the center layer. Scale bar equals 250 μm . (C) Magnified view of the pore structure in the outer layer. Scale bar equals 400 μm . **61**
- Table 3-1.** DNA incorporation efficiency for scaffolds loaded with different amounts of DNA. **62**
- Figure 3-2.** *In vitro* DNA release kinetics and agarose gel electrophoresis. (A) Cumulative DNA release from scaffolds loaded with 200, 400, or 800 μg of plasmid (n=4 per dose) (B) Image of an agarose gel containing DNA released from a scaffold at different times. Lane 1, molecular weight marker. Lane 2, unincorporated plasmid. Lanes 3-7: DNA released at days 1, 3, 7, 14, and 21, respectively. **63**
- Table 3-2.** Conformational analysis of plasmid released from scaffolds. **64**
- Figure 3-3.** *In vivo* luciferase transgene expression for scaffolds loaded with 200, 400, or 800 μg of pLuc (n=4 per dose per timepoint). **66**
- Figure 3-4.** H&E staining of cellular infiltration into outer layers of scaffolds. Scaffold cross-section at (A) day 7 and (B) day 14. 25x magnification, scale bars equal 1 mm. Labels indicate adipose tissue (AT) and scaffold (S). Dashed line indicates interface of scaffold edges with surrounding tissue. **68**
- Figure 3-5.** Immunohistochemical staining to determine the distribution and identity of transfected cells. Images were taken from a scaffold loaded with 400 μg of GFP plasmid that was retrieved after 7 days. For (A-C), 100x magnification images were captured at the interface of the scaffold with surrounding adipose tissue (scale bars equal 200 μm). (A) GFP antibody staining. (B) GFP antibody staining with Hoechst staining for cell nuclei. (C). F4/80 (macrophage) antibody staining with Hoechst. “S” indicates scaffold region, “AT” indicates adipose tissue, and dashed line indicates interface. For (D-F), 200x magnification images were captured in adipose tissue outside scaffold (scale bars equal 100 μm). (D) GFP antibody staining with Hoechst. (E) F4/80 antibody staining with Hoechst. (F) GFP antibody and F4/80 antibody staining. Yellow indicates co-localization of GFP and F4/80, and thus transfected macrophages. For (G-I), 200x magnification images were captured within the scaffold (scale bars equal 100 μm). (G) GFP antibody staining with Hoechst. (H) F4/80 antibody staining with Hoechst. (I) GFP and F4/80 antibody staining. **69**

- Figure 3-6.** Quantitative analysis of angiogenesis by microcomputed tomography. (A) Total vascular volume fraction for scaffolds releasing pFGF-2, pHIF-1 α , or pGFP (control) (n=3 per condition, per time point). (B) Histogram of vessel diameters for FGF-2 and control scaffolds at 2 weeks. ** P < 0.01, * P < 0.05. **72**
- Figure 3-7.** Microcomputed tomography 3-D renderings of vascular networks. (A,B) control scaffolds at 2 and 4 weeks. (C,D) pFGF-2 scaffolds at 2 and 4 weeks. (E,F) pHIF-1 α scaffolds at 2 and 4 weeks. **73**
- Figure 3-8.** Blood glucose levels of mice receiving 175 islets transplanted on scaffolds loaded with 400 μ g of GFP plasmid or no DNA. Red circles indicate control scaffolds without DNA, and blue squares indicate scaffolds with DNA. Values represent averages \pm standard errors (n=3 scaffolds per condition). **74**
- Table 4-1.** Microsphere encapsulation efficiency. **86**
- Figure 4-1.** *In vitro* exendin release kinetics from traditional scaffolds: effect of PLG concentration and molecular weight. Scaffolds were fabricated from microspheres made with 3% PLG, 100% HMW (red circles), 3% PLG, 75% HMW / 25% LMW (blue squares), 6% PLG, 100% HMW (green diamonds), or 6% PLG, 75% HMW / 25% LMW (black x). Values represent averages \pm standard deviations (n=3 scaffolds per condition). **87**
- Figure 4-2.** *In vitro* exendin release kinetics from scaffolds fabricated with a traditional or layered design. Both traditional (red circles) and layered (black squares) scaffolds were fabricated using the same microsphere formulation (3% PLG, 75/25 copolymer, HMW). Values represent averages \pm standard deviations (n=3 scaffolds per condition). **89**
- Figure 4-3.** *In vitro* exendin release kinetics from layered scaffolds fabricated with the 50/50 copolymer. The concentration of the PLG solution used in the microsphere emulsion process was varied from 3% (red circles) to 6% (blue squares). Values represent averages \pm standard deviations (n=3 scaffolds per condition). **90**
- Figure 4-4.** *In vitro* exendin release kinetics from layered PLG scaffolds fabricated with an equal weight blend of the 50/50 and 75/25 copolymers. The concentration of the PLG solution used in the microsphere emulsion process was varied from 3% (green circles) to 6% (black squares). Values represent averages \pm standard deviations (n=3 scaffolds per condition). **91**
- Figure 4-5.** Blood glucose levels of mice receiving 75 islets transplanted on exendin-4 or control scaffolds. Data combines 2 separate transplant experiments comparing control scaffolds (red circles) and exendin-4 scaffolds (blue squares). Experiment 1 was monitored for 48 days (n=3 per condition), and experiment 2 was

monitored for 20 days (n=3 per condition). Blood glucose levels of < 200 mg/dl are defined as normal. Values represent averages \pm standard errors. **93**

- Figure 6-1.** Images of lyophilization products with different physical properties. Both samples contained 7 mg of PLG microspheres, 800 μ g of DNA, and 1 mg of lactose. The size of the hole(s) created in the top of the plastic tube prior to lyophilization regulated the physical properties of the final product. (A) A 25-gauge needle was used to make three small holes. (B) An 18-gauge needle was used to make one large hole. The lyophilization product in (A) occupies a smaller volume and exhibits increased porosity and brittleness relative to (B). **108**
- Figure 6-2.** Image of a cracked scaffold after gas foaming. The scaffold was fabricated with an undesirable lyophilization product that could not be homogeneously mixed with salt particles, resulting in aggregates of polymer. During the gas foaming process, expansion of the polymer aggregates created fractures through the scaffold, compromising its structural integrity. **109**
- Figure 6-3.** Bioluminescence imaging of luciferase transgene expression for scaffolds containing 50 μ g or 100 μ g of pLuc dried onto their surface. The images are of a single mouse at different time points. Two scaffolds were implanted subcutaneously in the dorsal region of the mouse. The scaffold on the left had 50 μ g of pLuc, while the one on the right had 100 μ g of pLuc. **111**
- Figure 6-4.** Bioluminescence imaging of luciferase transgene expression at the intraperitoneal fat site following implantation of a scaffold containing 100 μ g of pLuc dried onto its surface. The images are of a single mouse at different time points. **112**
- Figure 6-5.** Structure of cetyltrimethylammonium bromide (CTAB). **114**
- Figure 6-6.** Adsorption-based strategies for DNA delivery from scaffolds. **115**
- Figure 6-7.** Images of PEI/PLG microspheres fabricated with different concentrations of PEI. (A) 1% PEI, (B) 2.5% PEI, (C) 5% PEI, and (D) 10% PEI. All images are the same magnification, 400x. **119**
- Figure 6-8.** Zeta potential measurements of PEI/PLG microspheres. **120**
- Figure 6-9.** Forward scatter vs. side scatter plot showing the gated cell population. **123**
- Figure 6-10.** Percentage of F4/80⁺ macrophages present within scaffolds as a function of time. Empty bars represent control scaffolds without DNA and black bars represent scaffolds loaded with 800 μ g of GFP plasmid. Values represent averages \pm standard deviations (n=3 per condition per time point). **124**

- Figure 6-11.** Image of a subcutaneous vascular network that has been completely perfused with Microfil® injection compound. **127**
- Figure 6-12.** Scout view of a tissue sample defining the measurement area for μ CT imaging. The green reference line determines the position of the first slice, and the total thickness measured is determined by the number of slices and slice thickness. **128**
- Figure 6-13.** *In vitro* VEGF release kinetics from scaffolds. VEGF was incorporated into scaffolds by mixing with alginate (red circles) or encapsulation inside microspheres (blue squares). Values represent averages \pm standard deviations (n=3 scaffolds per condition). **130**
- Figure 6-14.** Microcomputed tomography 3-D renderings of vascular networks within scaffolds. Control scaffolds at (A) 1 week and (C) 3 weeks post-implantation. VEGF-releasing scaffolds at (B) 1 week and (D) 3 weeks post-implantation. Images are composed of 360 serial slices, and represent a total measurement thickness of \sim 3 mm. **131**
- Figure 6-15.** Microcomputed tomography 3-D rendering of the vascular network within a VEGF-releasing scaffold at 3 weeks post-implantation, with a color-coded vessel diameter scale mapped to the 3-D image surface. **132**
- Figure 6-16.** *In vitro* DNA release kinetics for a layered scaffold containing 3 mg of polymer microspheres in the center layer. Values represent averages \pm standard deviations (n=3). **134**
- Figure 6-17.** *In vitro* DNA release kinetics for layered scaffolds containing different masses of polymer within the center layer. Scaffolds were loaded with 500 μ g of DNA. Values represent measurements from a single scaffold (n=1 per condition). **135**
- Figure 6-18.** Bioluminescence imaging of luciferase transgene expression at the intraperitoneal fat site following implantation of a non-layered scaffold loaded with 800 μ g of pLuc. The images are of a single mouse at different time points. **136**

1. CHAPTER 1

1.1. Introduction and Research Objectives

The ever increasing demand for organ transplants and the limited number of donors spawned the emergence of tissue engineering.¹ Tissue engineering is an interdisciplinary field that applies the principles of engineering and biological sciences in an effort to create new tissues that restore, maintain, or improve tissue function.¹ The underlying premise is that cells can be induced to repair an injury or develop into a desired tissue if subjected to the appropriate environmental conditions.² Scaffolds are a central component of tissue engineering strategies, providing a physical structure that serves as a template for organizing cells into the proper architecture.^{3,4} However, the ability to regulate cellular behavior and coordinate tissue formation is thought to require the development of cell-instructive scaffolds capable of presenting a variety of biological signals.⁵ To this end, controlled drug delivery from scaffolds has been proposed as a means for introducing bioactive proteins and peptides into the local environment.⁶⁻¹⁰ Proteins can be delivered directly from scaffolds, or a gene therapy approach can be employed where the encoding genes are delivered and cells are exploited to locally produce and secrete the desired proteins (illustrated in **Fig. 1-1**). Protein delivery systems have been widely used in tissue engineering applications and their effectiveness is well established,⁹ although it can be challenging to maintain protein bioactivity and adequately control the release kinetics. Additionally, the delivery system may need to be optimized for each protein delivered, due to the large variability in protein properties. In comparison, DNA delivery systems offer improved versatility and the potential to provide prolonged expression of the desired protein at stable levels, but the requirements for effective gene transfer are not well understood.^{11,12}

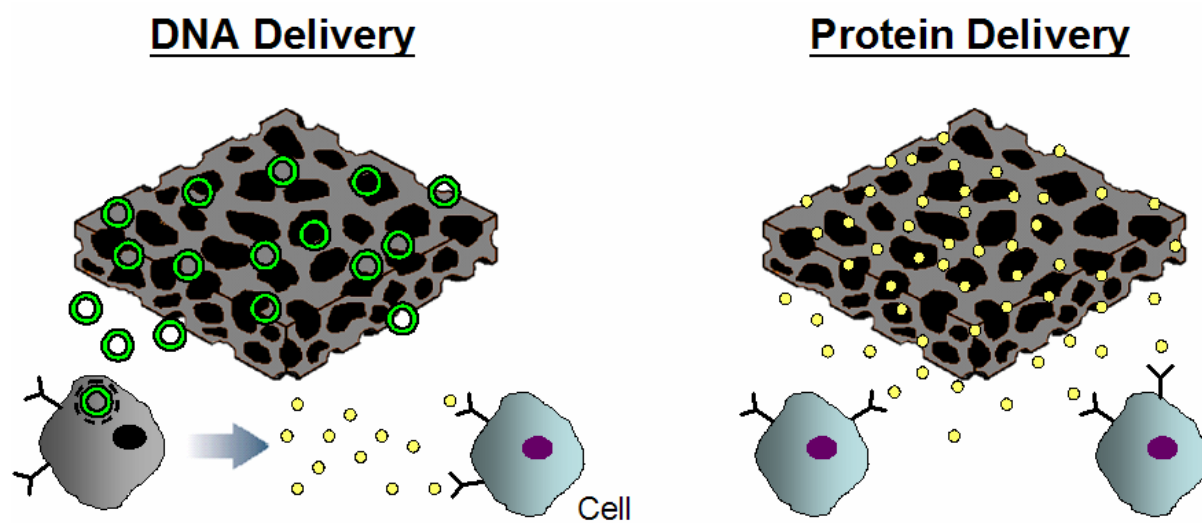


Figure 1-1. Drug delivery strategies from tissue engineering scaffolds.

Tissue engineering scaffolds capable of controlled drug delivery have the potential to enhance the efficacy of islet transplantation through creation of a supportive microenvironment. Clinical islet transplantation has shown the ability to normalize blood glucose levels in patients with type I diabetes following infusion of large numbers of islets into the liver.^{13, 14} However, this approach is limited by poor islet survival, where clinical estimates suggest that only 25-50% of the transplanted islet-mass successfully engrafts in patients.¹⁵ Also, progressive islet failure is observed over time, with less than 10% of patients remaining insulin-independent after 5 years,¹⁶ suggesting that the liver may not be the optimal transplant site. Thus, the exploration of alternative transplant sites and development of strategies to enhance the engraftment and long-term function of islets are needed. Drug-releasing scaffolds can provide localized delivery of angiogenic factors to induce the formation of a supportive vascular network, or they can deliver therapeutic factors that act directly on islets to promote cell survival and function. Towards this goal, the primary objective of this dissertation was to develop scaffold technologies for controlled delivery of DNA and proteins. In chapters 2 and 3, scaffolds were developed for DNA delivery and evaluated for their ability to promote gene transfer *in vivo*, in order to establish the capabilities of the delivery system and identify factors that regulate the extent and duration of transgene expression. In chapter 4, protein delivery strategies were employed to develop scaffolds for controlled delivery of the peptide exendin-4, which is known to exhibit several therapeutic effects on islet cells.

1.2. Background

1.2.1. *Tissue engineering scaffolds*

Tissue engineering scaffolds are intended to mimic key functions of the natural extracellular matrix (ECM), including organizing cells into structures, providing a support for cell adhesion, and serving as a reservoir for growth factors.^{3, 4} Scaffolds can create and maintain a three-dimensional space to guide new tissue formation, as well as provide a platform for delivering transplanted cells to specific sites within the body. Several fundamental requirements have been identified for the design of tissue engineering scaffolds, including being biodegradable and biocompatible, having sufficient mechanical strength, and providing a suitable environment for tissue growth and survival.⁴ In addition to providing a suitable physical structure, scaffolds can be designed to deliver a variety of biological signals to regulate cellular behavior.⁵ Physical signals in the form of adhesion-promoting molecules or peptides can be immobilized on the biomaterial surface to control cellular interactions with the scaffold.¹⁷⁻¹⁹ Also, scaffolds can deliver soluble signals (i.e. growth factors and cytokines) that bind to cell surface receptors and initiate a variety of cellular responses.²⁰ The creation of controllable microenvironments with the appropriate combination of signals needed to direct tissue formation represents a major challenge in the field of tissue engineering.

A variety of polymers, both natural and synthetic, have been used for the fabrication of tissue engineering scaffolds. Scaffolds fabricated from natural polymers, such as collagen, can mediate specific cellular interactions, but are limited by a narrow range of physical properties and poorly controlled degradation kinetics.²¹ In contrast, the mechanical strength and degradation rates of synthetic polymers can be readily controlled, allowing scaffolds to be

tailored for specific applications. For example, poly(lactide-co-glycolide) (PLG) can be designed to degrade over times ranging from a few weeks to more than a year by varying the polymer composition.

1.2.2. *Gene delivery from scaffolds*

Gene delivery from scaffolds is a versatile and promising approach for controlling soluble signals present within the local tissue microenvironment, yet successful implementation remains challenging due to the complexity of the gene transfer process. Gene therapy approaches may overcome some of the limitations associated with direct protein delivery.^{8, 21, 22} For example, since proteins exhibit a wide range of physical properties, the delivery of different proteins often requires modified strategies to maintain protein bioactivity, and ensure efficient incorporation and appropriate release kinetics. Additionally, proteins typically have short *in vivo* half-lives and are sensitive to inactivation.²³ Thus, it can be difficult to achieve sustained release kinetics needed to maintain the protein at therapeutic levels for extended periods of time. Rather than directly administering proteins, the encoding genes can be delivered and the transcriptional and translational machinery of cells can be exploited to locally produce and secrete the proteins of interest.

Gene delivery approaches can be divided into two main categories, viral and non-viral.²⁴ Viral approaches attempt to exploit the innate properties of viruses, as they have developed highly evolved and efficient mechanisms for infecting cells to ensure their own propagation.²⁵ Although highly efficient, virus-based gene delivery systems pose serious safety concerns.²⁶ Non-viral gene delivery or plasmid-based therapies provide a safe alternative, yet are much less

effective than viral vectors. Additionally, since plasmids do not integrate into the host genome, they provide only transient gene expression ranging from hours to months depending on the cell type.²⁷ However, transient expression of the encoded gene for several weeks may be desirable for many tissue engineering applications, such that expression subsides when the new tissue has formed or transplanted cells have successfully engrafted. The barriers of efficient non-viral DNA delivery can be separated into two categories – extracellular and intracellular.²⁸ The extracellular limitations refer to the process by which DNA traffics near the target cell membrane so that it can be internalized by the cell via endocytosis. Intracellular limitations include escape from the endosomal compartment, traffic through the cytoplasm, internalization into the nucleus, and finally protein expression.

Tissue engineering scaffolds for DNA delivery have been proposed to enhance gene transfer *in vivo* by (i) delaying clearance from the desired tissue, (ii) protecting DNA from degradation, and (iii) providing sustained delivery to maintain the vector at effective levels within the target tissue.²⁹ Scaffold-mediated DNA delivery has demonstrated the ability to achieve localized cellular transfection, with sufficient protein production to stimulate physiological responses that lead to tissue formation.³⁰⁻³³ DNA-loaded collagen matrices, also termed gene-activated matrices (GAMs), function to retain the DNA at the implant site and act as a scaffold for migration of repair cells (i.e. fibroblasts) into the matrix.²² Once inside the matrix, fibroblasts can internalize the DNA and serve as local bioreactors to produce and secrete the plasmid-encoded proteins.²² Collagen/DNA constructs have been implanted into an adult rat femur³¹ and a canine bone defect model,³⁰ and demonstrated the ability to induce new bone formation. In the canine model, a 1 mg DNA dose resulted in local transfection of ~30-50% of

infiltrating fibroblasts and expression of picogram quantities of the transgene product at 2-3 weeks post-implantation.³⁰ However, a 100 mg DNA dose was required to achieve regeneration of the bone defect.³⁰ PLG scaffolds have also demonstrated the capacity for controlled DNA delivery and *in vivo* gene transfer.³² Whereas collagen matrices generally retain DNA locally until cells arrive, PLG scaffolds function to provide controlled release of DNA. Subcutaneous implantation of DNA-loaded PLG scaffolds has resulted in transfection of cells within the scaffold and surrounding tissue, with protein production sufficient to promote physiological responses such as angiogenesis and granulation tissue formation.³² Although these initial studies have yielded promising results, more work is needed to better understand the requirements for achieving sustained and robust transgene expression at a variety of implant sites.

1.2.3. Islet transplantation

Islets of Langerhans are aggregates of endocrine cells dispersed throughout the exocrine tissue of the pancreas. Islets are composed of four major cell types: α , β , δ , and PP cells, which secrete glucagon, insulin, somatostatin, and pancreatic polypeptide, respectively.³⁴ The cellular distribution within islets is generally seen as a core of β -cells surrounded by a mantle of the other three cell types, although the distribution can vary depending on the species.^{35, 36} Islets constitute ~1% of the pancreas by mass, yet they receive 5-15% of the pancreatic blood supply.³⁷ The microvascular architecture in pancreatic islets is seen as a dense network of branching capillaries that is ideal for efficient delivery of oxygen and nutrients and the rapid dispersal of secreted hormones.³⁸ The competing roles of glucagon and insulin maintain glucose homeostasis within

the body. Insulin facilitates the uptake of glucose by tissues throughout the body and inhibits glucose synthesis in the liver, whereas glucagon increases glucose production in the liver.

Type I diabetes is caused by the autoimmune destruction of insulin-producing beta cells, rendering patients completely dependent on exogenous insulin for survival. The current standard of care for managing patients with type I diabetes is intensive insulin treatment, as it significantly delays the development and progression of secondary complications such as kidney failure and blindness.³⁹ However, insulin therapy does not provide perfect blood glucose control, and thus cannot guarantee the prevention of these complications. This is especially true for patients with volatile forms of type I diabetes, where large fluctuations in blood sugar are not adequately stabilized by insulin injections. Islet transplantation is a cell-based therapy that aims to restore normal blood glucose control through replacement of a patient's insulin-secreting beta cells. Recent clinical successes employing the Edmonton protocol have demonstrated that islet transplantation is a viable approach for reversing type I diabetes.^{13, 14, 40} However, a number of problems remain, including poor islet engraftment and progressive islet failure over time. Clinical estimates suggest that only 25-50% of the transplanted islet mass successfully engrafts in patients, necessitating two or more successive islet transplants to generate enough islets capable of establishing euglycemia.¹⁵ This extensive islet cell death in the early post-transplant period is likely related to disruption of the islet's native microenvironment during the isolation/purification process. Additionally, long-term follow-up on islet transplant recipients has revealed progressive islet failure, where less than 10% of patients remain insulin-independent after five years.¹⁶ Although reasons for this remain unclear, the current approach of transplanting islets into the liver may contribute to islet failure by exposing them to high levels of circulating

toxins, and placing them in the immediate proximity of resident macrophages within hepatic sinusoids.

Native islets are surrounded by a continuous peri-insular basement membrane composed of collagen IV, laminin, and fibronectin which can engage integrins on the cell surface to mediate adhesion, provide structural support, and activate intracellular chemical signaling pathways. The isolation of islets via enzymatic digestion results in complete destruction of the basement membrane, along with increased cell death by apoptosis.⁴¹⁻⁴⁵ Studies have suggested that early islet cell death occurs by an anoikis-like mechanism, which is related to an integrin signal defect that induces apoptosis in epithelial cells that are separated from their extracellular matrix (ECM).^{43, 45} For example, incompletely digested islets retaining an outer ring of ECM show dramatically lower rates of apoptosis relative to purified islets.⁴³ Consistent with these findings, the increase in apoptosis of isolated islets is paralleled by a progressive decrease in integrin expression,^{41, 42, 46} while islets cultured on solid matrices composed of ECM molecules exhibit improved cell survival.^{47, 48} Thus, the provision of a matrix to support islet attachment will likely be important for maintaining the viability of transplanted islets.

In addition to being stripped from their native ECM, newly transplanted islets are avascular, relying on nutrient and oxygen diffusion for survival before reestablishing their vascular supply.³⁸ This avascular state creates an oxygen concentration gradient within the islet decreasing radially from the periphery to the core, which can have a detrimental effect on cell survival and insulin biosynthesis and secretion.^{49, 50} The effects of hypoxia are exacerbated by chronic hyperglycemia, which places an increased metabolic demand on the beta-cells leading to increased oxygen consumption.⁴⁹ Islet revascularization requires 2-5 days post-transplantation to

initiate and approximately 2 weeks for the establishment of blood flow.⁵¹ Even at one month post-transplantation when vascularization is thought to be complete, the mean oxygen tension within the islets is <15% of that in native pancreatic islets regardless of the implantation site.^{38, 52} Also, the vascular density in transplanted islets is 25-50% lower than that seen in endogenous islets.⁵³ Thus, strategies to improve the rate and extent of islet revascularization will likely lead to enhanced cell survival and improved function.

1.2.3. Angiogenesis

Angiogenesis, or the sprouting of new capillaries from a preexisting network, is a critical component of tissue engineering since a sufficient vascular supply must be established to support the survival of transplanted cells and developing tissues. Blood vessel formation involves a coordinated sequence of events including: (i) vasodilation, (ii) increased vascular permeability, (iii) proteolytic degradation of the basement membrane, (iv) migration and proliferation of endothelial cells, and (v) reformation of the basement membrane.⁵⁴ This remodeling process is regulated by a delicate balance between angiogenic and anti-angiogenic factors.⁵⁵

Numerous angiogenic growth factors have been identified, of which basic fibroblast growth factor (FGF-2) and vascular endothelial growth factor (VEGF) have been the most widely studied. VEGF is a secreted homodimeric glycoprotein with four known splicing variants, consisting of 121, 165, 189, or 206 amino acids.⁵⁶ The larger isoforms (165, 189, and 206) bind to heparan sulfate present on cell surfaces and in the ECM with increasingly greater affinity, which limits diffusibility of the VEGF molecule but increases its mitogenic potency.⁵⁷ VEGF acts almost exclusively on endothelial cells (ECs) to stimulate their proliferation and migration,

promote their survival, increase vascular permeability, and induce vasodilation.^{56, 58} Despite its potency, VEGF is commonly associated with the formation of leaky blood vessels, and in some cases can cause aberrant angiogenesis characterized by formation of hemangioma-like structures.⁵⁹⁻⁶² Also, since VEGF is a survival factor for endothelial cells, long-term presence is generally required to prevent regression of newly formed vessels.⁶³ FGF-2 similarly acts on endothelial cells to induce proliferation and migration, stimulate secretion of proteolytic enzymes, and upregulate expression of integrins.⁶⁴ However, in comparison with VEGF, FGF-2 affects a broad range of cell types in addition to ECs, and is not known to induce vascular leakage. FGF-2 also exists in multiple isoforms (18, 22, 23, and 24 kD), but lacks a conventional signal peptide sequence for cellular secretion; however, an alternative export pathway specific to the 18 kD isoform has been identified making it an appropriate target for gene therapy.⁶⁵

The transcription factor hypoxia inducible factor-1 (HIF-1) plays a central role in regulating the process of angiogenesis.⁶⁶⁻⁶⁸ HIF-1 is a heterodimer consisting of two protein subunits, HIF-1 α and HIF-1 β .^{66, 67} Although both subunits are constitutively expressed independent of the tissue oxygen tension, HIF-1 α contains an oxygen-sensitive degradation domain (ODD) and is therefore rapidly degraded under normoxic conditions. Under hypoxic conditions, however, the degradation of HIF-1 α is inhibited resulting in increased formation of intact HIF-1 heterodimers. HIF-1 stimulates angiogenesis by upregulating VEGF expression, as well as a range of other molecules important for extracellular matrix metabolism and vessel maturation (e.g., matrix metalloproteinases, plasminogen activators and their receptors, and collagen prolyl hydroxylase).⁶⁷ Also, the expression of additional angiogenic molecules (e.g., angiopoietin-2 and its receptor, platelet-derived growth factor, and fibroblast growth factors) is

increased through secondary cascades of gene regulation.⁶⁶ In comparison to delivery of individual angiogenic factors, the HIF-1 transcription factor may offer a more effective therapeutic target by providing simultaneous induction of multiple angiogenic factors. As a result, oxygen-insensitive variants of HIF-1 α have been created to allow stabilization of the protein under normoxic conditions.⁶⁹

2. CHAPTER 2: PLG Scaffolds for Plasmid Delivery: *In Vivo* Transgene Expression at a Subcutaneous Site

2.1. Introduction

Tissue engineering involves the creation of biological tissue substitutes to replace those damaged by disease or injury.^{1, 2} The underlying premise is that cells have the potential to organize into new tissues when cultured in three dimensions under the appropriate environmental conditions.² Polymer scaffolds are typically used to create these three-dimensional environments. Fundamental design considerations for scaffolds include biodegradability, biocompatibility, and mechanical strength.⁴ Additionally, scaffolds are typically highly porous to allow cellular infiltration and integration with host tissue following implantation into the body.⁴ However, in order to direct cellular behavior and coordinate tissue formation, the controlled presentation of biological signals is thought to be required.⁵ Cells are constantly sensing and interpreting signals in their environment, and their response to these signals ultimately determines their behavior. Soluble growth factors and cytokines represent an important category of signals involved in regulating a variety of cellular processes such as migration, differentiation, proliferation, and apoptosis. Thus, the development of scaffolds capable of controlled drug delivery has been widely studied.^{6, 8-10} The effectiveness of protein delivery from scaffolds has been well established,⁹ although these systems can be limited by a lack of versatility. Since proteins exhibit a wide range of physical properties, different proteins often require separate delivery strategies to ensure efficient encapsulation and appropriate release kinetics.

Gene delivery from polymer scaffolds is an alternative approach for introducing soluble factors into the local environment, providing improved versatility and the potential for prolonged expression of desired proteins.¹¹ With a plasmid delivery system, genes can be interchanged

without significantly altering the physical properties of the plasmid.⁷⁰ Thus, a single delivery system could potentially be used for the delivery of a wide range of therapeutic targets. Successful implementation of a gene therapy approach *in vivo* will likely require transfection of sufficient numbers of cells and expression of the protein at physiologically relevant levels for sustained periods of time. Previous studies examining plasmid delivery from polymer scaffolds have demonstrated localized transfection of cells, with sufficient expression levels to promote tissue formation.³⁰⁻³² However, the extent and duration of transgene expression has generally not been well characterized. Additionally, the effects of scaffold design parameters (e.g. DNA dose, scaffold structure) on transgene expression are not well understood.

In this chapter, the ability of plasmid-releasing scaffolds to achieve localized and sustained transgene expression *in vivo* was evaluated at a subcutaneous site. Porous poly (lactide-co-glycolide) (PLG) scaffolds were fabricated using an established gas foaming process.^{71, 72} The extent and duration of transgene expression was monitored using bioluminescence imaging for a range of plasmid doses. Also, the effects of scaffold structure on transgene expression were examined by varying the polymer molecular weight and pore size. Histological analysis was performed to assess the distribution of transfected cells and the extent of cellular infiltration into scaffolds.

2.2. Materials and methods

2.2.1 Materials

DNA was purified from bacteria culture using Qiagen reagents (Santa Clara, CA), and stored in Tris-EDTA (TE) buffer at -20°C or 4°C. The pLuc plasmid contains the firefly

luciferase gene within the pNGVL vector backbone (National Gene Vector Labs, University of Michigan), and is driven by a CMV promoter. A control vector was created by removing the luciferase gene from the pNGVL backbone. PLG (75/25 mole ratio of D,L lactide to glycolide, i.v. = 0.6-0.8 dl/g) was obtained from Alkermes, Inc. (Cincinnati, OH) or Lakeshore Biomaterials (Birmingham, AL). PLG (75/25 mole ratio of D,L lactide to glycolide, i.v. = 0.16-0.24 dl/g) was purchased from Boehringer Ingelheim (Petersburg, VA).

2.2.2 *Fabrication of DNA-loaded scaffolds*

Scaffolds were fabricated using a previously described gas foaming/particulate leaching process.^{32, 71, 72} First, PLG was dissolved in dichloromethane and emulsified in 1% poly(vinyl alcohol) (PVA) to form microspheres. The concentration of the PLG solution was varied from 2% (w/w) to 10% (w/w) to alter the microsphere size and density. Microsphere size was assessed by light microscopy. Additionally, two different PLG molecular weight formulations were used: (1) high molecular weight (i.v. = 0.6-0.8 dl/g), and (2) high/low molecular weight blend (equal weights of i.v. = 0.6-0.8 dl/g and i.v. = 0.16-0.24 dl/g). To incorporate DNA, PLG microspheres (7 mg) were reconstituted in an aqueous solution containing DNA (300-800 µg) and lactose (1 mg, 5.5 mM), frozen in liquid nitrogen, and lyophilized overnight. The resulting powder was then mixed with NaCl particles (135 mg, $250 < d < 425$ µm or $106 < d < 250$ µm) in the presence of 1-2 µl of water (wet granulation technique).⁷³ Notably, the mixing process was influenced by the physical properties of the lyophilization product, which were found to be dependent on the drying rate (**Appendix 6.1**). The polymer/salt mixture was compressed in a 5 mm KBr die (International Crystal Labs, Garfield, NJ) at 1500 psi using a Carver press, and the resulting

construct was equilibrated with CO₂ (800 psi) for 16 hours in a custom-made pressure vessel. Afterwards, the pressure was rapidly released over a period of 25 minutes, which serves to fuse adjacent microspheres creating a continuous polymer structure. To remove the salt, scaffolds were immersed in water for 4 hours, with fresh water replacement after 2 hours.

2.2.3 *Characterization of in vitro release kinetics and incorporation efficiency*

The DNA incorporation efficiency is defined as the mass of DNA left in the scaffold after the leaching step divided by the mass of DNA initially input. Hereafter, the amount of input DNA will be referred to as the dose. After leaching, scaffolds were dissolved in chloroform (600 μ L), and the DNA was extracted from the organic solution. TE Buffer (400 μ L) was added to the organic phase, vortexed, and centrifuged at 14,000 rpm for 3 minutes. The aqueous layer was collected, and two more extraction cycles were performed to maximize DNA recovery. The amount of DNA was quantified using a fluorometer and the fluorescent dye Hoechst 33258. To determine the *in vitro* release kinetics of DNA, scaffolds were placed in 500 μ L of phosphate-buffered saline (PBS) (pH 7.4), and the solution was replaced at each time point.

2.2.4 *Measuring in vivo transgene expression with bioluminescence imaging*

Animal studies were performed in accordance with the NIH Guide for the Care and Use of Laboratory Animals, and protocols were approved by the IACUC at Northwestern University. Scaffolds loaded with pLuc plasmid were implanted subcutaneously into male CD-1 mice (20-22 g). *In vivo* luciferase expression was monitored using an IVIS imaging system (Xenogen Corp., Alameda, CA), which includes a cooled CCD camera. For imaging, the animals were injected IP with D-luciferin (Molecular Therapeutics Inc., MI, 150 mg/kg body weight). The animals were

placed in a light-tight chamber and bioluminescence images were acquired (every 5 minutes for a total of 20 minutes) until the peak light emission was confirmed. Gray scale and bioluminescence images were superimposed using the Living Image software (Xenogen Corp., CA). A constant size region of interest (ROI) was drawn over the implantation site. The signal intensity was reported as an integrated light flux (photons/sec), which was determined by IGOR software (WaveMetrics, OR). Background photon fluxes were obtained using the same procedures prior to the injection of D-luciferin. For these and other results, statistical comparison between conditions were performed using the software package JMP (SAS Institute Inc., NC).

2.2.5 Histological analysis and immunohistochemistry

Histological analysis was performed to evaluate the distribution of transfected cells and the extent of cellular infiltration into scaffolds following subcutaneous implantation. Scaffolds were surgically retrieved from mice at specific time points, fixed in 4% paraformaldehyde overnight at 4°C, and immersed in 10% and 30% sucrose solutions. Tissue samples were embedded in OCT and frozen in an isopentane bath cooled over dry ice. Sections were cut using a cryostat and mounted on glass slides. To evaluate cellular infiltration, sections were stained with hematoxylin and eosin (H&E) and visualized by light microscopy. To determine the distribution of transfected cells, immunohistochemical staining with antibodies directed against the luciferase transgene product was performed. After blocking, sections were incubated with primary rabbit anti-luciferase antibody (Cortex Biochem, CA, USA) diluted (1:100) in PBS/0.1% BSA for 1 h at 37°C. A biotinylated goat anti-rabbit secondary antibody (Vector Laboratories, Burlingame, CA, USA) was added, followed by incubation with the ABC reagent (Vector

Laboratories). After rinsing, the slide was incubated in 3-amino-9-ethylcarbazole (AEC) (Sigma, St. Louis, MO, USA) peroxidase substrate, which produced a red product for visualization.

2.3. Results

2.3.1 Scaffold fabrication

The polymer molecular weight significantly affected the scaffold's mechanical strength *in vivo*. Scaffolds fabricated with the high/low molecular weight polymer blend typically exhibited collapsed pore structures following implantation, and in turn did not allow for cellular infiltration (**Fig. 2-1A**). In comparison, scaffolds fabricated solely with the high molecular weight polymer maintained their structural integrity, but still failed to support cellular infiltration (**Fig. 2-1B**). In this case, the lack of cellular infiltration was hypothesized to be the result of a low degree of interconnectivity between adjacent pores within the scaffold. As a first attempt to address this problem, the salt-to-polymer ratio was increased from 19:1 up to 50:1. However, visual inspection of scaffolds under a light microscope did not reveal any noticeable improvement in pore interconnectivity for the increased salt-to-polymer ratios.

The ability to fabricate scaffolds with improved pore interconnectivity was further investigated by altering the physical properties of the polymer microspheres. Increasing the concentration of the PLG solution used in the emulsion process from 2% up to 10% substantially increased microsphere size, and presumably microsphere density (**Fig. 2-2**). The increase in particle size is due to the increased viscosity of the organic phase.⁷⁴ Scaffolds fabricated with the larger microspheres exhibited a greater degree of pore interconnectivity, but at the expense of decreased mechanical strength. Thus, it became clear that an important balance must be satisfied

between pore interconnectivity and mechanical strength in order to achieve a structure that both resists collapse and promotes cellular infiltration. Scaffolds fabricated from microspheres made with a 6% PLG solution satisfied this balance, as they supported complete cellular infiltration by 2 weeks post-implantation (**Fig. 2-3**).

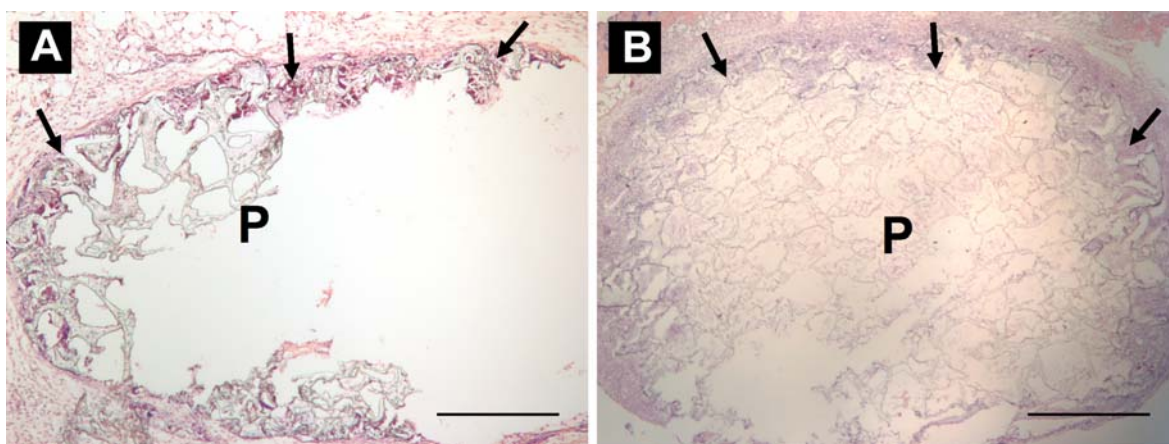


Figure 2-1. H&E staining of scaffold cross-sections at 14 days post-implantation to evaluate structural integrity and the extent of cellular infiltration. (A) A scaffold fabricated with the high/low molecular weight polymer blend exhibited a collapsed pore structure and supported only minimal cellular infiltration at the scaffold periphery (indicated by arrows). “P” indicates polymer. Note that the center of the scaffold tore out during sectioning due to the lack of cellular infiltration and weak mechanical strength of the polymer. Image was taken at 50x magnification, scale bar equals 0.5 mm. (B) A scaffold fabricated with the high molecular weight polymer maintained an intact pore structure, but supported only minimal cellular infiltration at the scaffold periphery (indicated by arrows). Image was taken at 25x magnification, scale bar equals 1 mm.

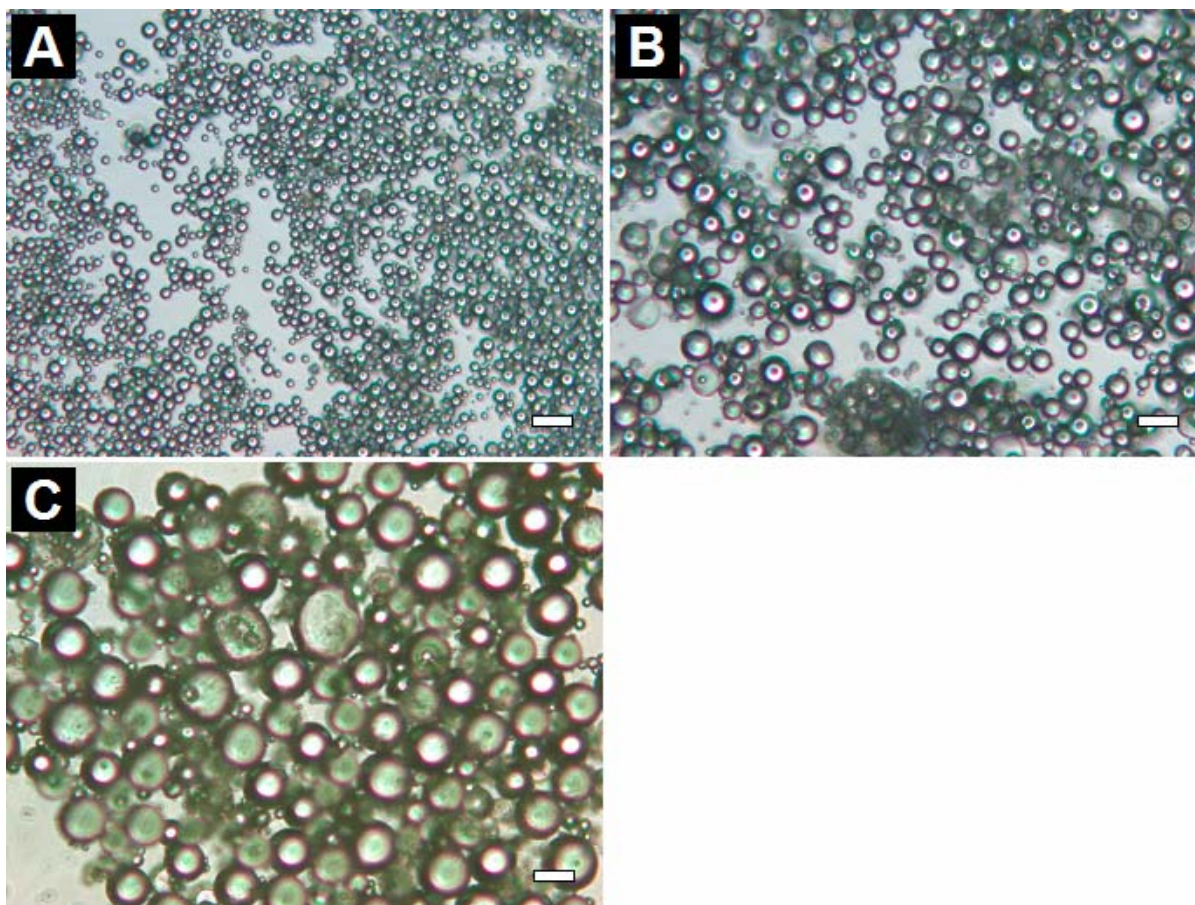


Figure 2-2. Microsphere size increases with increasing concentration of the PLG solution. Images of microspheres made with a (A) 2% PLG solution, (B) 6% PLG solution, and (C) 10% PLG solution. All images were taken at the same magnification, 400x. Scale bars equal 20 μm .

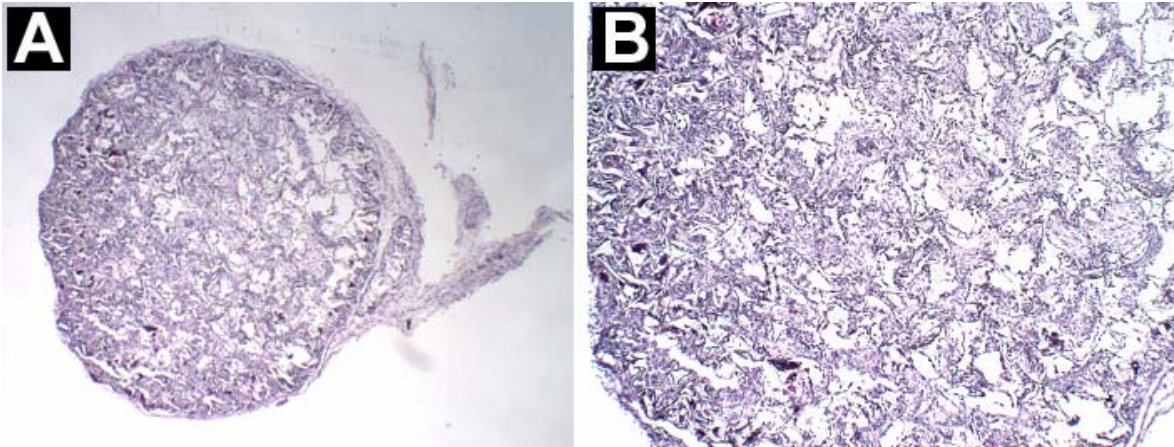


Figure 2-3. H&E-stained cross-section of a scaffold fabricated from microspheres made with a 6% PLG solution. Hematoxylin stains cell nuclei a blue/purple color, and thereby indicates the distribution of cells within the scaffold. Complete cellular infiltration throughout the scaffold interior was observed by 2 weeks post-implantation. Images were taken at (A) 10x or (B) 40x magnification.

2.3.2 Plasmid incorporation efficiency and *in vitro* release kinetics

Plasmid incorporation efficiencies of 50-60% have typically been obtained for porous PLG scaffolds made with the gas foaming/particulate leaching method.³² In the current studies, implementation of a wet granulation mixing technique increased plasmid incorporation from $46.5 \pm 3.9\%$ to $59.5 \pm 2.4\%$ ($P < 0.001$) (**Fig. 2-4A**), presumably by facilitating more homogeneous mixing.³³ The scaffolds exhibited rapid plasmid release kinetics *in vitro*, characterized by an initial burst equal to $53 \pm 8.1\%$ within the first 3 days, followed by a slower release that was sustained through 3 weeks (**Fig. 2-4B**).³³ Notably, the scaffolds used in these studies were made with 2% PLG microspheres, which resulted in a pore structure that typically failed to support cellular infiltration (as described above). However, when the scaffold's pore interconnectivity was improved to promote cellular infiltration (by using 6% PLG microspheres), the plasmid incorporation efficiency decreased to $< 20\%$. As a result, scaffolds made with 6% PLG microspheres were not evaluated *in vivo* for plasmid delivery.

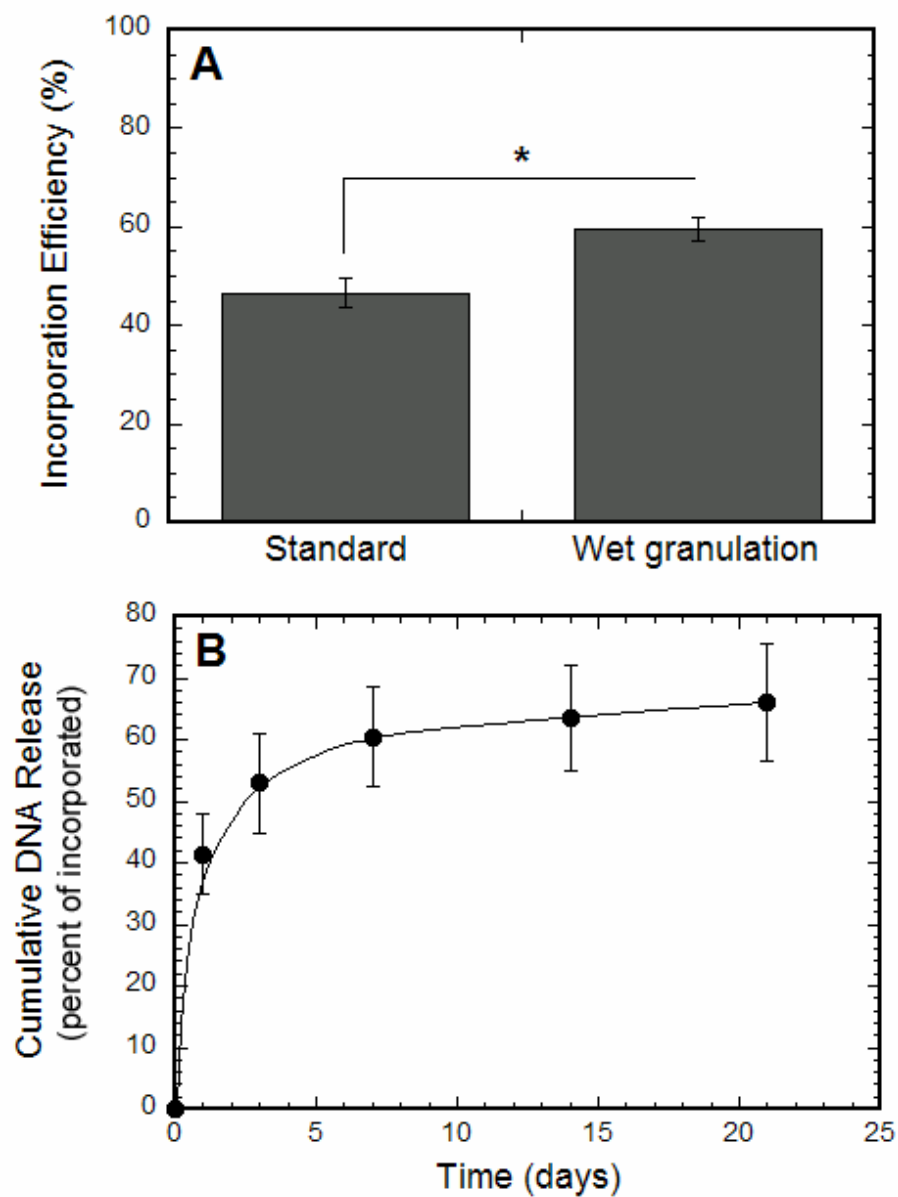


Figure 2-4. Characterization of plasmid incorporation and *in vitro* release kinetics. (A) DNA incorporation efficiency with standard mixing and wet granulation. *Significance at $P < 0.001$. (B) *In vitro* cumulative DNA release from scaffolds fabricated by wet granulation and subsequent gas foaming process.

2.3.3. *In vivo* transgene expression

DNA-releasing scaffolds provided localized and sustained transgene expression *in vivo* following subcutaneous implantation, with the extent and duration of expression regulated by the DNA dose. Scaffolds loaded with 500 μg of plasmid DNA produced light emission in 89% of the animals (8 of 9, **Fig. 2-5A**), with levels at day 3 that were significantly above background or empty scaffold controls (**Fig. 2-5B**, $P < 0.05$).³³ Light emission was visualized at subsequent time points, but the levels were not significantly above controls (**Fig. 2-5**, $P > 0.05$).³³ Increasing the plasmid loading to 800 μg dramatically increased the duration of transgene expression to at least 105 days (**Fig. 2-6**).³³ Light emission was observed directly over the implant in all samples (7 of 7, **Fig. 2-6A**), at levels significantly greater than the control conditions (**Fig. 2-6B**, $P < 0.05$).³³ Control conditions included scaffolds without DNA, or with plasmid lacking the luciferase cDNA, which produced light emission equivalent to background (**Fig. 2-6B**).³³ After 105 days, average levels of light emission for the pLuc-loaded scaffolds were not significantly different than the control conditions, because half of the samples decreased to background levels ($P > 0.05$). The remaining samples, however, continued to have luciferin-induced light emission above background, with one sample having consistently elevated levels through 189 days. To further examine this dose-dependent effect on transgene expression, additional DNA doses were tested. Scaffolds loaded with 600 μg of DNA provided sustained transgene expression (in 5 of 5 mice) for at least 56 days at similar or higher levels to those previously observed for the 800 μg DNA dose, suggesting a threshold above which further increases in dose do not increase expression (**Fig. 2-7**). Scaffolds loaded with 400 μg of DNA also provided sustained expression (in 5 of 5 mice) for at least 28 days, but at lower levels than the 600 μg or 800 μg dose (**Fig. 2-7**). Unlike

the 500 μg dose (discussed above), expression levels for the 400 μg dose were significantly above background for all time points ($P < 0.05$, **Fig. 2-7**). It is unclear why the 400 μg dose provided higher expression levels than the 500 μg dose, but may be related to variability in the plasmid incorporation efficiency. Decreasing the DNA dose further to 300 μg resulted in only short-term transgene expression, where light emission was observed in only 2 of 5 mice by day 7 (**Fig. 2-7**).

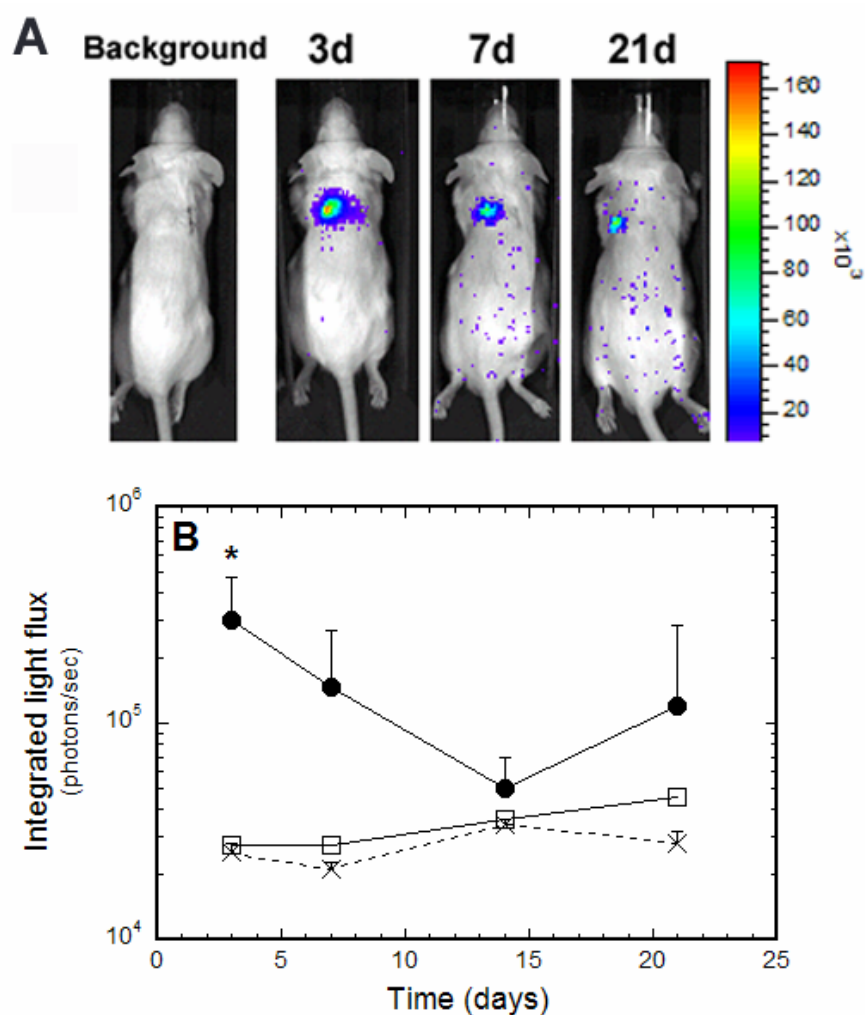


Figure 2-5. Bioluminescence imaging of firefly luciferase expression for scaffolds loaded with 500 μg of pLuc. Scaffolds were made with the high/low molecular weight blend. (A) Images showing light emission for a single mouse at different time points. (B) Emitted light intensity (photons/s) in region of interest over the implant sites ($n=8$) for scaffolds incorporating pLuc (circles), scaffolds without DNA (squares), and background (x). *Statistical significance at $P < 0.05$ relative to control.

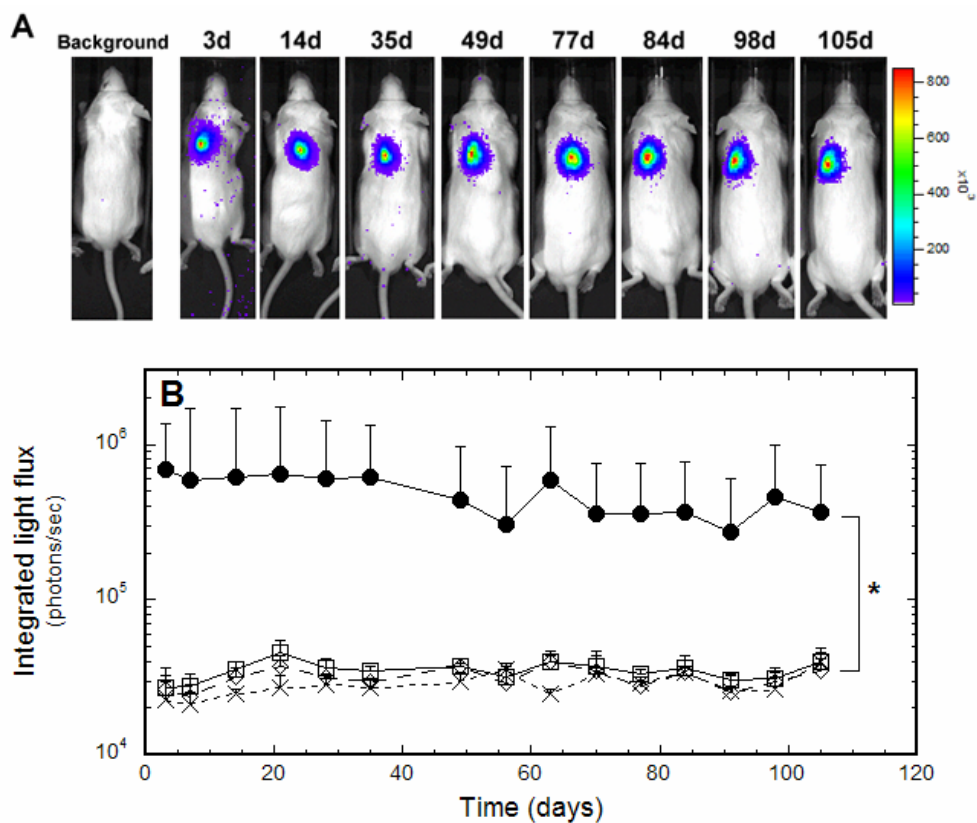


Figure 2-6. Bioluminescence imaging of firefly luciferase expression for scaffolds loaded with 800 μg of pLuc. Scaffolds were made with the high/low molecular weight blend. (A) Images showing a single mouse at different time points. (B) *In vivo* CCD signal intensity (photons/s) in region of interest over implant sites ($n=6$) for scaffolds with pLuc (circles), scaffolds without DNA (squares), scaffolds with empty vector (diamonds), and background (x). *Statistical significance at $P < 0.05$ between pLuc and all other conditions for all time points.

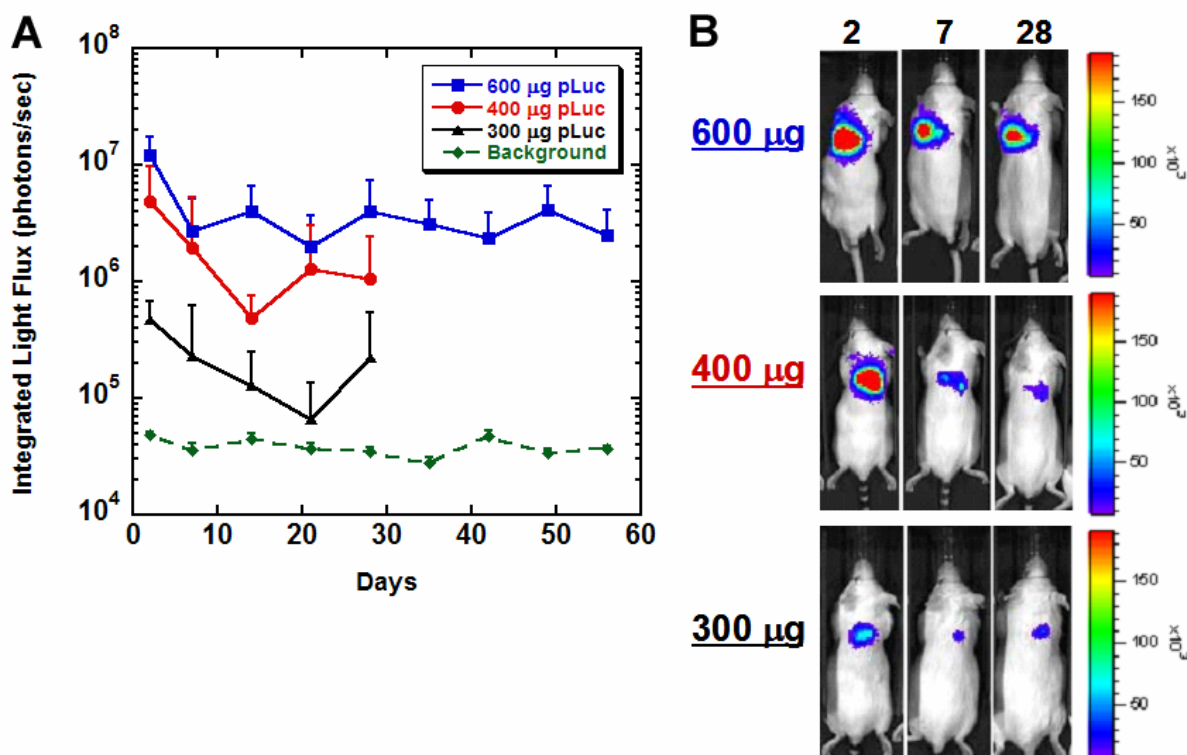


Figure 2-7. Bioluminescence imaging of firefly luciferase expression for scaffolds fabricated with different DNA doses. All scaffolds were made with the high/low molecular weight blend. (A) Emitted light intensity (photons/s) in region of interest over the implant sites ($n = 5$) for scaffolds loaded with 600 µg of pLuc (blue squares), 400 µg of pLuc (red circles), or 300 µg of pLuc (black triangles). Background is indicated by green diamonds. (B) Images showing a single mouse for each condition at different time points.

Initial studies suggested that the scaffold's porous structure may play an important role in promoting transgene expression *in vivo*, by providing a large surface area over which DNA can be released.³³ First, we observed that several scaffolds that failed to provide sustained transgene expression had collapsed pore structures, which was hypothesized to limit DNA release. Second, immunohistochemical staining with antibodies directed against the luciferase transgene product demonstrated transfected cells immediately adjacent to the polymer surface, suggesting that gene transfer may preferentially occur at the polymer surface (**Fig. 2-8**).³³ In this case, maintaining a large surface area (i.e. non-collapsed structure) would be important for maximizing the number of cells that contact the polymer, which in turn would promote gene transfer. However, in comparing scaffolds made with different molecular weight polymers, it was later found that the scaffold structure had no effect on transgene expression. Specifically, scaffolds fabricated from the high/low molecular polymer blend collapsed following implantation, yet they consistently (5 of 5 mice) promoted robust and sustained expression, similar to the high molecular weight scaffolds that maintained their structure (**Fig. 2-9**). In another experiment, the scaffold pore size was varied to further examine potential effects of scaffold structure on transgene expression. Scaffolds with decreased pore sizes of 106-250 μm resulted in lower levels of expression and shortened duration in some samples, with light emission observed in only 3 of 5 mice by day 7 (**Fig. 2-10**). The reasons for the decreased expression observed here are unclear, but may be related to decreased plasmid incorporation, which depends on the scaffold structure. Notably, these scaffolds were made from the high/low molecular weight polymer, and collapsed following implantation, limiting cellular infiltration. Thus, the decreased expression cannot be explained by altered kinetics of cellular infiltration or differences in the total surface area for cell contact.

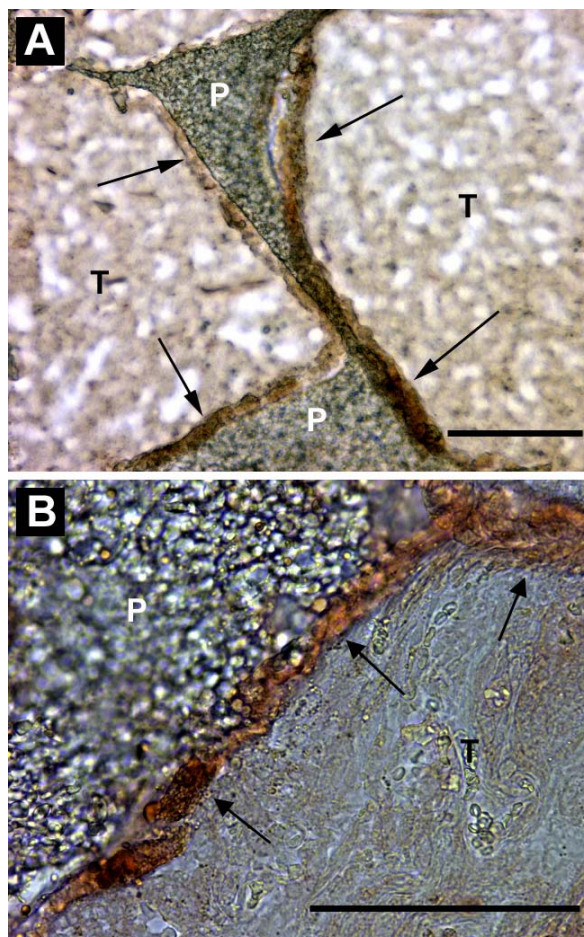


Figure 2-8. Immunohistochemical staining with luciferase antibodies to determine the distribution of transfected cells. Images were taken from scaffolds loaded with 800 μg of pLuc that were retrieved at 17 days post-implantation. The scaffold was made with the high/low molecular weight blend, but unlike most of the other samples made with this formulation, it supported cellular infiltration. Transfected cells were found immediately adjacent to the polymer surface, as shown in (A) 200x and (B) 400x magnification. Scale bars equal 100 μm . Labels indicate polymer (P), surrounding tissue (T), and luciferase staining (arrows).

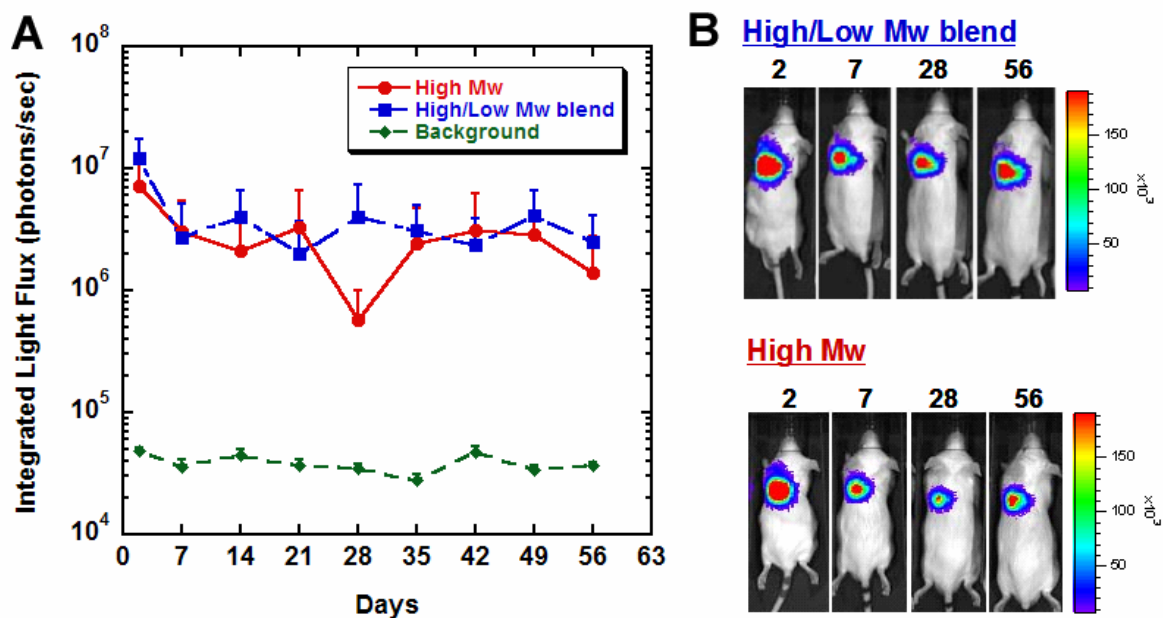


Figure 2-9. Bioluminescence imaging of firefly luciferase expression for scaffolds fabricated with different molecular weight polymers. All scaffolds were loaded with 600 μg of pLuc. (A) Emitted light intensity (photons/s) in region of interest over the implant sites ($n = 5$) for scaffolds made with the high/low molecular weight polymer blend (blue squares) or only the high molecular weight polymer (red circles). Background is indicated by green diamonds. (B) Images showing a single mouse for each condition at different time points.

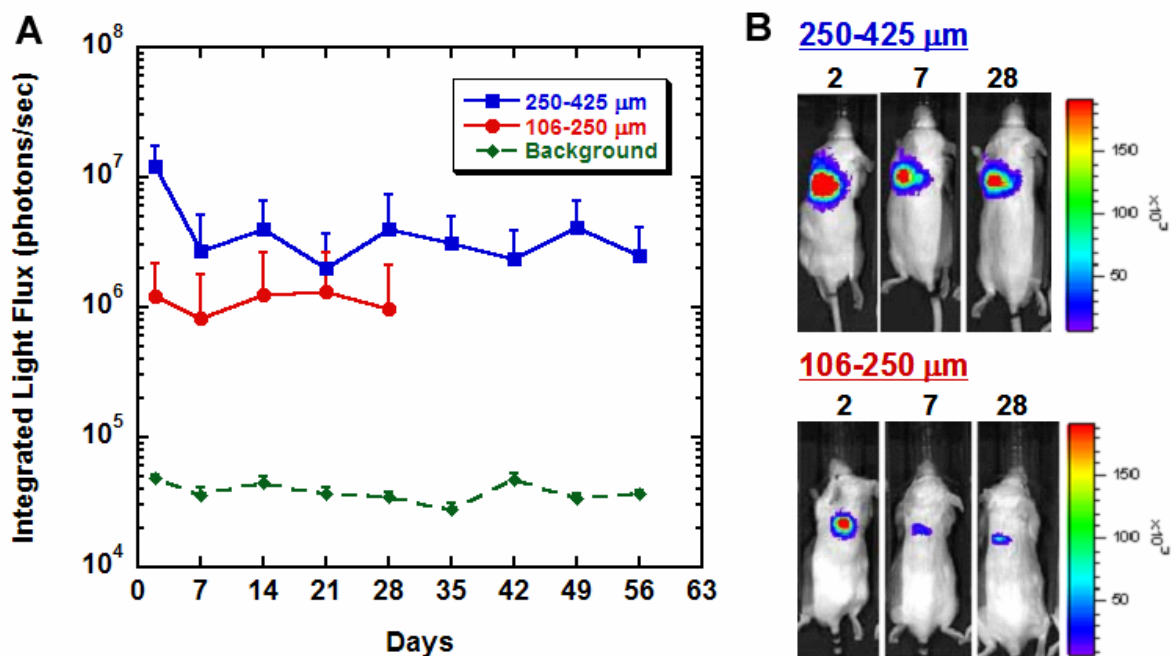


Figure 2-10. Bioluminescence imaging of firefly luciferase expression for scaffolds fabricated with different pore sizes. All scaffolds were loaded with 600 μg of pLuc and made with the high/low molecular weight polymer blend. (A) Emitted light intensity (photons/s) in region of interest over the implant sites ($n = 5$) for scaffolds with 250-425 μm pore sizes (blue squares) or 106-250 μm pore sizes (red circles). Background is indicated by green diamonds. (B) Images showing a single mouse for each condition at different time points.

2.4. Discussion

Gene delivery from tissue engineering scaffolds offers the potential to achieve localized expression of a wide range of proteins that can direct cellular behavior and ultimately stimulate new tissue formation. However, the requirements for designing effective gene delivery systems have not been well established. This chapter examined the ability of plasmid-releasing scaffolds to provide sustained *in vivo* transgene expression at a subcutaneous site, and evaluated the effects of DNA dose and scaffold structure. Monitoring of reporter gene expression over time using bioluminescence imaging demonstrated localized transgene expression that persisted for several months at sustained levels. The plasmid dose influenced the extent and duration of gene expression. Plasmid doses of 400, 600, and 800 μg all provided long-term expression, although the levels of expression were lower for the 400 μg dose. In contrast to the higher doses, scaffolds loaded with 300 μg of DNA provided only short-term expression, with expression subsiding in most of the animals by 7 days. Although initial studies suggested that the scaffold's porous structure may play an important role in promoting gene transfer, it was later determined that loss of structural integrity does not negatively affect transgene expression. In fact, scaffolds made with the high/low molecular weight blend consistently provided robust and sustained transgene expression, despite their collapsed pore structures. In comparison, scaffolds made with the high molecular weight polymer maintained intact pore structures, but provided similar transgene expression. However, regardless of the polymer molecular weight, scaffolds were unable to effectively support cellular infiltration. To address this problem, the scaffold pore interconnectivity was improved by increasing the microsphere size. Although the modified scaffold structure promoted cellular infiltration, it also substantially decreased the plasmid

incorporation efficiency. These studies demonstrated an important relationship between the scaffold structure and plasmid incorporation efficiency, and thereby revealed a major limitation of the current gene delivery system. A summary of these results is shown in **Table 2-1**.

The ability to achieve long-term transgene expression *in vivo* with non-viral gene delivery approaches is generally regarded as a challenge,²⁶ so it is important to consider possible explanations for the prolonged expression observed here. Plasmids are typically expressed in target cells for 1-2 weeks.⁷⁵ The rapid decrease in expression has traditionally been explained by phenomena such as (i) plasmid dilution due to cell division, (ii) transcriptional inactivation of the promoter, and (iii) death of the transfected cell.^{76, 77} Sustained plasmid release from scaffolds has been proposed as a means to extend transgene expression by maintaining elevated concentrations of the vector locally to allow for repeated cellular transfection.^{11, 29} However, the scaffolds in these studies exhibited rapid *in vitro* release kinetics, where most of the plasmid was released in an initial burst during the first few days. Notably, the release kinetics were determined using a decreased DNA dose of 50 μg , and the magnitude of the initial burst typically increases with dose; thus, the initial burst for scaffolds tested *in vivo* was likely even higher. Although the initial burst was followed by a slower release that continues for a few weeks, it seems unlikely that these smaller plasmid quantities released at later times would be sufficient to sustain transgene expression for several months. In another experiment, it was found that scaffolds with DNA dried onto their surface can provide robust transgene expression for at least 2 weeks (**Appendix 6.2**). Since the surface-adsorbed plasmid is rapidly released upon hydration of the scaffold, this experiment suggests that sustained DNA release may not be required for prolonging expression at this site. Another important observation is that the transgene expression levels are maintained

at relatively stable levels over time. If transgene expression were maintained through repeated cellular transfection (i.e. sustained plasmid release), more fluctuations in the expression levels over time would likely be observed. Additionally, one would expect expression levels at later times to be much lower than initial levels due to lower quantities of plasmid being delivered.

An alternative explanation for the sustained transgene expression is that the cell population initially transfected continues to express the plasmid for a prolonged period of time. It is well established that muscle can provide sustained expression of plasmids for at least 19 months without chromosomal integration.^{78, 79} Thus, muscle cells represent a likely explanation for the long-term transgene expression observed here. As partial support for this hypothesis, H&E-stained tissue sections clearly demonstrated the presence of striated muscle fibers (known as panniculus carnosus) in close proximity to the scaffold (**Fig. 2-11**). The panniculus carnosus is a system of muscle fibers present in subcutaneous tissue connecting skin to underlying fascia and bone. Previous immunostaining with antibodies directed against the luciferase transgene product demonstrated transfected cells within the scaffold, which are clearly not muscle fibers; but, at this time we were unaware that muscle fibers were even present.³³ Thus, it is possible that muscle cells were transfected in addition to cells within the scaffold, although more immunohistochemical analysis is needed to confirm this hypothesis.

The dependency of plasmid incorporation efficiency on the scaffold structure represents a major limitation of the current plasmid delivery system. A basic function of the scaffold is to provide a suitable physical structure for new tissue formation, which typically requires a high degree of porosity to support cellular infiltration. The efficient incorporation of plasmid into highly porous scaffolds is limited by the particulate leaching step which can result in the loss of

large quantities of plasmid. However, these studies revealed that alterations to the scaffold structure that increase porosity or improve pore interconnectivity can exacerbate this problem, leading to even greater losses of plasmid during the leaching step. A delivery system that decouples these two design considerations is needed, such that the scaffold structure can be optimized without affecting plasmid incorporation or release. A modified scaffold design was developed to address this limitation, and will be discussed in Chapter 3. Additionally, an absorption-based approach involving the fabrication of cationic microspheres was investigated to create an electrostatic interaction between the scaffold and DNA (**Appendix 6.3**).

Table 2-1
Summary of Results

Microspheres		Scaffold Structure			Transgene Expression	
% PLG	M _w	Pore stability	Tissue infiltration	DNA dose (μg)	Duration	Level
2	high/low blend	collapsed	minimal, only at scaffold periphery	800	105 days	high
				600	at least 56 days	high
				400	at least 28 days	med
				300	<7 days for 3 of 5 mice	low
2	high	intact	minimal, only at scaffold periphery	600	at least 56 days	high
6	high	intact	complete by 2 wks	---	not evaluated*	

*DNA incorporation efficiencies were <20%

Table 2-1. Summary of results.

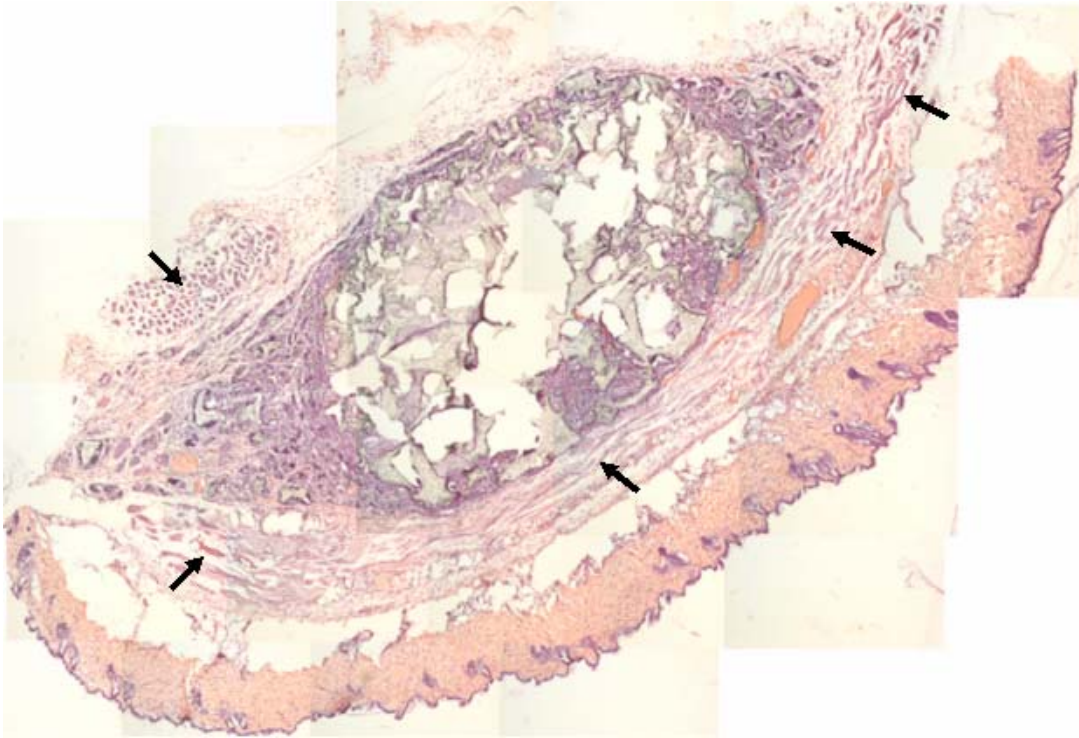


Figure 2-11. Image showing the presence of muscle fibers in tissue immediately adjacent to the scaffold. H&E stained cross-section of a high molecular weight scaffold at 62 days post-implantation (arrows indicate location of longitudinal and transverse muscle fibers).

3. CHAPTER 3: Layered PLG Scaffolds for Plasmid Delivery and Cell Transplantation: *In Vivo* Transgene Expression at an Intraperitoneal Fat Site

3.1. Introduction

The fundamental goal of tissue engineering is to develop novel strategies for the replacement of diseased or injured tissues.¹ Most approaches utilize biomaterials to create a three-dimensional structure, or scaffold, that will support and guide new tissue formation.^{3, 4} Scaffolds are typically fabricated from biocompatible and biodegradable polymers, and exhibit a highly porous structure that allows for cellular infiltration and integration of the scaffold with host tissue. In cell-based therapies, scaffolds can also serve as a platform for delivering transplanted cells to specific sites within the body. A classic paradigm for cell-based therapy is islet transplantation for the treatment for type I diabetes. The disease is caused by an autoimmune destruction of insulin-secreting β cells found within pancreatic islets, rendering patients completely dependent on exogenous insulin. Islet transplantation offers the potential to restore normal blood glucose control in diabetic patients through replacement of their insulin-producing cells. In general, the success of cell transplantation approaches is dependent on the scaffold's ability to create an environment that supports cell survival and promotes their ability to fulfill a given therapeutic function. The creation of such environments will likely not be accomplished simply through the provision of a suitable physical structure; rather, the controlled presentation of specific biological signals will be needed to direct cellular behavior.

Gene delivery from scaffolds offers a versatile approach for manipulating soluble signals present within the local microenvironment, and has the potential to provide prolonged expression of therapeutic proteins.^{11, 12, 80} The versatility arises from the fact that plasmid DNA maintains essentially constant physical properties despite changes in the nucleic acid sequence,⁷⁰ thereby

allowing delivery of multiple genes with a single delivery system. Previous studies have demonstrated that plasmid delivery from both collagen and poly(lactide-co-glycolide) (PLG) scaffolds can achieve localized transfection of cells, with sufficient protein production to stimulate new tissue formation.^{30-33, 81} The duration of transgene expression has been reported to persist for several weeks or even months. However, more studies are needed to determine whether these initial results can be translated to achieve effective gene transfer at a variety of anatomical sites.

In this chapter, the ability of DNA-releasing scaffolds to provide localized transgene expression in the intraperitoneal fat, a model site for cell transplantation,⁸² was investigated. Scaffolds were fabricated using an established gas-foaming/particulate leaching process,^{32, 71, 72} although a modified scaffold design including a non-porous layer was implemented to maximize DNA incorporation efficiency. The *in vivo* transgene expression levels were measured by a luciferase assay for multiple DNA doses, and the distribution and identity of transfected cells were determined by immunohistochemistry. The ability of DNA-releasing scaffolds to induce angiogenesis by providing expression of fibroblast-growth factor-2 (FGF-2) or hypoxia inducible factor-1 α (HIF-1 α) was evaluated using microcomputed tomography. Additionally, the impact of gene delivery on islet function was evaluated by monitoring blood glucose levels in diabetic mice receiving islets transplanted on DNA-releasing scaffolds.

3.2. Materials and Methods

3.2.1. DNA sources

Plasmids were purified from bacteria culture using Qiagen reagents (Santa Clara, CA), and stored in Tris-EDTA (TE) buffer at 4°C. All plasmids used in this study have a CMV promoter. The pLuc plasmid contains the firefly luciferase gene within the pNGVL vector backbone (National Gene Vector Labs, University of Michigan). The pEGFP-C2 plasmid (CLONTECH, Palo Alto, CA) encodes green fluorescent protein. The pFGF-2 plasmid was provided by Dr. Claudia Heilmann (University Hospital Freiburg, Germany), who cloned the cDNA for human fibroblast growth factor-2 (18 kDa) into the pCI-neo expression vector (Promega) between EcoRI and XbaI sites.⁸³ The pHIF-1 α plasmid was constructed by Dr. Navdeep Chandel's Lab (Northwestern University), and contains a degradation-resistant mutant form of HIF-1 α inserted into pcDNA3.1 (Invitrogen) at the BamHI site. The HIF-1 α mutant was generated by modifying the coding sequence of mouse HIF-1 α to achieve two "proline to alanine" exchanges at positions 402 and 564. These two proline residues within the oxygen-dependent-degradation domain (ODDD) have been shown to be crucial for the degradation of wild type HIF-1 α in the absence of hypoxia.⁸⁴⁻⁸⁶

3.2.2. Scaffold fabrication

DNA-loaded scaffolds were fabricated using a previously described gas foaming/particulate leaching process,^{32, 71, 72} with a modified scaffold design containing a non-porous center layer for DNA loading. PLG (75% D,L-lactide/25% glycolide, i.v. = 0.6-0.8 dl/g) (Lakeshore Biomaterials, Birmingham, AL) was dissolved in dichloromethane to make either a

2% (w/w) or 6% (w/w) solution, which was then emulsified in 1% poly(vinyl alcohol) to create microspheres. The scaffold outer layers were constructed by mixing 1.5 mg of 6% PLG microspheres with 50 mg of NaCl (250-425 μm), and then compressing the mixture in a 5 mm KBr die at 1500 psi using a Carver press. To make the center layer, 2 mg of 2% PLG microspheres were reconstituted in a solution containing plasmid (200, 400, or 800 μg) and lactose (1 mg), and then lyophilized. This lyophilized product was then sandwiched between two outer layers and compressed at 200 psi. The composite scaffold was then equilibrated with high pressure CO_2 gas (800 psi) for 16 hrs in a custom made pressure vessel. Afterwards, the pressure was rapidly released over a period of 25 minutes, which serves to fuse adjacent microspheres creating a continuous polymer structure. To remove the salt, each scaffold was leached in 4 mL of water for 2.5 hours while shaking at 110 rpm, with fresh water replacement after 2 hours.

3.2.3. *Scanning electron microscopy (SEM)*

Structural characteristics of scaffolds were imaged with a scanning electron microscope (Hitachi S-3400N-II) using the variable pressure mode and an ESED detector. The microscope was operated at an electron voltage of 15 kV.

3.2.4. *Characterization of DNA incorporation and in vitro release kinetics*

The DNA incorporation efficiency is defined as the mass of DNA left in the scaffold after the leaching step divided by the mass of DNA initially input. Hereafter, the amount of input DNA will be referred to as the dose. After leaching, scaffolds were dissolved in chloroform (600 μL), and the DNA was extracted from the organic solution. TE Buffer (400 μL) was added to the

organic phase, vortexed, and centrifuged at 14,000 rpm for 3 minutes. The aqueous layer was collected, and two more extraction cycles were performed to maximize DNA recovery. The amount of DNA was quantified using a fluorometer and the fluorescent dye Hoechst 33258. To determine the *in vitro* release kinetics of DNA, scaffolds were placed in 500 μ L of phosphate-buffered saline (PBS) (pH 7.4), and the solution was replaced at each time-point. The conformation of the released DNA was analyzed by agarose gel electrophoresis. A digital image of the gel was taken and NIH image software was used to evaluate the fraction of DNA remaining in the supercoiled conformation as previously described.⁸⁷

3.2.5. *Measuring in vivo transgene expression*

Animal studies were performed in accordance with the NIH Guide for the Care and Use of Laboratory Animals, and protocols were approved by the IACUC at Northwestern University. Scaffolds loaded with luciferase-encoding plasmid were sterilized in 70% ethanol, washed in islet growth medium (described in section 2.8) to mimic the cell transplantation procedure, and then implanted into intraperitoneal fat of 10-12 week old C57BL/6 male mice (Jackson Laboratories), as previously described.⁸² At 3, 7, 14, and 21 days post-implantation, scaffolds were retrieved and frozen over dry ice. The frozen tissue samples were cut into small pieces with scissors, immersed in 200 μ L of cell culture lysis reagent (Promega), and placed on a rotator for 30 minutes. Then, samples were snap frozen in liquid nitrogen, thawed in a 37°C water bath, and centrifuged at 14,000 rpm for 10 minutes at 4°C. The supernatant was mixed with luciferase assay reagent (Promega) and luciferase activity was measured with a luminometer using a 10

second integration time. Samples were normalized by total protein amount, which was measured using a BCA protein assay (Pierce Biotechnology Inc., Rockford, IL).

3.2.6. *Histological analysis and immunohistochemistry*

Histological analysis was performed to determine the cellular distribution and identity of transfected cells. Scaffolds loaded with 400 and 800 μg of GFP plasmid were retrieved at 7 and 14 days post-implantation and frozen in an isopentane bath cooled over dry ice. Tissue samples were embedded in OCT and sections were cut at 14 μm thickness using a cryostat. Prior to staining, sections were fixed with 4% paraformaldehyde for 10 min and washed in PBS. The extent of cellular infiltration into scaffolds was visualized by H&E staining of tissue sections at 7 and 14 days. The distribution of transfected cells was determined by performing immunohistochemistry using antibodies directed against green fluorescent protein (GFP). Additionally, antibodies directed against the macrophage surface marker (F4/80) were used to determine if the cell type transfected was macrophages. After blocking, the two primary antibodies (rabbit anti-GFP (Invitrogen) and rat anti-mouse F4/80 (AbD Serotec, Raleigh, NC) were applied for 2 hrs. at room temp., using dilutions of 1:500 and 1:100, respectively. Secondary antibodies (Alexa Fluor 546 nm goat anti-rat (Invitrogen) and Alexa Fluor 488 nm goat anti-rabbit (Invitrogen)) were used to visualize the antigens. Lastly, sections were incubated with Hoechst 33258 (10 mg/ml, 1:2000 dilution) for 5 min. to allow visualization of cell nuclei. Additionally, flow cytometry was used to quantify the percentage of F4/80⁺ macrophages present within scaffolds as a function of time (**Appendix 6.4.**).

3.2.7. Evaluation of angiogenesis using microcomputed tomography

A previously described method for contrast-enhanced microcomputed tomography (μ CT) was used to analyze blood vessel formation within scaffolds delivering DNA encoding angiogenic proteins.⁸⁸ Scaffolds loaded with 800 μ g of pFGF-2 or pHIF1- α were implanted into the intraperitoneal fat site as described above, and angiogenesis was evaluated at 2 and 4 weeks. Additionally, scaffolds loaded with recombinant VEGF protein were examined for their ability to induce vascular growth at the subcutaneous site (**Appendix 6.5.**). To prepare samples for μ CT imaging, animals were deeply anesthetized by an intraperitoneal injection of tribromoethanol and placed ventral side up on a perfusion tray. The thoracic cavity was opened and a 21 gauge needle was inserted into the left ventricle and secured in place. The right atrium was cut and a peristaltic pump was used to flush the vasculature with 25 ml of normal saline containing heparin sodium (10 U/ml) at a rate of \sim 5 ml/min. The specimen was then fixed by perfusion with 75 ml of 4% paraformaldehyde. The fixative was subsequently flushed from the vasculature with heparinized saline. A radiopaque silicone rubber compound containing lead chromate (Microfil MV-122, Flow Tech Inc, Carver, MA) was then manually injected into the vasculature. Specimens were stored at 4 °C overnight to allow for polymerization of the compound, and then tissue samples were surgically retrieved. Samples were stored in 4% paraformaldehyde at 4 °C until imaging.

Samples were imaged using a Scanco Micro-CT 40 system (Basserdorf, Switzerland) operated at a voltage of 45 kV and current of 88 μ A. Samples were scanned in a 16.4 mm diameter sample holder at high resolution, creating a 2,048 x 2,048 pixel image matrix and an isotropic voxel (volume element) size of \sim 8 μ m. Each scan consisted of 160 slices through the center of the sample. Reconstructed serial slices were globally thresholded based on X-ray

attenuation and used to create 3-D renderings of the vascular networks. The same threshold (200) was used for all samples. The vascular volume fraction was calculated directly from the 3-D renderings, based on the voxel size and the number of segmented voxels in the 3-D image. The distribution of vessel diameters was calculated using a model-independent method for assessing thickness in 3-D images.⁸⁹

3.2.8. *Islet transplantation*

Diabetes was chemically induced in male C57BL/6 mice (10-12 weeks old) by an intraperitoneal injection of 220 mg/kg streptozotocin (Sigma Aldrich, St. Louis, MO). Blood glucose levels were measured from tail vein samples using a One Touch Basic glucose monitor (Lifescan, Milpitas, CA), and mice with blood glucose levels of > 300 mg/dl on consecutive days were considered diabetic.

Islets were isolated from healthy male C57BL/6 mice as previously described.^{82, 90, 91} Donor mice were anesthetized with an intraperitoneal injection of tribromoethanol. The peritoneal cavity was opened with a midline abdominal incision, and the common bile duct was cannulated and injected with collagenase (type XI; Sigma, St. Louis, MO) in Hank's balanced salt solution. The pancreas was removed by dissection, and digested at 37°C for 15 min. The digested tissue was then filtered through a mesh screen, and the filtrate added to a discontinuous dextran (Sigma) gradient. Islets were collected and counted under a microscope.

Scaffolds were sterilized in 70% ethanol and washed in islet growth medium (RPMI-1640 medium (Gibco-BRL, Grand Island, NY) supplemented with 10% heat inactivated fetal calf serum (Hyclone, Logan, UT), 100 U/ml penicillin-G, 100 mg/ml streptomycin sulfate, and 1

mmol/L L-glutamine) in preparation for the seeding of purified islets. Islets were applied in a minimal volume of medium onto the surface of the microporous scaffold. The scaffolds were incubated for 15 min. at 37°C in 5% CO₂ and 95% air. At that time, ~20 µl of medium was added and scaffolds were incubated for another 15 min. Scaffolds were then immediately transplanted into intraperitoneal fat of diabetic mice.

3.2.9. *Statistical Analysis*

Values are reported as the mean \pm standard deviation. Statistical calculations were performed using JMP 4.0.4 software (SAS Institute, Cary, NC). P values were determined by a t-test.

3.3. Results

3.3.1. *Layered scaffold design*

A layered scaffold design was developed to facilitate the efficient incorporation of large quantities of plasmid, while retaining the open pore structure for cell transplantation. The design consists of a thin, non-porous center layer that is sandwiched between two highly porous outer layers (**Fig. 3-1A-C**). The center layer is used for plasmid delivery, while the outer layers provide a platform for cell-seeding and support tissue infiltration. By constructing a scaffold with different layers, the design requirements for the physical structure (i.e. outer layers) were decoupled from the delivery system (i.e. center layer).

3.3.2. DNA incorporation and in vitro release kinetics

The layered scaffold design substantially improved DNA incorporation efficiency relative to previous reports of scaffolds made with the gas foaming/particulate leaching process.^{32, 33} The incorporation efficiencies for 200 and 400 μg of DNA were $76.8 \pm 4.9\%$ and $75.7 \pm 4.5\%$, respectively (**Table 3-1**). For 800 μg of DNA, the incorporation efficiency was further increased to $86.8 \pm 6.3\%$ (**Table 3-1**), which was significantly higher than the other two doses ($P < 0.05$). In characterizing DNA release, a large initial burst was observed within the first 3 days, although the magnitude of the burst increased with increasing dose (**Fig. 3-2A**). The initial bursts were equal to $73.3 \pm 2.4\%$, $83.6 \pm 1\%$, and $89.9 \pm 2.5\%$ for the 200 μg , 400 μg , and 800 μg doses, respectively (**Fig. 3-2A**). Following the initial burst, a sustained DNA release was observed for up to 2 weeks (**Fig. 3-2A**). Overall, the DNA release profiles obtained here are similar to those previously reported.^{32, 33} Increasing the mass of polymer contained in the center layer above 2 mg (up to 5 mg) did not further improve the incorporation efficiency or slow the rate of DNA release (**Appendix 6.6**). Analysis by agarose gel electrophoresis confirmed that a large proportion of released DNA remains in the supercoiled conformation, although there is a gradual increase in the conversion to nicked and linear conformations as time progresses (**Fig. 3-2B, Table 3-2**).

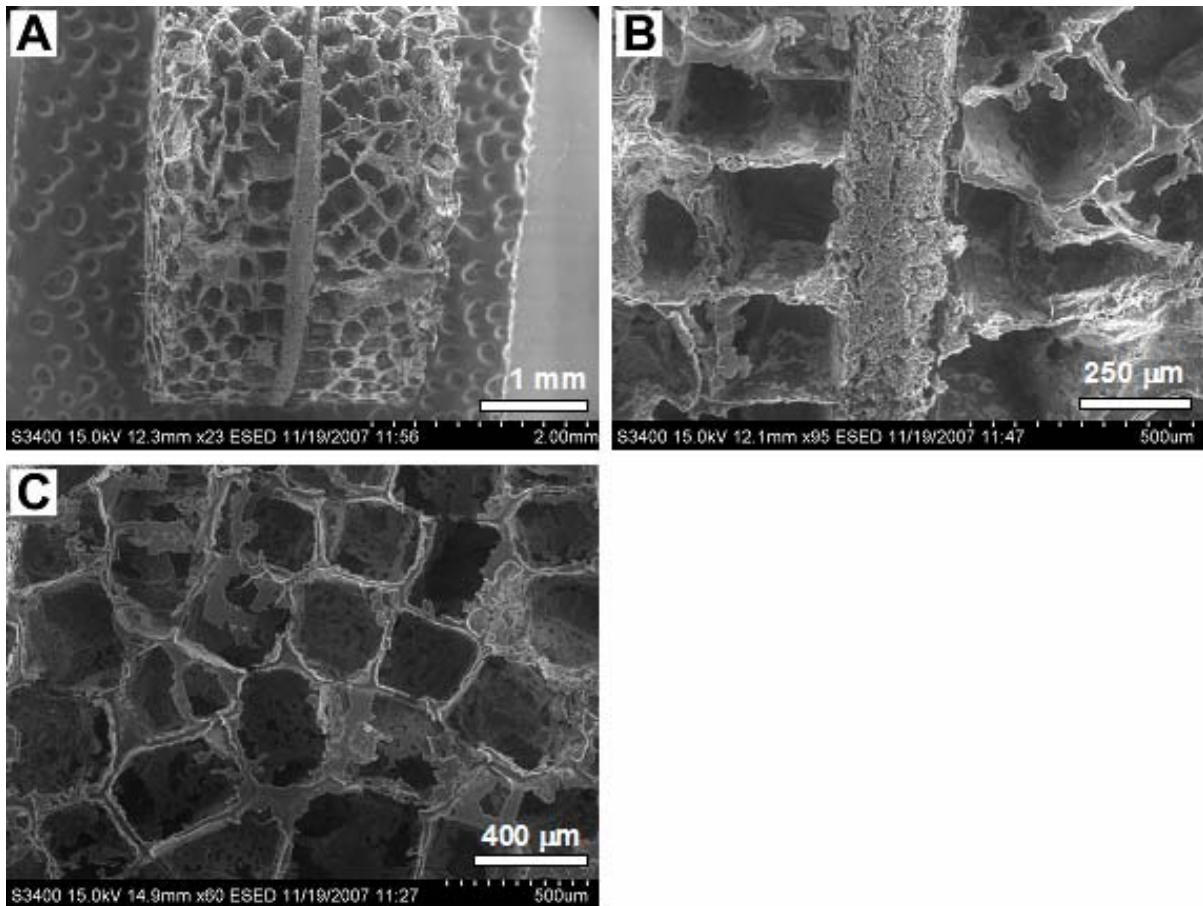


Figure 3-1. Scanning electron micrographs of a layered PLG scaffold. (A) Side view of the composite scaffold. Scale bar equals 1 mm. (B) Magnified view of the center layer. Scale bar equals 250 μm. (C) Magnified view of the pore structure in the outer layer. Scale bar equals 400 μm.

Table 1
DNA incorporation efficiency

Input DNA (μg)	Incorporated DNA (μg)	Incorporation efficiency (%)
200	153.7 ± 9.8	76.8 ± 4.9
400	302.7 ± 17.8	75.7 ± 4.5
800	694.5 ± 50.1	86.8 ± 6.3

Table 3-1. DNA incorporation efficiency for scaffolds loaded with different amounts of DNA.

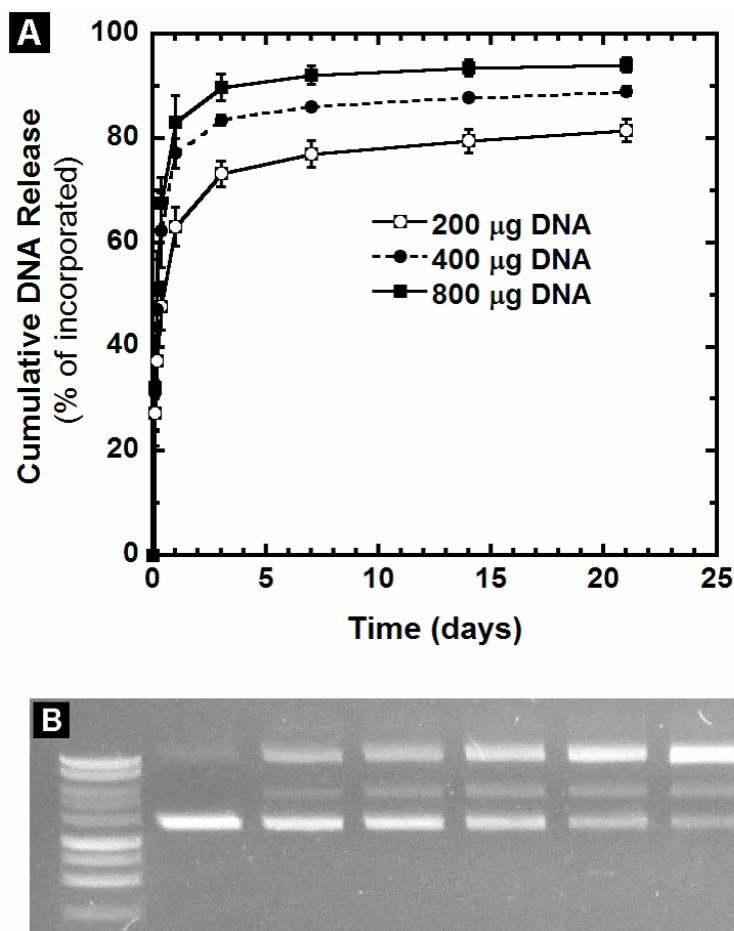


Figure 3-2. *In vitro* DNA release kinetics and agarose gel electrophoresis. (A) Cumulative DNA release from scaffolds loaded with 200, 400, or 800 µg of plasmid (n=4 per dose) (B) Image of an agarose gel containing DNA released from a scaffold at different times. Lane 1, molecular weight marker. Lane 2, unincorporated plasmid. Lanes 3-7: DNA released at days 1, 3, 7, 14, and 21, respectively.

Table 2

Conformational analysis of plasmid DNA released from scaffolds

Lane	Sample	Nicked (%)	Linear (%)	Supercoiled (%)
1	molecular weight marker	--	--	--
2	unincorporated DNA	14.7	0.0	85.3
3	DNA released between 8-24 hrs	36.3	10.3	53.5
4	DNA released between 1-3 days	38.2	14.4	47.4
5	DNA released between 3-7 days	45.8	16.1	38.2
6	DNA released between 7-14 days	53.9	16.9	29.2
7	DNA released between 14-21 days	61.8	17.1	21.1

Table 3-2. Conformational analysis of plasmid released from scaffolds.

3.3.3. *In vivo* transgene expression

The ability of DNA-releasing scaffolds to promote *in vivo* gene transfer at the intraperitoneal fat site was evaluated for a range of DNA doses. For all doses tested (200, 400, and 800 μg), a general trend was observed where transgene expression levels peaked during the first few days and then declined substantially over a period of 1-2 weeks (**Fig. 3-3**). The DNA dose had little effect on transgene expression levels at day 3, as all doses had similarly robust levels of expression (**Fig. 3-3**). This result indicates that the amount of DNA initially released is not a limiting factor in gene transfer for any of the doses tested (**Fig. 3-3**). At days 7 and 14, the 400 and 800 μg doses resulted in higher levels of transgene expression relative to the 200 μg dose (**Fig. 3-3**), indicating that delivery of increased quantities of DNA may help to sustain expression. However, transgene expression decreased to background levels in most animals by 21 days. Also noteworthy is the fact that the 400 and 800 μg doses provided similar expression levels at all time-points, suggesting a threshold above which further increases in dose do not increase expression (**Fig. 3-3**). Non-layered scaffolds described in chapter 2 were also evaluated for their ability to promote gene transfer at the intraperitoneal fat site, but displayed similar kinetics of transgene expression compared to layered scaffolds (**Appendix 6.7**).

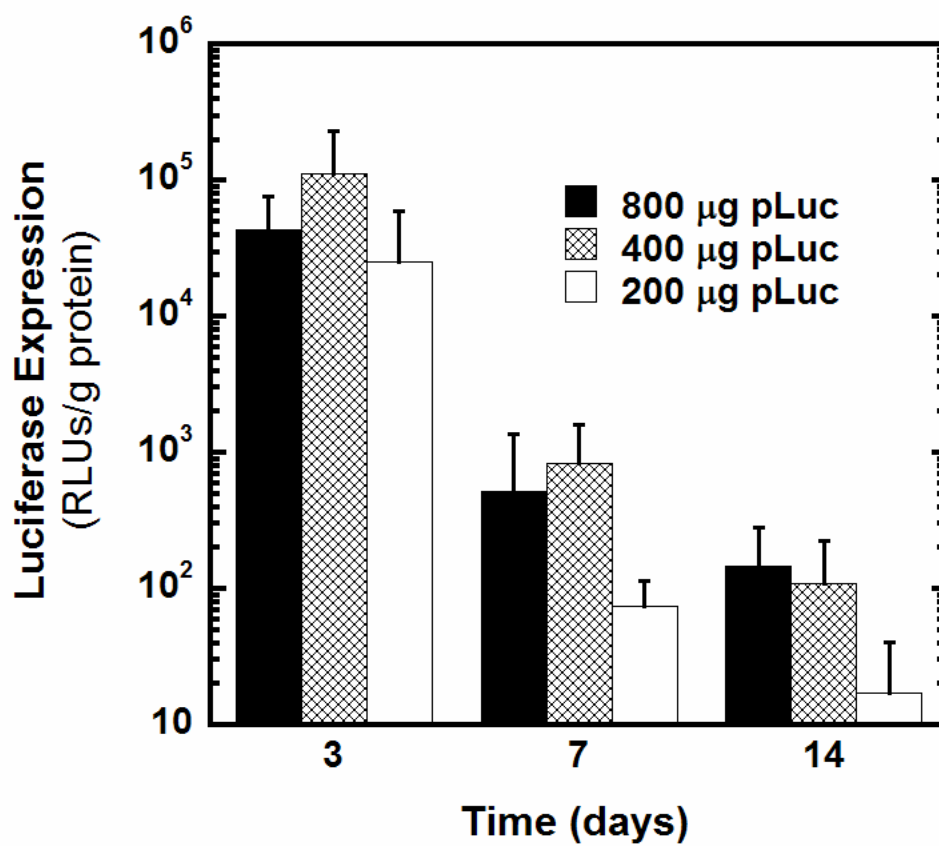


Figure 3-3. *In vivo* luciferase transgene expression for scaffolds loaded with 200, 400, or 800 µg of pLuc (n=4 per dose per timepoint).

3.3.4. *Histological analysis and immunohistochemistry*

The scaffold's outer layers provided a suitable physical structure that supported cellular infiltration, as shown by H&E staining at days 7 and 14 (**Fig. 3-4A,B**). Immunohistochemical staining was performed to determine the distribution and identity of transfected cells. Scaffolds loaded with 400 or 800 μg of GFP-encoding plasmid were retrieved at 7 and 14 days, and stained with antibodies directed against GFP (transgene product) and F4/80 (macrophage surface marker). Staining results were similar for both doses and time points. Low magnification images taken at the interface of the scaffold with surrounding adipose tissue demonstrate the presence of GFP⁺ transfected cells (green) and macrophages (red) in both regions (**Fig. 3-5A-C**). Higher magnification images focusing on the surrounding adipose tissue clearly indicate co-localization of GFP and F4/80 staining (yellow), revealing that a large number of the transfected cells are macrophages (**Fig. 3-5D-F**). Similarly, higher magnification images focusing on a region within the scaffold show co-localization of GFP and F4/80 staining immediately adjacent to the polymer, demonstrating that macrophages are the primary cell type transfected and revealing their propensity to align at the polymer surface (**Fig. 3-5G-I**). The presence of transfected cells immediately adjacent to the polymer surface has been observed previously,³³ although here we have identified them as macrophages.

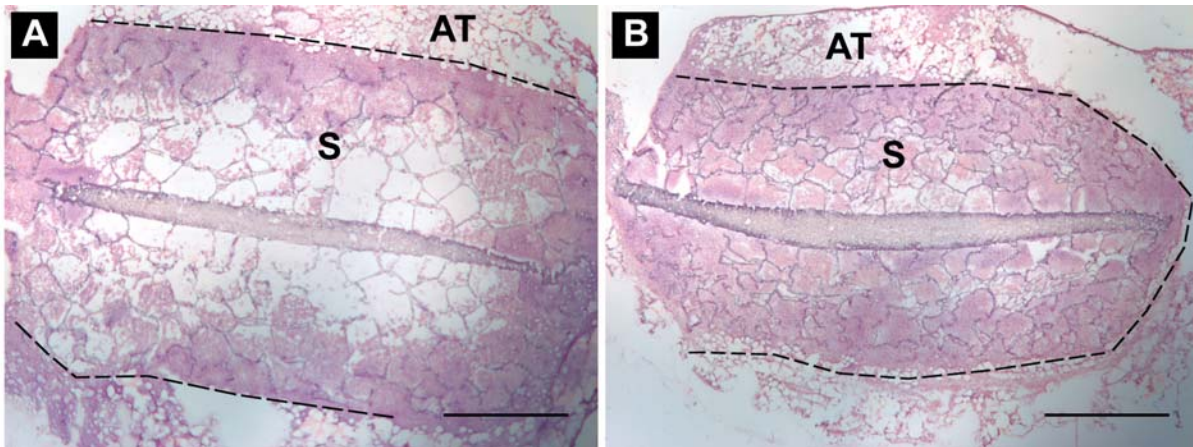


Figure 3-4. H&E staining of cellular infiltration into outer layers of scaffolds. Scaffold cross-section at (A) day 7 and (B) day 14. 25x magnification, scale bars equal 1 mm. Labels indicate adipose tissue (AT) and scaffold (S). Dashed line indicates interface of scaffold edges with surrounding tissue.

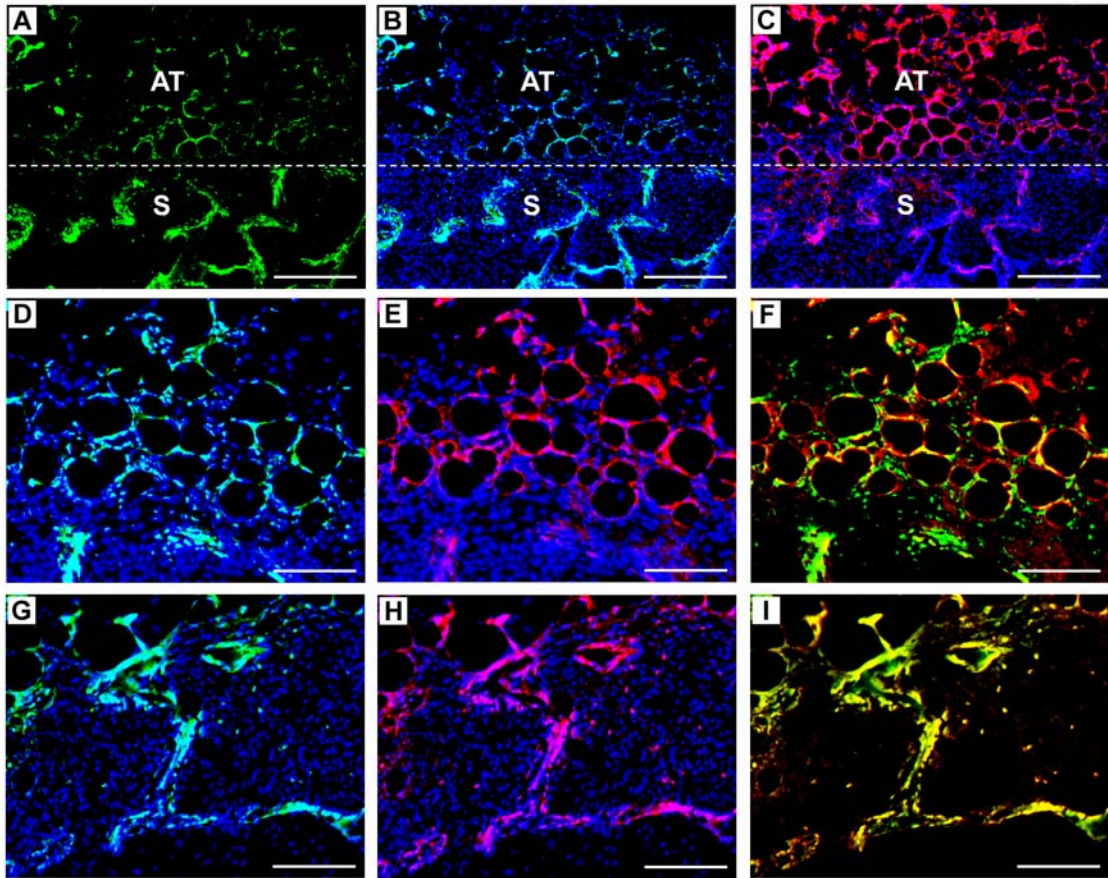


Figure 3-5. Immunohistochemical staining to determine the distribution and identity of transfected cells. Images were taken from a scaffold loaded with 400 μg of GFP plasmid that was retrieved after 7 days. For (A-C), 100x magnification images were captured at the interface of the scaffold with surrounding adipose tissue (scale bars equal 200 μm). (A) GFP antibody staining. (B) GFP antibody staining with Hoechst staining for cell nuclei. (C). F4/80 (macrophage) antibody staining with Hoechst. “S” indicates scaffold region, “AT” indicates adipose tissue, and dashed line indicates interface. For (D-F), 200x magnification images were captured in adipose tissue outside scaffold (scale bars equal 100 μm). (D) GFP antibody staining with Hoechst. (E) F4/80 antibody staining with Hoechst. (F) GFP antibody and F4/80 antibody staining. Yellow indicates co-localization of GFP and F4/80, and thus transfected macrophages. For (G-I), 200x magnification images were captured within the scaffold (scale bars equal 100 μm). (G) GFP antibody staining with Hoechst. (H) F4/80 antibody staining with Hoechst. (I) GFP and F4/80 antibody staining.

3.3.5. Angiogenesis

Scaffolds releasing plasmid encoding FGF-2 or HIF1- α were evaluated for their ability to induce new blood vessel formation. Angiogenesis is a critical component of cell transplantation approaches, where the establishment of a sufficient vascular supply is required to support cell survival. Microcomputed tomography was used for three-dimensional visualization and quantitative analysis of the vascular networks formed within scaffolds at 2 and 4 weeks post-implantation. At 2 weeks, scaffolds releasing pFGF-2 provided a 40% increase in the total vascular volume fraction relative to controls ($P < 0.01$), while no effect was observed with the pHIF-1 α scaffolds at this time-point (**Fig. 3-6A**). This moderate increase in vascularization for the pFGF-2 scaffolds was also apparent in the 3-D renderings (**Fig. 3-7A,C,E**). A histogram showing the distribution of vessel diameters demonstrated a significant increase in the presence of larger vessels ($>200 \mu\text{m}$) for the FGF-2 scaffolds relative to controls ($P < 0.05$, **Fig. 3-6B**). This result indicates that the increase in vascular volume fraction for FGF-2 scaffolds was partly the result of an increase in vessel sizes. From 2 to 4 weeks, the vascular volume fraction decreased by 50% for pFGF-2 scaffolds and 60% for control scaffolds, indicating regression of initially formed blood vessels (**Fig. 3-6A**). This decrease in vascularization can also be visualized in the 3-D renderings (**Fig. 3-7A-D**). Although reasons for the decreased vascular volume fractions at 4 weeks are not known, it may be related to a subsiding inflammatory response due to partial scaffold resorption and integration with host tissue. In contrast, the vascular volume fraction for pHIF-1 α scaffolds was similar or perhaps higher at 4 weeks relative to 2 weeks, indicating HIF-1 α treatment may counteract the vessel regression (**Fig. 3-6A, Fig. 3-**

7E,F). Also, at 4 weeks, the vascular volume fractions for pHIF-1 α scaffolds were significantly higher than controls ($P < 0.05$, Fig. 3-6A).

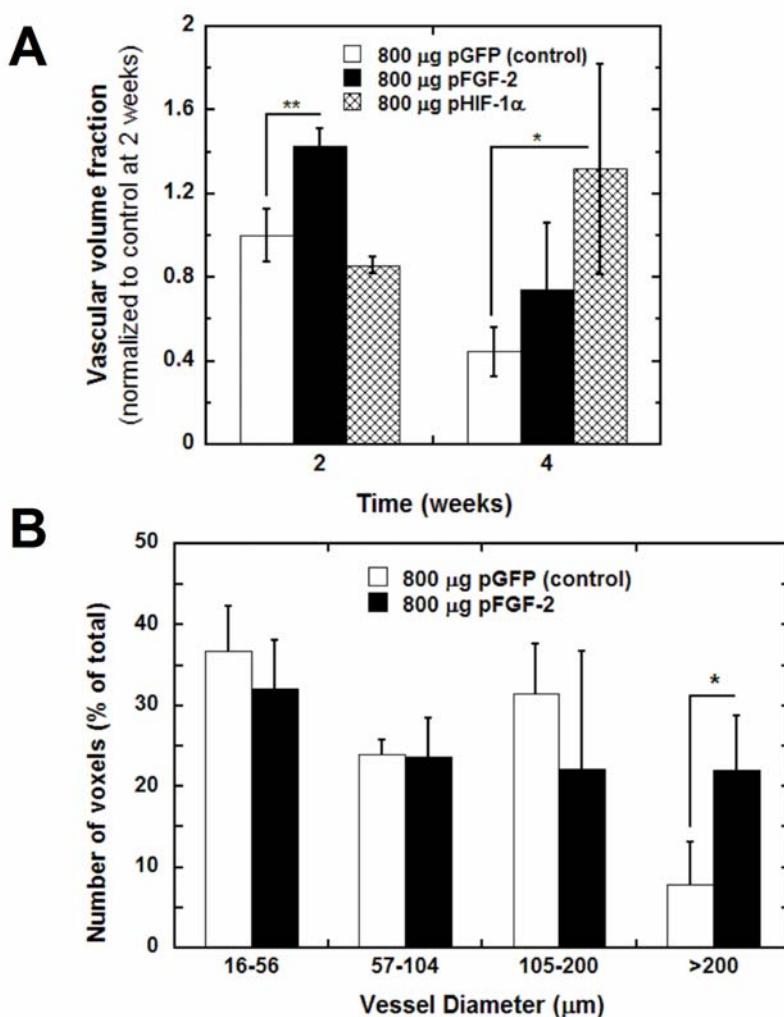


Figure 3-6. Quantitative analysis of angiogenesis by microcomputed tomography. (A) Total vascular volume fraction for scaffolds releasing pFGF-2, pHIF-1 α , or pGFP (control) ($n=3$ per condition, per time-point). (B) Histogram of vessel diameters for FGF-2 and control scaffolds at 2 weeks. ** $P < 0.01$, * $P < 0.05$.

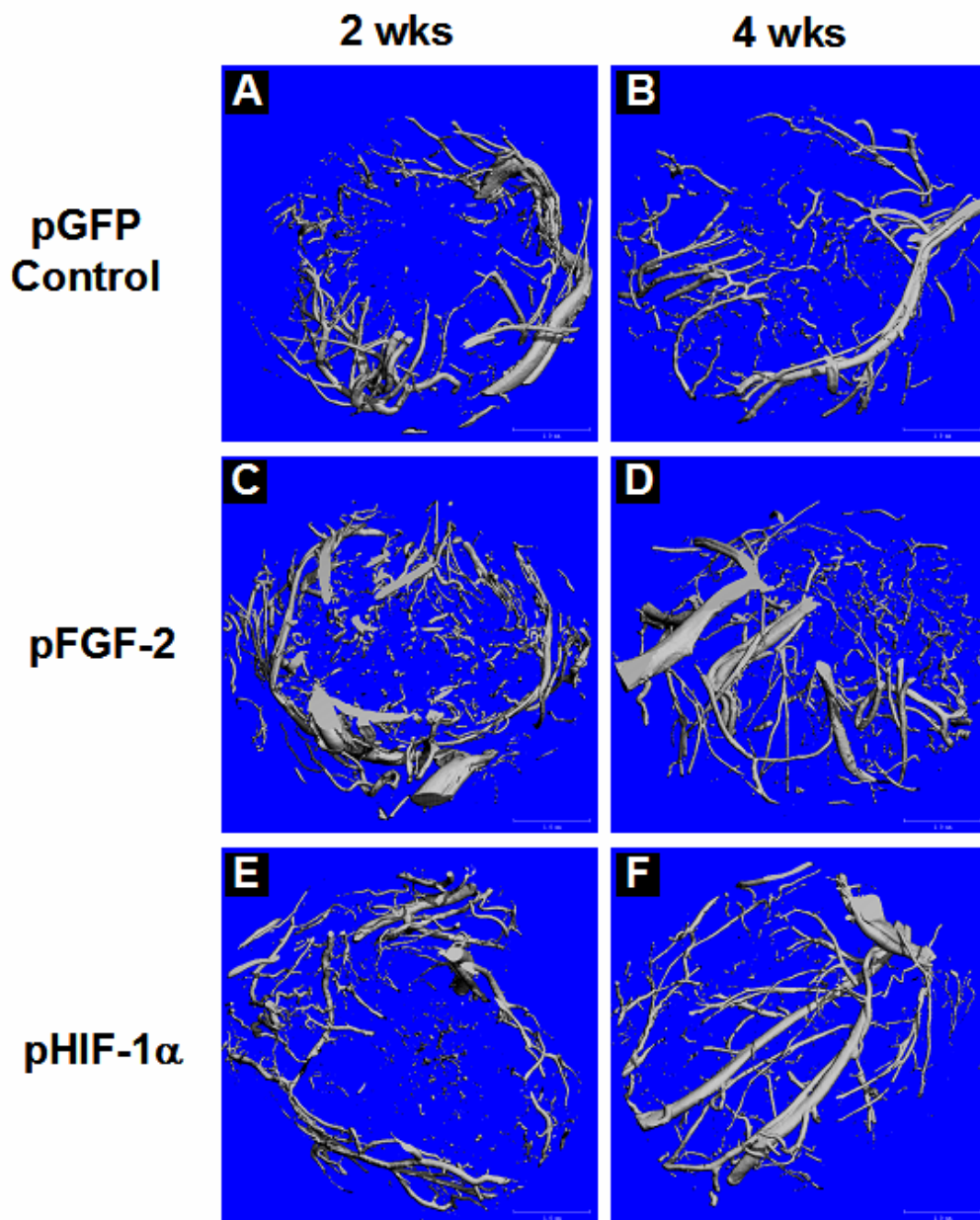


Figure 3-7. Microcomputed tomography 3-D renderings of vascular networks. (A,B) control scaffolds at 2 and 4 weeks. (C,D) pFGF-2 scaffolds at 2 and 4 weeks. (E,F) pHIF-1 α scaffolds at 2 and 4 weeks.

3.3.6. Islet transplantation

We have previously established the ability of microporous PLG scaffolds to support islet transplantation at the intraperitoneal fat site,⁸² but the effect of plasmid delivery on islet function has not been tested. To address this question, 175 islets were transplanted on scaffolds loaded with 400 μg of GFP plasmid or control scaffolds containing no DNA, and blood glucose levels were monitored over time to evaluate graft function. The mean blood glucose levels were found to be similar for both conditions, suggesting no difference in islet function (**Fig. 3-8**).

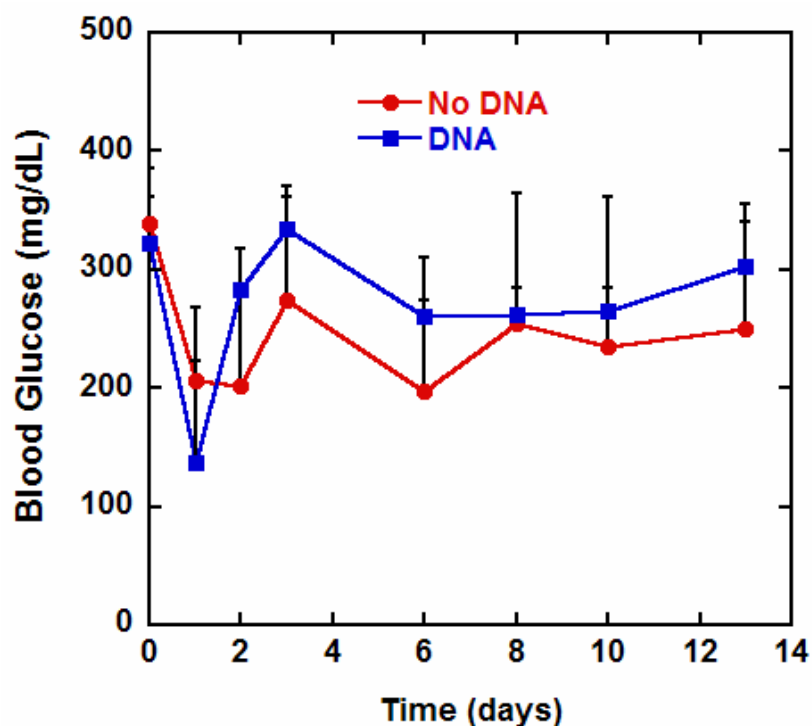


Figure 3-8. Blood glucose levels of mice receiving 175 islets transplanted on scaffolds loaded with 400 μg of GFP plasmid or no DNA. Red circles indicate control scaffolds without DNA, and blue squares indicate scaffolds with DNA. Values represent averages \pm standard errors (n=3 scaffolds per condition).

3.4. Discussion

In this chapter, a novel layered scaffold design was developed to facilitate efficient incorporation of large quantities of plasmid. These scaffolds were evaluated for their ability to promote *in vivo* gene transfer following implantation into intraperitoneal fat, a model site for cell transplantation. All DNA doses (200, 400, and 800 μg) provided similarly robust levels of expression at day 3, indicating that the amount of DNA initially released was not a limiting factor. However, a substantial decline in transgene expression was observed from days 3 to 7 for all doses. This rapid drop in expression represents a common obstacle encountered with *in vivo* administration of plasmid.⁷⁷ Increasing the DNA dose had only a modest effect on prolonging transgene expression. Although the levels of reporter gene expression were decreased at days 7 and 14, immunohistochemical analysis demonstrated the presence of abundant transfected cells both within the scaffold and in the surrounding adipose tissue. A large number of the transfected cells were identified as macrophages. Scaffolds delivering FGF-2 plasmid stimulated a modest increase in vascularization at 2 weeks relative to control scaffolds, indicating that transgene expression levels, at least initially, were physiologically relevant. However, by 4 weeks, a substantial decline in vascularization was observed for both FGF-2 and control scaffolds, indicating regression of initially formed vessels. In contrast, scaffolds delivering HIF-1 α plasmid did not show any decrease in vascularization from 2 to 4 weeks.

The kinetics of *in vivo* transgene expression obtained in this study are consistent with those typically seen for the human cytomegalovirus (CMV) promoter, where expression peaks within the first few days and declines rapidly over 1-2 weeks.⁹² Reasons for this rapid inactivation are not well understood, although several possibilities have been suggested including

cytokine-mediated inhibition,⁹³ binding of repressor proteins,⁹⁴ methylation,⁹⁵ or loss of a positive activator.⁹⁶ In some cases, the use of alternative promoters has allowed for more sustained gene expression.⁹² Thus, the continued design of synthetic or custom promoters may facilitate sustained transgene expression at appropriate levels. Additionally, modification of the plasmid vector through depletion of CpG motifs has shown the potential to provide more prolonged transgene expression.⁹⁷ The kinetics of plasmid delivery may also play an important role in determining the duration of gene expression. The rapid plasmid release observed here likely provides an excess amount of plasmid initially, yet insufficient quantities of plasmid at later times. A more sustained release profile may extend transgene expression by maintaining higher concentrations of the vector over time, thereby allowing for continued cellular transfection. Decreasing the burst effect is also desirable from the perspective of an inflammatory response, as large quantities of bacterially derived plasmid are known to activate inflammatory cells due to the presence of unmethylated CpG sequences. The rate of DNA release can be slowed by encapsulating DNA within polymer microspheres, and fabricating scaffolds from these DNA-loaded microspheres.^{81, 98, 99} However, the amount of DNA that can be delivered with this approach is limited based on the loading capacity of the microspheres and the amount of polymer required to make the scaffold (i.e. scaffold size). An alternative approach for slowing plasmid release is to include cationic microspheres within the center layer to create an electrostatic interaction with the plasmid, and thereby modulate the release kinetics (**Appendix 6.3**). Overall, more studies are needed to establish the appropriate plasmid doses and release kinetics that maximize the extent and duration of transgene expression.

A large number of transfected cells at the intraperitoneal fat site were identified as macrophages using immunohistochemistry. Previous studies investigating DNA delivery at other sites have typically implicated either fibroblasts or endothelial cells as the cell types responsible for expressing the plasmid.^{30, 81} The transfection of macrophages has been shown to involve a specific transport mechanism for the uptake of plasmid, involving scavenger receptors that recognize a variety of anionic macromolecules.^{100, 101} Although much of the internalized DNA is degraded in endosomal compartments, studies have demonstrated that some remains in an intact form and reaches the nucleus to be expressed especially when delivered in high concentrations.¹⁰² In a study investigating delivery of plasmid from a polymer-coated stent, *in vivo* transfection of macrophages was observed at 7 days after implantation.¹⁰³ Efficient *ex vivo* transfection of primary macrophages has also been demonstrated using gelatin particles complexed with plasmid.¹⁰⁴ An important implication for the transfection of macrophages is their potential to provide long-term transgene expression, since they are essentially non-dividing and are known to have long life-spans up to several months.¹⁰⁵ Also, macrophages are part of the normal inflammatory response following implantation of a biomaterial, and will be present regardless of the implant site. Thus, macrophages represent a widely applicable target for gene transfer. However, the intensity and duration of the inflammatory response may be closely related to the transfection profile obtained. The fact that transfected macrophages were observed within the scaffold pores immediately adjacent to the polymer surface is also an interesting finding. Although this same observation was noted in a previous report, it was hypothesized that cellular transfection preferentially occurs near the polymer surface because the concentration of DNA would be highest there (given that plasmid was distributed throughout the entire

scaffold).³³ However, in the current study all of the plasmid is loaded into the center layer, so the highest concentration of DNA would be found at the surface of this layer, not at the surface of the pores in the outer layers. Thus, the initial hypothesis does not fit here. Instead, the presence of transfected cells next to the polymer surface may be related to the propensity of macrophages to attach to the surface of a biomaterial.¹⁰⁶

4. CHAPTER 4: Exendin-4 Releasing Scaffolds for Islet Transplantation

4.1. Introduction

Type I diabetes is an autoimmune disease that destroys insulin-secreting β -cells within the pancreas, resulting in an absolute insulin deficiency.¹⁰⁷ An estimated 1 million people in North America have type I diabetes and approximately 30,000 new cases are diagnosed each year, with prevalence rates rising annually.^{107, 108} Although intensive insulin treatment significantly delays the development and progression of secondary complications (e.g. kidney failure, blindness), it does not perfectly recreate normal blood glucose regulation and greatly increases the risk of severe hypoglycemic events.^{15, 39} As a result, the replacement of a patient's insulin-producing β -cells via islet transplantation has been pursued as a means to restore normal blood glucose control.

Recent successes in clinical islet transplantation using the Edmonton protocol have demonstrated the feasibility of this approach,^{13, 14, 40} although several major problems remain including the need for multiple transplants to achieve euglycemia and progressive islet failure over time.¹⁶ Although reasons for these problems are unclear, the requirement for multiple transplants likely reflects an early loss of functional islet mass caused by disruption of the islet's native microenvironment during isolation (i.e. loss of cell-matrix interactions and vascular connections).^{41, 45, 49, 109} Additionally, the current practice of transplanting islets into the liver may contribute to islet failure by exposing them to high levels of circulating toxins and placing them in immediate proximity of resident macrophages.^{34, 110} Recognition of the potential importance of environmental factors on islet survival and function has increased interest in the

exploration of alternative transplant sites, and the development of strategies to improve the microenvironment of transplanted islets.¹¹⁰

Tissue engineering scaffolds capable of controlled drug delivery may offer a powerful tool for creating a supportive environment that will promote islet survival and function. Scaffolds are commonly employed in tissue engineering applications as platforms for cell transplantation, providing a support for cell attachment and maintaining a three-dimensional structure to guide new tissue formation.⁴ Fundamental design requirements for scaffolds include biocompatibility, biodegradability, and adequate mechanical strength. Also, scaffolds typically have porous structures to (i) provide a large surface area-to-volume ratio for high-density cell-seeding, (ii) promote nutrient and waste transport, and (iii) support cellular infiltration and integration of the scaffold with host tissue.⁴ The development of a vascular network throughout the three-dimensional space is crucial for supporting the survival of transplanted cells and newly formed tissues. In addition to providing a suitable physical structure, scaffolds can be designed to deliver bioactive proteins that will bind to cell surface receptors and initiate specific cellular processes. The delivered proteins can act on cells in the surrounding tissue to increase vascularization, or they can act directly on the islet cells to prevent apoptosis, promote function, and/or stimulate proliferation.

Exendin-4 is a 39 amino acid peptide originally isolated from the Gila monster lizard that exhibits several anti-diabetic actions of the mammalian hormone glucagon-like peptide-1 (GLP-1).¹¹¹⁻¹¹³ GLP-1 has been shown to stimulate β -cell proliferation,¹¹⁴ inhibit apoptosis,¹¹⁵ and increase glucose-stimulated insulin secretion.¹¹⁶ However, GLP-1 has a short circulating half-life of < 2 minutes that greatly limits its potential as a therapeutic target.¹¹³ Exendin-4 shares 53%

sequence homology to GLP-1 and acts as a GLP-1 receptor agonist; but, unlike GLP-1, exendin-4 exhibits an extended half-life of ~4 hours making it a more effective therapeutic target.^{112, 113} As a result, researchers have begun to investigate exendin-4 treatment as a means to promote the function of transplanted islets. A recent study demonstrated that daily intra-peritoneal injections of exendin-4 for one week substantially improved metabolic control following transplantation of rat islets into diabetic athymic mice, where 88% of treated mice maintained functioning grafts compared to only 22% of untreated mice.¹¹⁷ We hypothesize that controlled delivery of exendin-4 from polymer scaffolds will maximize the therapeutic benefit by maintaining high concentrations of the peptide within the immediate islet microenvironment for extended periods of time.

In this chapter, scaffolds were designed for controlled delivery of exendin-4 and evaluated for their ability to improve the outcome of islet transplantation in a syngeneic mouse model. Poly(D,L-lactide-co-glycolide) (PLG) scaffolds were fabricated using an established gas foaming/particulate leaching procedure.^{71, 72} Exendin-4 was encapsulated inside PLG microspheres using a double emulsion process, and protein-loaded microspheres were used to fabricate the scaffolds. Iodinated exendin was used to determine protein encapsulation efficiency and release kinetics for a range of polymer formulations. Islets were then transplanted on exendin-4 releasing scaffolds, and blood glucose levels were monitored over time to evaluate the impact of sustained exendin-4 delivery on islet graft function.

4.2. Materials and Methods

4.2.1. Materials

PLG (75/25 mole ratio of D,L-lactide to glycolide, i.v. = 0.6-0.8 dl/g) and (50/50 mole ratio of D,L-lactide to glycolide, i.v. = 0.4-0.5 dl/g) were purchased from Lakeshore Biomaterials (Birmingham, AL). PLG (75/25 mole ratio of D,L-lactide to glycolide, i.v. = 0.16-0.24 dl/g) was purchased from Boehringer Ingelheim (Petersburg, VA). Exendin-4 was purchased from AnaSpec (San Jose, CA). Iodinated exendin was purchased from Perkin Elmer (Boston, MA).

4.2.2. Encapsulation of exendin-4 inside PLG microspheres

Exendin-4 was encapsulated inside PLG microspheres using a double emulsion procedure. Different PLG formulations were dissolved in dichloromethane to make either 3% or 6% (w/w) solutions. An aqueous protein solution (total volume = 17 μ L) containing 73 μ g of exendin-4, 700 μ g of bovine serum albumin (BSA), 50 mg/mL sucrose, and 3% wt. MgCO_3 /wt. BSA²³ was also prepared. The first emulsion was created by adding 500 μ L of the PLG solution to the aqueous protein solution, and sonicating for 15 seconds at 40 W over ice. The first emulsion was then poured into 25 mL of 5% poly(vinyl alcohol) (PVA) (with 50 mg/mL sucrose) and homogenized for 45 seconds to form the second emulsion. Lastly, the second emulsion was poured into 15 mL of 1% PVA (with 50 mg/mL sucrose) and stirred for 1.5 hours to allow evaporation of dichloromethane. Microspheres were washed with water, centrifuged at 4000 rpm for 10 min, and then frozen in liquid nitrogen and lyophilized overnight.

4.2.3. *Fabrication of exendin-4 loaded scaffolds*

PLG scaffolds were fabricated using an established gas foaming/particulate leaching procedure.^{71, 72} However, exendin-4 loaded microspheres were incorporated into scaffolds using two different structural designs (i.e. traditional and layered). First, for the traditional scaffold design, exendin-4 loaded microspheres were distributed throughout the entire three-dimensional polymer structure. In this case, exendin-4 loaded microspheres (3.7 mg) were mixed with NaCl particles (100 mg, $250\ \mu\text{m} < d < 425\ \mu\text{m}$) in the presence of 0.5 μL of water, and then compressed in a 5 mm KBr die at 1500 psi using a Carver press. The resulting construct was equilibrated with CO_2 (800 psi) for 16 hours in a custom-made pressure vessel. Afterwards, the pressure was rapidly released over a period of 25 minutes, which serves to fuse adjacent microspheres creating a continuous polymer structure. To remove the salt, scaffolds were immersed in water for 3 hours, with fresh water replacement after 2 hours.

For the layered design (described in Chapter 3), exendin-4 loaded microspheres were packed into a thin center layer that was sandwiched between two highly porous outer layers. The outer layers were fabricated by mixing 1.5 mg of empty microspheres (for release kinetics) or exendin-4 loaded microspheres (for islet transplantation) with 50 mg of NaCl particles ($\mu\text{m} < d < 425\ \mu\text{m}$). Then, 2 mg of exendin-4 loaded microspheres were compressed between two outer layers, and the composite scaffold was processed as described above.

4.2.4. *Characterization of release kinetics*

To characterize protein release kinetics from scaffolds, iodinated exendin was encapsulated inside PLG microspheres, and the resulting radioactive microspheres were used to

fabricate scaffolds. After leaching, scaffolds were immersed in 1 mL of phosphate-buffered saline (PBS) and incubated in a 37°C water bath. At specific time-points, scaffolds were transferred to fresh PBS, and the activity of release buffer was determined using a gamma counter (Micromedic 4/600 Plus, Micromedic, Horsham, PA). At the last time-point, scaffolds were dissolved in 1 mL of 5 M NaOH, and the activity was measured to determine the amount of protein left in the scaffold. The initial amount of protein in the scaffold was determined by adding the total amount released to the amount left in the scaffold at the end. Microsphere encapsulation efficiencies were determined by dissolving a known mass of microspheres in 1 mL of 5 M NaOH, and measuring the activity on a gamma counter.

4.2.5. *Islet transplantation*

Diabetes was chemically induced in male C57BL/6 mice (10-12 weeks old) by an intraperitoneal injection of 220 mg/kg streptozotocin (Sigma Aldrich, St. Louis, MO). Blood glucose levels were measured from tail vein samples using a One Touch Basic glucose monitor (Lifescan, Milpitas, CA), and mice with blood glucose levels of > 300 mg/dl on consecutive days were considered diabetic. Normal blood glucose levels are defined as < 200 mg/dl.

Islets were isolated from healthy male C57BL/6 mice as previously described.^{82, 90, 91} Donor mice were anesthetized with an intraperitoneal injection of tribromoethanol. The peritoneal cavity was opened with a midline abdominal incision, and the common bile duct was cannulated and injected with collagenase (type XI; Sigma, St. Louis, MO) in Hank's balanced salt solution. The pancreas was removed by dissection, and digested at 37°C for 15 min. The

digested tissue was then filtered through a mesh screen, and the filtrate added to a discontinuous dextran (Sigma) gradient. Islets were collected and counted under a microscope.

Scaffolds were sterilized in 70% ethanol and washed in islet growth medium (RPMI-1640 medium (Gibco-BRL, Grand Island, NY) supplemented with 10% heat inactivated fetal calf serum (Hyclone, Logan, UT), 100 U/ml penicillin-G, 100 mg/ml streptomycin sulfate, and 1 mmol/L L-glutamine) in preparation for the seeding of purified islets. Islets were applied in a minimal volume of medium onto the surface of the microporous scaffold. The scaffolds were incubated for 15 min. at 37°C in 5% CO₂ and 95% air. At that time, ~20 µl of medium was added and scaffolds were incubated for another 15 min. Scaffolds were then immediately transplanted into intraperitoneal fat of diabetic mice.

4.3. Results

4.3.1. In vitro release kinetics

PLG microspheres encapsulating radiolabeled exendin were fabricated using a range of polymer formulations in order to evaluate the effects of the polymer molecular weight (Mw), copolymer composition, and polymer concentration on the release kinetics. The first set of studies used a traditional scaffold design, where the exendin-loaded microspheres were distributed throughout the entire three-dimensional scaffold structure. The concentration of the PLG solution was varied from 3% to 6%, and two Mw formulations were tested: (1) high Mw (i.v. = 0.6-0.8 dl/g) (HMW), and (2) a blend of 25 wt. % low Mw (i.v. = 0.16-0.24 dl/g) (LMW) and 75 wt. % HMW. The copolymer ratio was kept constant (75/25 mole ratio D,L-lactide-to-glycolide). The microsphere encapsulation efficiencies ranged from 70 to 90% (**Table 4-1**). For

the 3% PLG solution, the polymer molecular weight had no effect on the release kinetics, where a large burst release within the first 2 days was observed for both conditions ($71.2 \pm 6.5\%$ for the high Mw and $66.1 \pm 3.1\%$ for the high/low Mw blend) (**Fig. 4-1**). Increasing the PLG solution concentration from 3% to 6% substantially decreased the initial burst for both Mw formulations, although to a greater extent for the high Mw polymer ($20.2 \pm 2.4\%$ for the high Mw and $36.2 \pm 3\%$ for the high/low Mw blend) (**Fig. 4-1**). However, all 4 of these conditions failed to provide a continued protein release following the initial burst (**Fig. 4-1**).

Table 4-1
Microsphere encapsulation efficiency

PLG% (w/w)	Mole ratio of D,L-lactide/glycolide	Molecular weight (inherent viscosity, dl/g)		Encapsulation efficiency (%)
		0.16-0.24	0.6-0.8	
3	75/25	--	100%	92.4
3	75/25	25%	75%	89.7
6	75/25	--	100%	67.8
6	75/25	25%	75%	65.8

Table 4-1. Microsphere encapsulation efficiency.

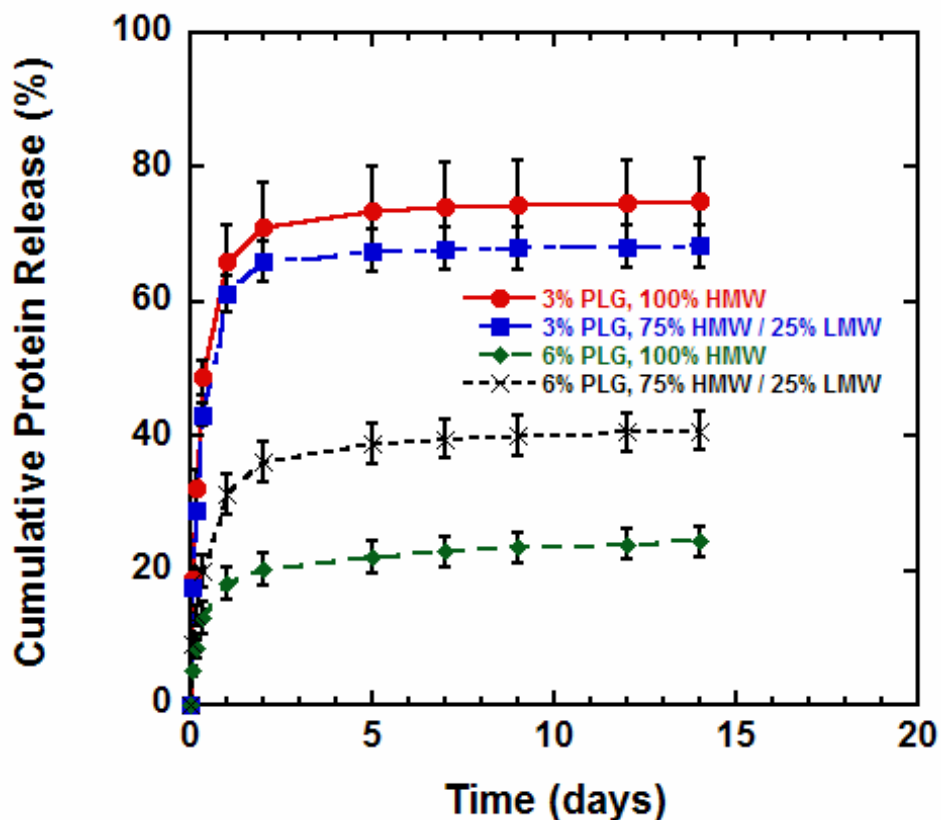


Figure 4-1. *In vitro* exendin release kinetics from traditional scaffolds: effect of PLG concentration and molecular weight. Scaffolds were fabricated from microspheres made with 3% PLG, 100% HMW (red circles), 3% PLG, 75% HMW / 25% LMW (blue squares), 6% PLG, 100% HMW (green diamonds), or 6% PLG, 75% HMW / 25% LMW (black x). Values represent averages \pm standard deviations (n=3 scaffolds per condition).

The second set of studies utilized a layered scaffold design, in which exendin-loaded microspheres were packed into a thin layer in the center of the scaffold. Layered scaffolds were first fabricated using the microsphere formulation that provided the fastest release profile for the traditional scaffold design (i.e. 3% PLG, HMW). In comparing the release kinetics for the two scaffold designs, a 4-fold decrease in the initial burst was observed for the layered design, although protein release was not sustained in either case (**Fig. 4-2**). In an effort to promote continued protein release, the lactide-to-glycolide ratio was varied to achieve a faster polymer degradation rate. The high Mw polymer used in the first set of studies (75 D,L-lactide/25 glycolide, i.v. = 0.6-0.8 dl/g) degrades over a timeframe of ~4-5 months, according to the manufacturer's specifications. In contrast, the "50 D,L-lactide/50 glycolide, i.v. = 0.4-0.5 dl/g" formulation degrades over a period of ~3-4 weeks. To test the effect of polymer degradation rate on protein release kinetics, microspheres were fabricated using this 50/50 copolymer alone, or as an equal weight blend with the 75/25 copolymer. Microsphere encapsulation efficiencies were approximately 90% for both of these formulations, and were not affected by the concentration of the PLG solution. When used alone, the 50/50 copolymer provided a biphasic release profile, characterized by an initial burst over the first 5 days and another burst beginning after 3-4 weeks (**Fig. 4-3**). The magnitude of the initial burst was larger for the lower PLG concentration ($37.3 \pm 1.9\%$ for 3% PLG and $21.8 \pm 2.6\%$ for 6% PLG), which is consistent with the first set of studies (**Fig. 4-3**). However, an opposite trend was observed in the secondary phase (i.e. between days 21 and 70), where the extent of release was greater for the higher PLG concentration (26.1% for 3% PLG and 41.5% for 6%). When the 50/50 copolymer was blended with the 75/25 copolymer, more sustained release profiles were obtained, especially with the 3% PLG (**Fig. 4-4**). For the

3% PLG formulation, ~50 % of the encapsulated protein was released over the first week, followed by another 33% that was released through 56 days in a relatively sustained manner (Fig. 4-4). In comparison, the 6% PLG formulation had a lower initial burst, but followed a similar release trend (Fig. 4-4).

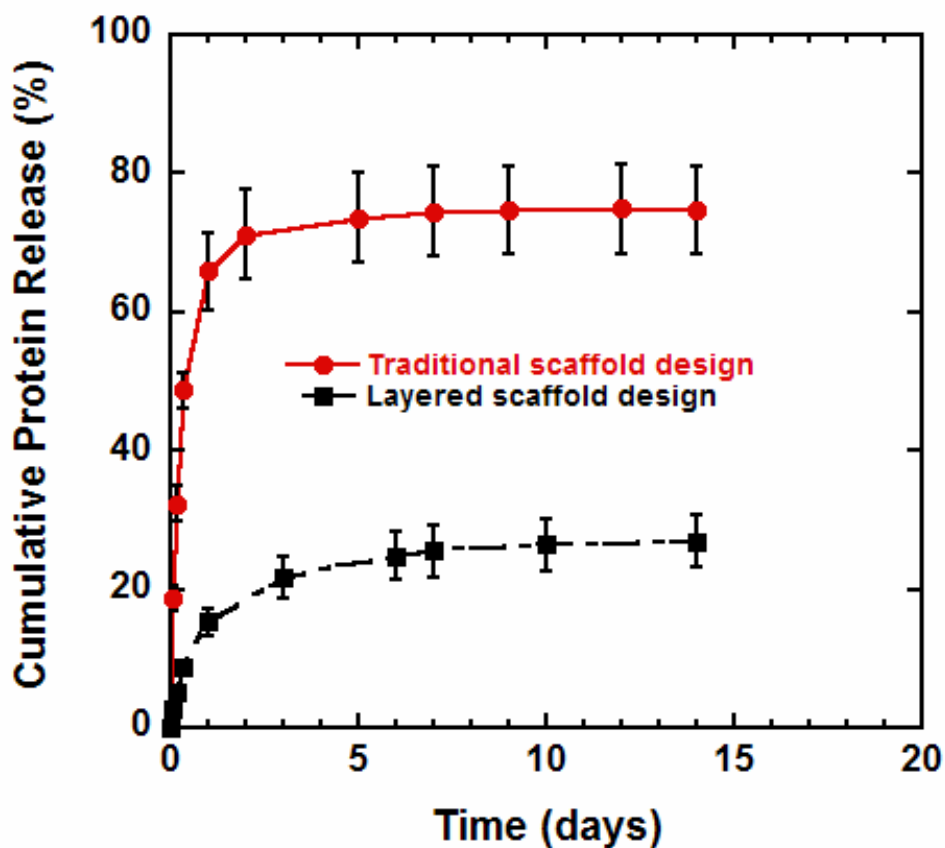


Figure 4-2. *In vitro* exendin release kinetics from scaffolds fabricated with a traditional or layered design. Both traditional (red circles) and layered (black squares) scaffolds were fabricated using the same microsphere formulation (3% PLG, 75/25 copolymer, HMW). Values represent averages \pm standard deviations (n=3 scaffolds per condition).

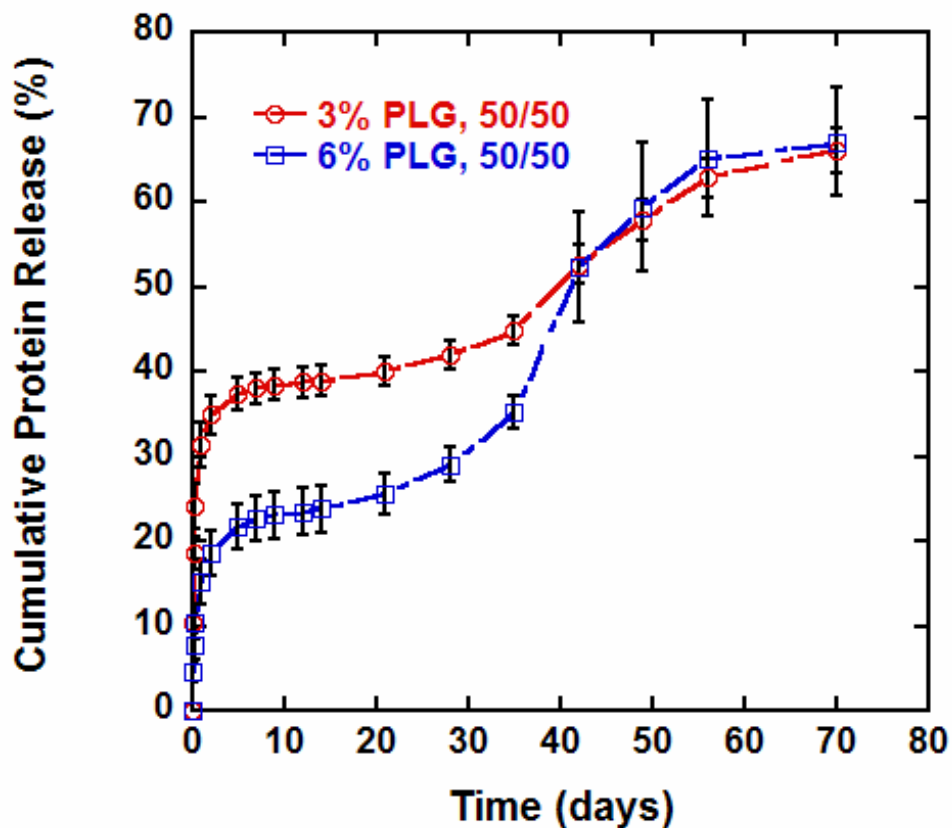


Figure 4-3. *In vitro* exendin release kinetics from layered scaffolds fabricated with the 50/50 copolymer. The concentration of the PLG solution used in the microsphere emulsion process was varied from 3% (red circles) to 6% (blue squares). Values represent averages \pm standard deviations (n=3 scaffolds per condition).

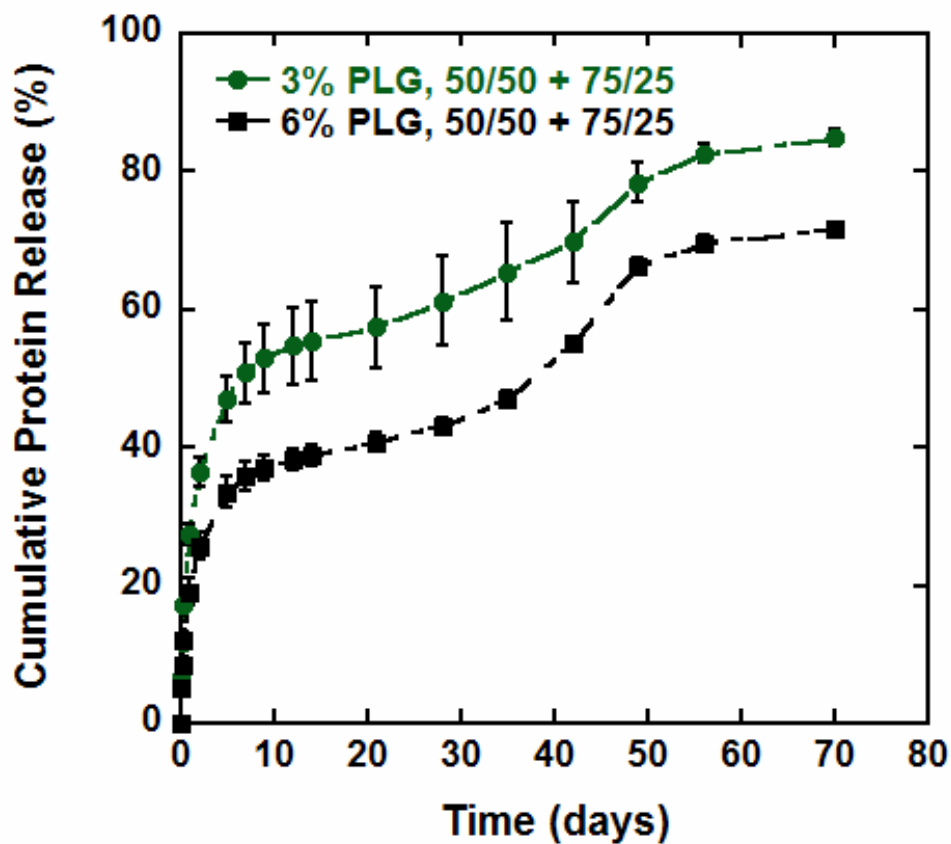


Figure 4-4. *In vitro* exendin release kinetics from layered PLG scaffolds fabricated with an equal weight blend of the 50/50 and 75/25 copolymers. The concentration of the PLG solution used in the microsphere emulsion process was varied from 3% (green circles) to 6% (black squares). Values represent averages \pm standard deviations (n=3 scaffolds per condition).

4.3.2. *Islet transplantation*

Islets were seeded onto exendin-4-loaded scaffolds and transplanted into the intraperitoneal fat of syngeneic mice with streptozotocin-induced diabetes to evaluate the effect of sustained exendin-4 delivery on islet graft function. Scaffolds were fabricated using the layered design, with both the outer and center layers containing exendin-4 loaded microspheres. The outer layers were made with the “3% PLG, 75/25 copolymer, HMW” formulation, while the center layer was made with the “3% PLG, 50/50 + 75/25 copolymer blend” formulation. Thus, the outer layers provide a large burst release during the first few days, while the center layer provides a sustained release for approximately 2 months. Using a marginal islet mass of 75 islets, it was found in two separate experiments that islets transplanted on exendin-4-releasing scaffolds exhibited enhanced function relative to those transplanted on control scaffolds (**Fig. 4-5**). In experiment 1, blood glucose levels of transplant recipients were monitored for 48 days, and all 3 mice receiving islets on control scaffolds failed to convert to euglycemia. Notably, one of the control mice displayed excessive weight loss and had to be sacrificed after 22 days. In contrast, 2 of 3 mice receiving islets on exendin-4 scaffolds rapidly converted to euglycemia on days 1 and 10. In the second experiment, blood glucose levels were monitored for 20 days, and again 2 of 3 mice in the exendin-4 group rapidly converted to euglycemia on days 1 and 6. For the control group, 1 of 3 mice converted to euglycemia on day 17, but the other 2 mice remained diabetic with consistently high blood glucose levels > 400 mg/dl.

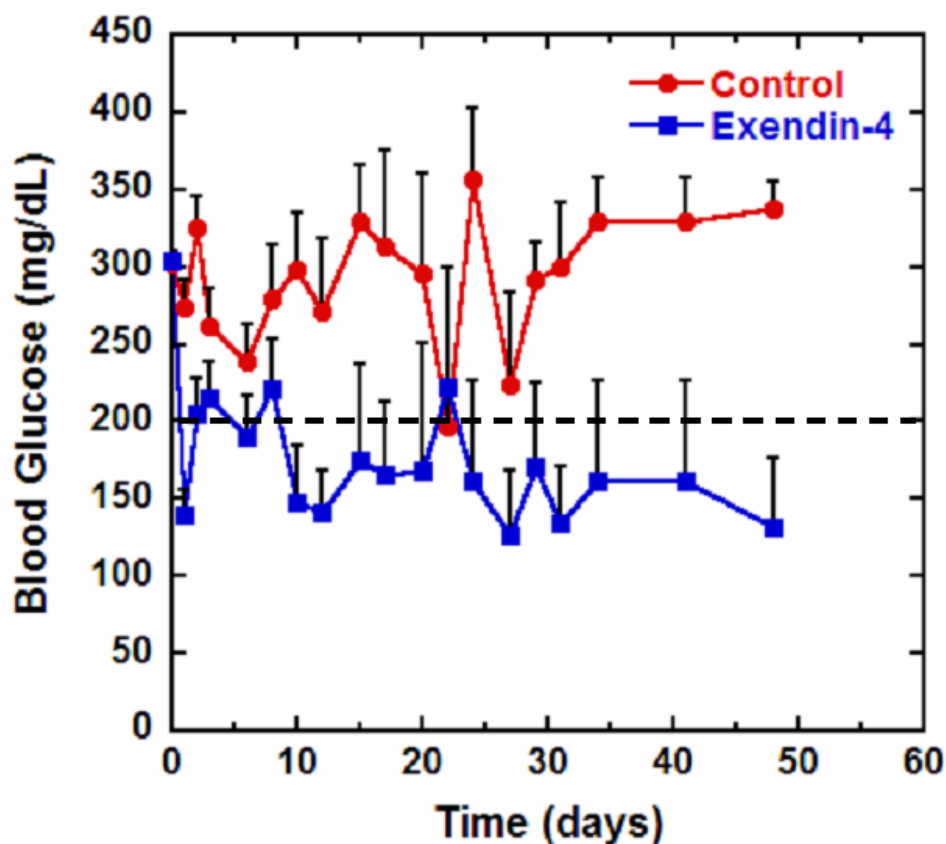


Figure 4-5. Blood glucose levels of mice receiving 75 islets transplanted on exendin-4 or control scaffolds. Data combines 2 separate transplant experiments comparing control scaffolds (red circles) and exendin-4 scaffolds (blue squares). Experiment 1 was monitored for 48 days (n=3 per condition), and experiment 2 was monitored for 20 days (n=3 per condition). Blood glucose levels of < 200 mg/dl are defined as normal. Values represent averages \pm standard errors.

4.4. Discussion

In this chapter, PLG scaffolds were developed for sustained exendin-4 delivery in order to create a supportive platform for islet transplantation. Exendin-4 acts directly on β -cells to inhibit apoptosis, stimulate proliferation, and increase glucose-stimulated insulin secretion.¹¹⁴⁻¹¹⁶ Studies have already demonstrated the potential of exendin-4 to promote islet graft function when administered via intraperitoneal injections.¹¹⁷ However, localized and sustained delivery of exendin-4 within the islet microenvironment may enhance the therapeutic benefit. Tissue engineering scaffolds provide an ideal system for studying the effects of controlled delivery of bioactive factors on cellular function. Exendin-4 was encapsulated inside PLG microspheres using a range of polymer formulations in an effort to identify conditions that provide sustained release kinetics. Using the 75/25 PLG copolymer, non-sustained release profiles were obtained, with the magnitude of the initial burst regulated by the polymer concentration, polymer molecular weight, and scaffold design. Using the layered scaffold design and blending the 75/25 copolymer with the 50/50 copolymer promoted more sustained protein release, presumably due, in part, to the faster degradation rate of the 50/50 copolymer. Interestingly, when used alone, the 50/50 copolymer did not further increase the rate of release (as may be expected due to faster degradation), but rather decreased the extent of protein release. This indicates that other factors in addition to the polymer degradation rate influenced protein release. For islet transplantation studies, layered scaffolds were fabricated using two different polymer formulations, where the outer layers delivered a large burst of exendin-4 in the first few days and the center layer provided sustained exendin-4 release over approximately 2 months. Importantly, the layered scaffold design allows flexibility in choosing a polymer formulation that provides appropriate

protein release kinetics, since the center layer can be designed independently of the structural requirements for the outer layers. Initial studies have demonstrated that islets transplanted on exendin-4-releasing scaffolds exhibit enhanced function relative to those transplanted on control scaffolds, providing the first evidence that drug-releasing scaffolds can improve the outcome of islet transplantation. However, more studies are needed to increase the n values and confirm these findings.

Drug release from PLG microspheres is known to be controlled by a complex interplay of different factors including polymer molecular weight, copolymer composition, and microsphere size.¹¹⁸ The encapsulated drug is released from microspheres via diffusion through the polymer matrix, and as a result of polymer erosion.¹¹⁹ Diffusion rates of drugs through the polymer phase generally decrease with increasing polymer molecular weight.¹¹⁸ Also, as microsphere size decreases, drug release typically increases due to the larger surface area-to-volume ratio and faster water penetration.¹¹⁸ Since microsphere size decreases with decreasing polymer concentration,⁷⁴ this may partially explain why the lower PLG concentration resulted in increased protein release. Furthermore, microspheres made with the higher PLG concentration presumably have increased densities, which may limit protein diffusion. In general, microspheres typically exhibit an initial burst of drug release within the first few hours or days that is thought to be the result of drug located at or near the microsphere surface or in the pores/voids connected to the surface.^{118, 119} After the initial burst, the drug diffuses out of the microsphere interior through a network of water-filled pores, which grows over time due to erosion of the polymer matrix.¹¹⁸ If diffusivity of the drug through the polymer matrix is limiting, drug release will primarily be controlled by the polymer degradation rate.¹¹⁹ In this case, there may be a lag phase

after the initial burst until the polymer achieves bulk erosion, which results in a significant increase in the formation of pores for drug diffusion.¹¹⁹ This type of release profile was observed in these studies for the layered scaffolds fabricated with the 50/50 copolymer. The secondary phase of release after 3-4 weeks likely corresponds to time required for bulk erosion of this polymer formulation. It is unclear why blending the 50/50 copolymer with the 75/25 copolymer resulted in more sustained protein release (since the degradation rate was likely slower), but may be related to increased diffusivity of the protein through the polymer matrix or partitioning of the protein closer to the microsphere surface.

An important consideration for future studies is that the thickness of the scaffold's outer layer may limit the efficacy of exendin-4 delivery by creating a large diffusion distance that the protein must overcome in order to reach the islets. The scaffolds used in these studies had an outer layer thickness of ~1.5 mm, and seeded islets typically do not penetrate deep within the scaffold; rather they remain on the surface. Thus, exendin-4 released from the center layer must diffuse the full distance of ~1.5 mm in order to reach the islets. Decreasing the thickness of the outer layers to place the seeded islets in direct contact with the center layer (i.e. source of exendin-4) may maximize the therapeutic benefit by minimizing the protein diffusion distance. Future studies should also investigate dose effects of exendin-4 delivery. Additionally, administration of exendin-4 via intraperitoneal injections should be performed as a control to establish whether controlled delivery leads to a greater enhancement in islet function.

5. CONCLUSIONS AND RECOMMENDATIONS

5.1. Perspective

Tissue engineering holds great promise for the treatment of a wide range of medical problems associated with tissue or organ loss, but requires harnessing the inherent capacity of cells to assemble into functional tissues. The underlying idea is that cellular behavior can be controlled by manipulating environmental signals. Although the concept is simple, the ability to adequately control cellular behavior and coordinate the formation of complex tissues remains a challenge, partly due to the diversity of biological signals and a lack of effective strategies for presenting these signals in a spatially and temporally controlled manner. Scaffolds are a central component of tissue engineering, as they provide a three-dimensional template for organizing cells into the proper architecture, and offer the potential to create controllable environments with the appropriate cellular cues required to direct tissue formation. To this end, scaffolds have been developed for controlled drug delivery as a means for introducing bioactive proteins or peptides into the local environment. Encapsulation of proteins inside biodegradable polymer microspheres has been one of the most common approaches for promoting controlled delivery. The main challenges include obtaining high encapsulation efficiencies, maintaining the protein's bioactivity prior to release, and achieving continued protein release for the desired timeframe. Additionally, since proteins exhibit a wide range of physical properties, the delivery system may need to be optimized for each protein delivered, limiting the versatility of this approach.

Bioactive proteins and peptides can also be indirectly delivered via a gene therapy approach, where a plasmid vector containing the encoding gene is delivered and cells are exploited to locally produce and secrete the protein of interest. This approach is attractive due to

its versatility and potential to induce prolonged expression of proteins at stable levels. The primary challenge is achieving transfection of sufficient numbers of cells and maintaining expression of the delivered plasmid at effective levels for the desired time frame. Previous studies have demonstrated proof of principle that plasmid delivery from scaffolds can achieve localized cellular transfection and sufficient protein production to induce physiological responses. However, an understanding of the important factors that regulate the extent and duration of transgene expression is lacking. For example, it is not known how the plasmid dose and release rate correlate with the transgene expression profile. Additionally, the relationship between key scaffold design parameters and transgene expression has not been investigated. Also, the cell types responsible for expressing the plasmid have generally not been identified, and it is not known how the transgene expression profile will vary for different anatomical locations. Chapters 2 and 3 aimed to address some of these questions and improve our overall understanding of scaffold-mediated gene delivery. These fundamental studies are needed to establish the capabilities/limitations of the current approach and may help to direct new strategies for continued development of effective gene delivery systems. Ultimately, it will be important to develop an ability to regulate the levels, duration, and location of transgene expression, since the requirements for tissue formation are generally not known, and will likely vary for different applications.

This dissertation focused on developing scaffold technologies for controlled delivery of proteins and DNA, and then applying these systems to create an effective platform for islet transplantation, which is a promising cell-replacement therapy for the treatment of type I diabetes. The current clinical approach of infusing large numbers of islets into a patient's liver

has demonstrated the potential to achieve insulin independence, although multiple transplants are typically required and the reversal of diabetes is not maintained due to progressive islet failure over time. Poor islet survival and concerns with the liver as a transplant site are thought to contribute to the limited success. The application of tissue engineering principles to this problem offers the potential to create a more supportive environment for transplanted islets that will promote engraftment and continued function. In chapter 4, scaffolds were developed for controlled delivery of the peptide exendin-4, which acts on islet β -cells to inhibit apoptosis, stimulate proliferation, and increase glucose-stimulated insulin secretion. Initial studies demonstrated that exendin-4 delivery from scaffolds can enhance islet graft function, providing the first evidence that drug-releasing scaffolds can promote the success of islet transplantation. Further development of this scaffold-based approach will require delivery of a variety of other therapeutic targets, such as angiogenic factors to induce the formation of a sufficient vascular supply. As discussed above, plasmid delivery provides an alternative drug delivery strategy that would afford improved versatility to deliver a wide range of therapeutic targets with a single delivery system. However, it is not known whether the extent and duration of transgene expression currently obtained at the intraperitoneal fat site will be sufficient to provide a therapeutic benefit for transplanted islets. Importantly, the requirements for transgene expression will likely depend on the therapeutic target. For example, anti-apoptotic factors expressed at high levels for only a few days may be effective for promoting islet engraftment, since substantial islet cell death is known to occur in the early post-transplant period. For other factors such as angiogenic factors, sustained expression for several weeks will likely be required to achieve formation of robust and stable vascular networks.

5.2. Chapter 2: PLG Scaffolds for Plasmid Delivery: *In Vivo* Transgene Expression at a Subcutaneous Site

5.2.1. Conclusions

These studies demonstrated the ability of DNA-releasing scaffolds to provide localized and sustained transgene expression *in vivo* following implantation at a subcutaneous site. The extent and duration of transgene expression was strongly regulated by the plasmid dose. High plasmid doses (>600 μg) resulted in robust expression that persisted for several months, while low doses (<300 μg) provided only short-term expression that subsided within a few days. Immunohistochemical analysis demonstrated the presence of transfected cells within the scaffold, immediately adjacent to the polymer surface. It was initially hypothesized that the scaffold's porous structure played an important role in promoting transgene expression. However, in comparing scaffolds made with different molecular weight polymers, it was found that maintaining an intact pore structure was not required for sustained transgene expression. Scaffolds made with low molecular weight polymer typically collapsed following implantation, but consistently provided robust and sustained transgene expression, similar to high molecular weight scaffolds that maintained structural integrity. Additionally, histological analysis demonstrated that scaffolds failed to effectively support cellular infiltration, regardless of the polymer molecular weight. To address this problem, the scaffold's pore interconnectivity was improved by increasing the microsphere size and density. Although the modified scaffold structure promoted cellular infiltration, it also substantially lowered the plasmid incorporation efficiency. This dependency of the plasmid incorporation efficiency on the scaffold structure was an important finding that revealed a critical limitation of the current delivery system.

5.2.2. Recommendations

The mechanism responsible for long-term transgene expression observed at the subcutaneous site remains undetermined, but is likely the result of continued expression of the plasmid by initially transfected cells, rather than repeated cellular transfection. Sustained plasmid delivery from scaffolds has been proposed as a means to extend transgene expression by maintaining elevated concentrations of the vector in the local environment. However, the scaffolds described in this chapter exhibited rapid plasmid release kinetics *in vitro*, with most of the plasmid released within a few days. Thus, the kinetics of plasmid release are not consistent with the prolonged and stable transgene expression profile obtained. To more rigorously prove that sustained plasmid delivery is not required for long-term expression at this site, plasmid should be locally delivered via a bolus injection during implantation of a control scaffold. Additionally, identifying the cell type(s) transfected will likely provide insight into the mechanism. Specifically, more immunohistochemical analysis should be performed to determine whether muscle cells are transfected at this site. It is well established that muscle can provide sustained expression of plasmids for several months at stable levels, and abundant striated muscle fibers were observed in the immediate scaffold periphery. Importantly, if muscle cells are found to be responsible for the sustained expression, the applicability of results obtained at this site would likely be limited given that many anatomical sites do not contain muscle tissue. In fact, we have already found that these results do not translate well to the intraperitoneal fat site, where the duration of expression was found to be substantially shorter. Thus, the subcutaneous site may not be suitable as a model site for studying *in vivo* gene transfer.

In addition to determining whether muscle cells are transfected in the surrounding tissue, the cell type(s) transfected within the scaffold should also be identified. At both the subcutaneous and intraperitoneal fat sites, immunohistochemical analysis demonstrated the presence of transfected cells within the scaffold, immediately adjacent to the polymer surface. At the intraperitoneal fat site, these cells were identified as macrophages. Thus, given the same pattern of staining at the subcutaneous site, it is reasonable to expect these cells may also be macrophages. However, since transgene expression at the intraperitoneal fat site persisted for only a few weeks, transfected macrophages within the scaffold are not expected to contribute to long-term expression at the subcutaneous site.

The dependency of the plasmid incorporation efficiency on the scaffold structure represents a major limitation of the current delivery system. Improving the scaffold's pore interconnectivity was necessary to promote cellular infiltration, but resulted in unacceptably low plasmid incorporation efficiencies. Thus, an alternative or modified delivery system that would allow the scaffold structure to be changed without affecting DNA incorporation or release was needed. As a result, a novel layered scaffold design was developed in chapter 3 to overcome this problem.

5.3. Chapter 3: Layered PLG Scaffolds for Plasmid Delivery and Cell Transplantation: *In Vivo* Transgene Expression at an Intraperitoneal Fat Site

5.3.1. Conclusions

A novel layered scaffold design was developed to facilitate the efficient incorporation of large quantities of plasmid, while maintaining a well-interconnected open-pore structure for cell

transplantation. These scaffolds promoted gene transfer *in vivo* at an intraperitoneal fat site, with transgene expression persisting for up to 2 weeks. Regardless of the plasmid dose (200, 400, or 800 μg), a similar trend was observed where expression levels peaked during the first few days and then rapidly declined. This rapid drop in expression represents a common obstacle encountered with *in vivo* plasmid delivery. Despite the decreased expression at 1 and 2 weeks, immunohistochemical analysis demonstrated abundant transfected cells both in the surrounding tissue and within the scaffold pores. A large number of these transfected cells were identified as macrophages. Scaffolds delivering FGF-2 plasmid induced a modest increase in vascularization at 2 weeks relative to control scaffolds, demonstrating that expression levels, at least initially, were physiologically relevant. However, no effect was seen for delivery of HIF-1 α at 2 weeks. Additionally, by 4 weeks, a substantial decrease in vascularization was observed for both FGF-2 and control scaffolds, suggesting that vessel regression had occurred. Taken together, the microcomputed tomography results indicate that the current transgene expression profile is likely insufficient to induce the formation of a robust and stable vascular network.

5.3.2. Recommendations

The layered scaffold design substantially increased plasmid incorporation efficiency, but did not provide sustained plasmid release kinetics or promote long-term transgene expression at the intraperitoneal fat site. The underlying reasons limiting the duration of transgene expression are not known, but are likely related to both extracellular and intracellular barriers. First, extracellular barriers refer to the process by which DNA diffuses from the scaffold to the target cell membrane so that it can be internalized by the cell via endocytosis. Sustained plasmid

release from scaffolds has been proposed as a means to maintain elevated concentrations of the vector within the cellular microenvironment to increase opportunities for internalization and facilitate repeated cellular transfection. However, layered scaffolds exhibited rapid *in vitro* plasmid release kinetics (similar to those in chapter 2), where most of the plasmid was released in the first few days. In order to test whether expression can be extended by sustained plasmid delivery, more work is needed to develop strategies for controlling plasmid release from scaffolds. One potential approach for slowing plasmid release is to include cationic microspheres within the center layer to create an electrostatic interaction with the plasmid, and thereby modulate the release kinetics (**Appendix 6.3**). Alternatively, the rate of DNA release can be slowed by encapsulating DNA within polymer microspheres, and fabricating scaffolds from these DNA-loaded microspheres.^{81, 98, 99} However, the amount of DNA that can be delivered with this approach is limited based on the loading capacity of the microspheres and the amount of polymer required to make the scaffold (i.e. scaffold size). In addition to controlling plasmid release, we will likely need to address intracellular barriers. For example, once the plasmid is internalized into the cell and successfully traffics to the nucleus, rapid inactivation of the plasmid promoter commonly occurs. Reasons for this rapid inactivation are not well understood, although several possibilities have been suggested including cytokine-mediated inhibition,⁹³ binding of repressor proteins,⁹⁴ methylation,⁹⁵ or loss of a positive activator.⁹⁶ In some cases, the use of alternative promoters has allowed for more sustained gene expression.⁹² Additionally, modification of the plasmid vector through depletion of CpG motifs has shown the potential to provide more prolonged transgene expression.⁹⁷

5.4. Chapter 4: Exendin-4 Releasing Scaffolds for Islet Transplantation

5.4.1. Conclusions

PLG scaffolds were developed for controlled delivery of exendin-4 and evaluated for their ability to enhance the function of transplanted islets. Exendin-4 was encapsulated inside PLG microspheres using a double emulsion procedure, and scaffolds were fabricated from the protein-loaded microspheres. The PLG copolymer ratio and molecular weight were varied in order to identify formulations that provide sustained protein release. Scaffolds made with the 75/25 copolymer provided only an initial burst of protein release during the first few days, with the magnitude of the burst regulated by the polymer concentration, molecular weight, and scaffold design (i.e. layered vs. traditional). Using the layered scaffold design and blending the 75/25 copolymer with the 50/50 copolymer promoted more sustained protein release, presumably due, in part, to a faster polymer degradation rate. With this formulation, 50 % of the encapsulated protein was released over the first week, followed by another 33% that was released through 56 days in a relatively sustained manner. The layered scaffold design was an important aspect of these studies, as it allowed the center layer to be designed independently of the structural requirements of the outer layers, thereby providing more flexibility in choosing a polymer formulation that provides appropriate protein release kinetics. After identifying a formulation with desirable release kinetics, exendin-4-releasing scaffolds were evaluated for their ability to enhance islet transplantation. Initial studies have demonstrated that islets transplanted on exendin-4-releasing scaffolds provide improved blood glucose control relative to those transplanted on control scaffolds.

5.4.2. Recommendations

In order to confirm our initial results indicating that exendin-4-releasing scaffolds promote islet graft function, more islet transplants are needed to increase the n values. Additionally, the effect of scaffold thickness on the efficacy of exendin-4 delivery should be investigated. Specifically, decreasing the thickness of the outer layers to place the seeded islets in direct contact with the center layer (i.e. source of exendin-4) may maximize the therapeutic benefit by minimizing the protein diffusion distance. Also, administration of exendin-4 via intraperitoneal injections should be performed as a control to establish whether controlled delivery leads to a greater enhancement in islet function.

6. APPENDIX

6.1. Lyophilization of DNA with PLG microspheres

To incorporate DNA into porous PLG scaffolds, polymer microspheres are reconstituted in a concentrated DNA solution and lyophilized to form a powder. This powder is mixed with salt particles, compressed into a pellet, and processed by gas foaming and particulate leaching. Importantly, the physical properties of the lyophilization product can affect its ability to be mixed effectively with salt particles. A desirable lyophilization product is brittle, such that it can be easily pulverized into a fine powder (**Fig. 6-1A**). However, in some cases, the lyophilization product can exhibit a “foam-like” quality and occupy a significantly larger volume (**Fig. 6-1B**). This type of lyophilization product cannot be broken up into a powder, and the addition of a small volume of water (i.e. wet granulation technique) causes formation of a “gum-like” substance that is extremely sticky and difficult to mix. Furthermore, scaffolds fabricated with this undesirable lyophilization product typically become cracked during the gas foaming process, presumably due to the expansion of large aggregates of polymer that were not homogeneously mixed (**Fig. 6-2**). Given these difficulties in fabricating DNA-loaded scaffolds, it was important to understand how to consistently achieve formation of desirable lyophilization products. It was found that the size of the holes created in the top of the microcentrifuge tube prior to lyophilization significantly influenced the physical properties of the lyophilization product (**Fig. 6-1**). Using an 18-gauge needle to make 1 large hole in the top of the tube resulted in the formation of an undesirable lyophilization product (**Fig. 6-1B**). In contrast, using a 25-gauge needle to make 3 small holes in the top of the tube resulted in a lyophilization product that occupied less volume, and exhibited increased porosity and brittleness (**Fig. 6-1A**). This effect is

likely related to the drying rate of the product during lyophilization, where the larger hole allows for an accelerated drying rate.

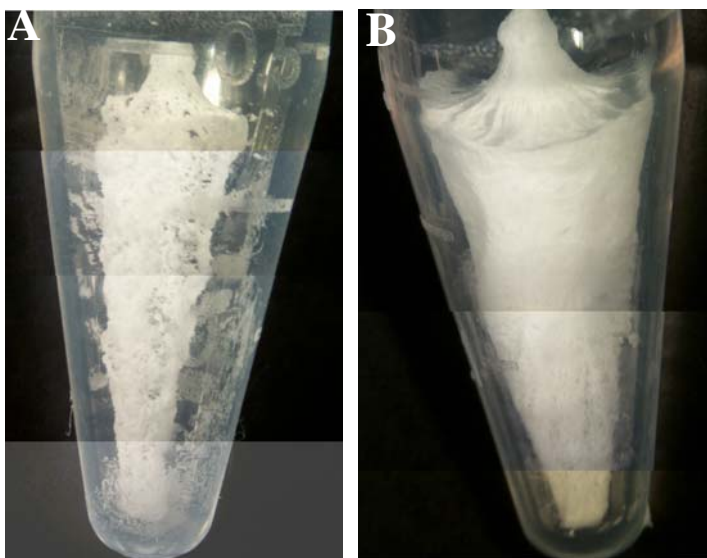


Figure 6-1. Images of lyophilization products with different physical properties. Both samples contained 7 mg of PLG microspheres, 800 μg of DNA, and 1 mg of lactose. The size of the hole(s) created in the top of the plastic tube prior to lyophilization regulated the physical properties of the final product. (A) A 25-gauge needle was used to make three small holes. (B) An 18-gauge needle was used to make one large hole. The lyophilization product in (A) occupies a smaller volume and exhibits increased porosity and brittleness relative to (B).

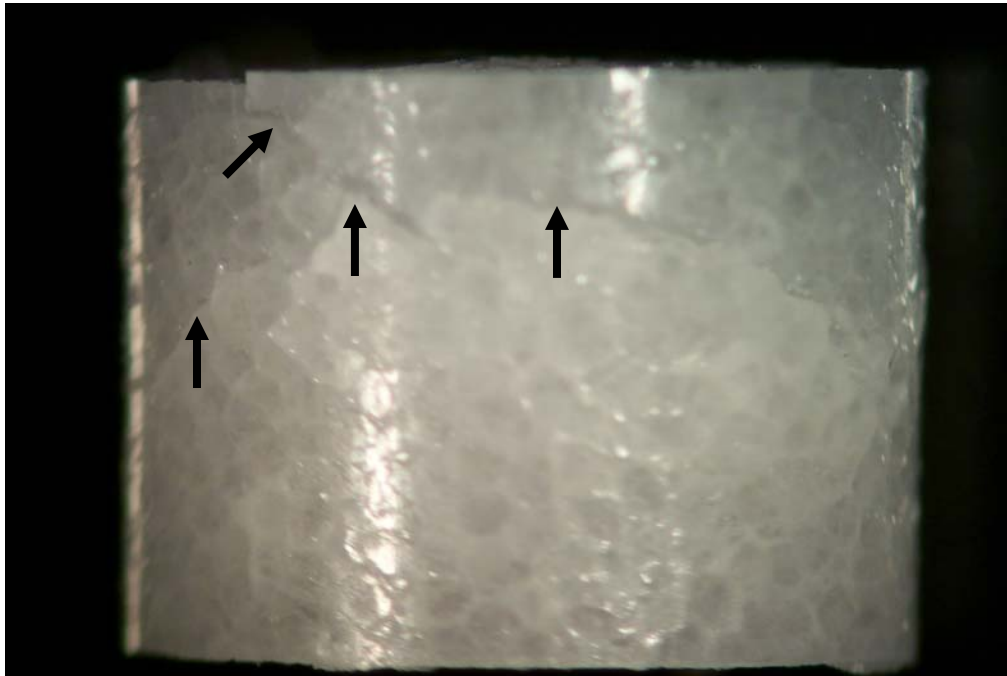


Figure 6-2. Image of a cracked scaffold after gas foaming. The scaffold was fabricated with an undesirable lyophilization product that could not be homogeneously mixed with salt particles, resulting in aggregates of polymer. During the gas foaming process, expansion of the polymer aggregates created fractures through the scaffold, compromising its structural integrity.

6.2. *In vivo* transgene expression obtained by drying DNA onto the surface of scaffolds

Scaffolds with 50 or 100 μg of DNA dried onto their surface provided robust transgene expression at the subcutaneous site for at least 2 weeks. Prior to addition of DNA, scaffolds were wetted in ethanol, washed in water, and then partially dried. DNA was added in a drop-wise fashion to the scaffold surface in a minimal volume of TE buffer ($\sim 20 \mu\text{L}$), and scaffolds were incubated at 37°C to dry the DNA onto the surface. When immersed in water, the adsorbed DNA was quickly released from the scaffold, which is to be expected given that both the scaffold and DNA are negatively charged. Scaffolds containing 50 or 100 μg of luciferase plasmid were implanted subcutaneously and transgene expression was monitored using bioluminescence imaging. Both doses provided robust transgene expression that persisted for at least 2 weeks, with higher levels observed for the 100 μg dose (**Fig. 6-3**). It is important to note that transgene expression may have persisted for a longer period of time, but the mice were only monitored for 2 weeks. This experiment suggests that sustained plasmid release may not be required for prolonging transgene expression at the subcutaneous site. Although this approach worked well in the current situation, it would not be useful in any application that requires pre-hydration of the scaffold prior to implantation (as would be done in cell transplantation procedures). Furthermore, when this approach was applied to the intraperitoneal fat site, transgene expression persisted for only a few days (**Fig. 6-4**). Thus, these results may be specific to the subcutaneous site.

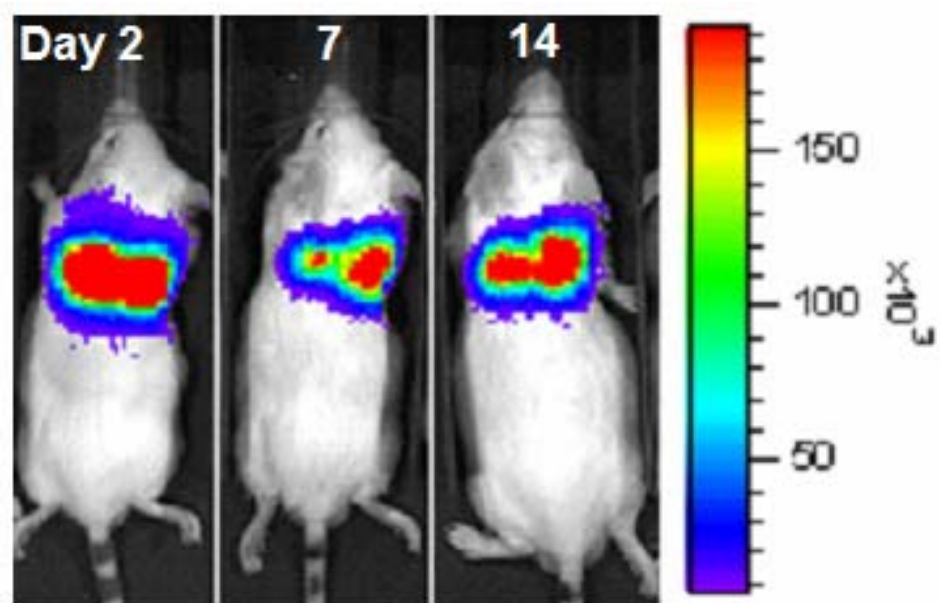


Figure 6-3. Bioluminescence imaging of luciferase transgene expression for scaffolds containing 50 µg or 100 µg of pLuc dried onto their surface. The images are of a single mouse at different time points. Two scaffolds were implanted subcutaneously in the dorsal region of the mouse. The scaffold on the left had 50 µg of pLuc, while the one on the right had 100 µg of pLuc.

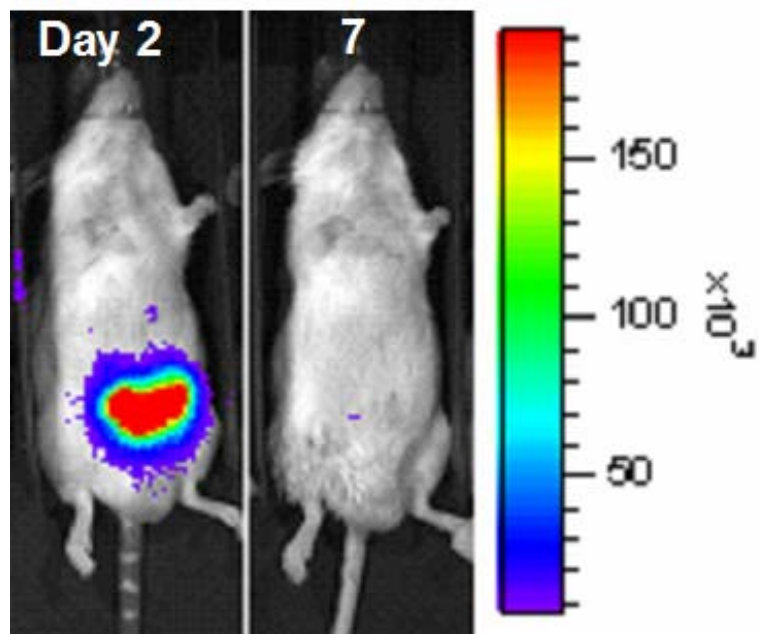


Figure 6-4. Bioluminescence imaging of luciferase transgene expression at the intraperitoneal fat site following implantation of a scaffold containing 100 μg of pLuc dried onto its surface. The images are of a single mouse at different time points.

6.3. Fabrication of cationic PLG microspheres for DNA adsorption

Introduction

Incorporation of DNA into porous PLG scaffolds via the methods described in chapter 2 is associated with several significant problems, including large losses of DNA during the particulate leaching step, rapid release kinetics, and a dependency of the incorporation efficiency on the scaffold structure. As a result, an alternative delivery strategy involving adsorption of DNA to PLG microspheres or scaffolds was investigated. With an adsorption based approach, DNA could potentially be adsorbed to a pre-made scaffold that has already been leached, such that no DNA is lost during leaching and the scaffold structure is not affected by addition of DNA. However, such an approach would likely require a specific interaction (e.g. electrostatic) between the scaffold and DNA, in order to allow efficient loading and prevent rapid release of the DNA. The strength of this interaction would be crucial, as it would need to promote DNA adsorption, yet still allow for DNA release.

The creation of cationic PLG microspheres capable of efficient DNA adsorption has already been explored by other groups as a means to deliver DNA vaccines.¹²⁰ Several studies have used the cationic lipid, cetyltrimethylammonium bromide (CTAB) (structure shown in **Fig. 6-5**), as a surfactant in the emulsion procedure to make cationic microspheres with highly positive zeta potentials of $>+50$ mV (in comparison, microspheres prepared with poly(vinyl alcohol) (PVA) as a surfactant have negative zeta potentials of approximately -15 mV).¹²⁰⁻¹²³ One study reported that the amount of CTAB on the microsphere surface can be controlled through the extent of washing, and the CTAB content regulates both the DNA loading efficiency and the extent of release.¹²¹ Other cationic polymers have also been explored to create positively

charged PLG microspheres, including polyethylenimine (PEI),¹²⁴⁻¹²⁶ chitosan,^{125, 127} and poly(2-dimethyl-amino)ethyl methacrylate (pDMAEMA).¹²⁵

The objective of these studies was to fabricate cationic PLG microspheres, and evaluate their capacity for DNA adsorption and release. Ultimately, these cationic microspheres could be used to fabricate three-dimensional scaffolds, providing a mechanism to modulate interactions between DNA and the scaffold. Examples of potential adsorption-based strategies for delivering DNA from scaffolds include: (1) pre-adsorbing DNA to microspheres before fabricating scaffolds, (2) adsorbing DNA to scaffolds after fabrication, and (3) pre-adsorbing DNA to nanospheres and then seeding the DNA-coated particles onto scaffolds (illustrated in **Fig. 6-6**).

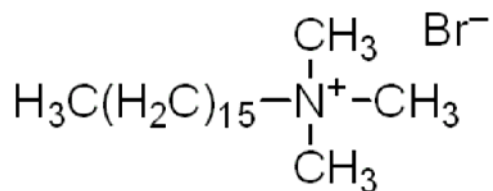


Figure 6-5. Structure of cetyltrimethylammonium bromide (CTAB).

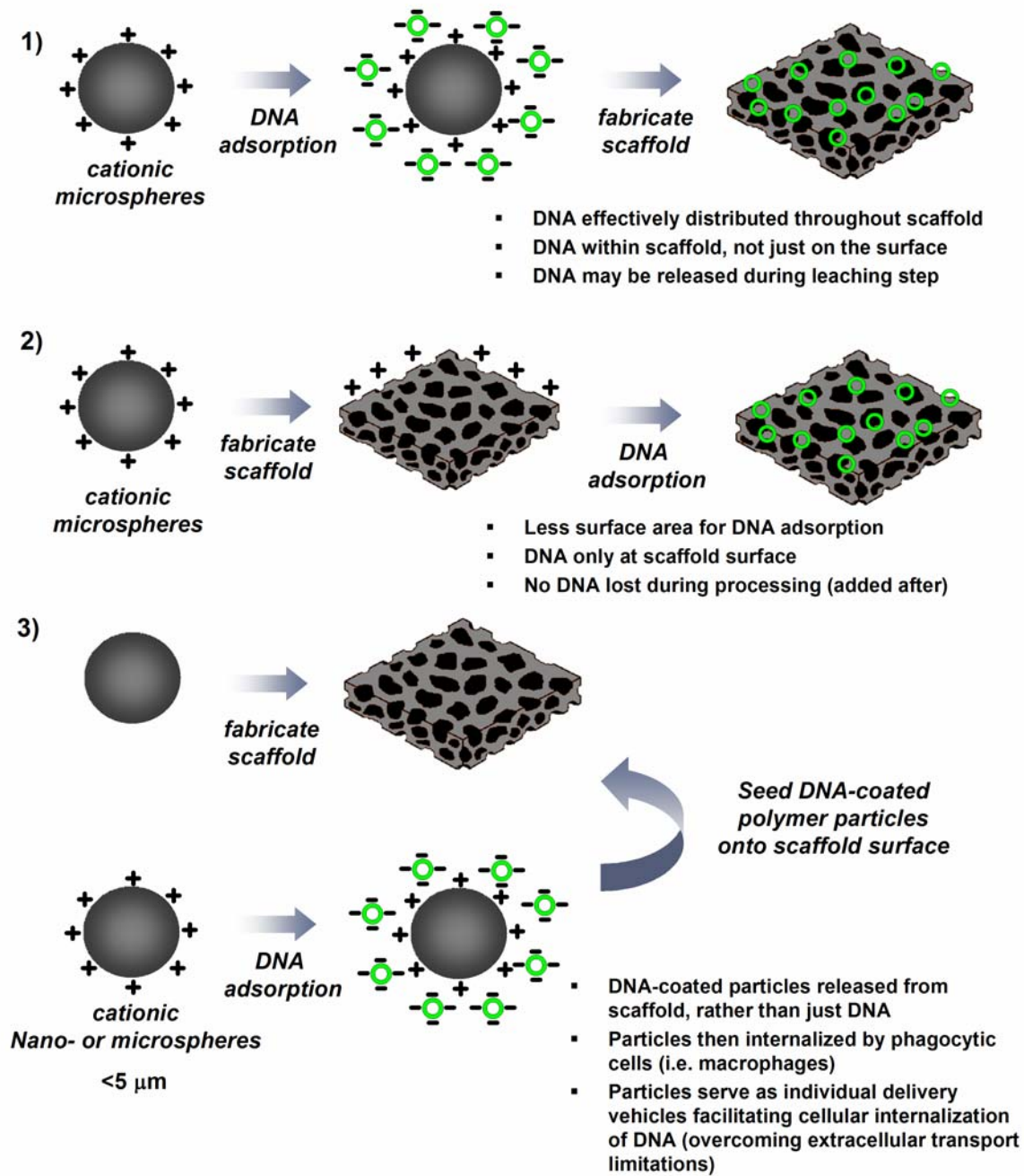


Figure 6-6. Adsorption-based strategies for DNA delivery from scaffolds.

Fabrication of CTAB-coated PLG microspheres

We initially attempted to fabricate cationic microspheres with CTAB, since it has been extensively studied in numerous reports. Microspheres were fabricated using a single emulsion procedure. PLG (75/25 mole ratio of D,L-lactide-to-glycolide, i.v. = 0.6-0.8 dl/g) was dissolved in dichloromethane to make a 6% (w/w) solution. To create the emulsion, 3 mL of the PLG solution was combined with 20 mL of an aqueous CTAB solution (0.1%, 0.5%, or 1% (w/v)) and homogenized at 7000 rpm for 45 sec. Other reports typically used a 0.5% (w/v) CTAB solution.¹²⁰ Note that CTAB can precipitate out of solution at room temperature at high concentrations above 0.5% (w/v). The emulsion was poured into 60 mL of an aqueous CTAB solution, and stirred for 3 hr. to allow evaporation of the organic solvent. Microspheres were washed with water and centrifuged at 4000 rpm for 10 min (repeated twice).

During washing, microspheres aggregated and adsorbed to the walls of conical tubes, presumably due to the removal of CTAB from the microsphere surface and subsequent exposure of the hydrophobic PLG surface. The inability to form a stable CTAB coating represents a major problem, since the CTAB must be present in order to impart a positive surface charge. This problem was not reported in any of the initial papers (all from a single group).^{120, 121, 123} However, a recent paper by another group did describe this same problem, and concluded that CTAB desorbs from the microsphere surface during washing, regardless of the CTAB concentration or polymer formulation.¹²⁸ CTAB desorption could only be prevented by inclusion of at least 0.1% (w/v) CTAB in the wash buffer. Given the problems associated with fabricating CTAB-coated PLG microspheres, alternative cationic molecules were examined.

Fabrication of PEI/PLG microspheres

Polyethylenimine (PEI) is a commonly used non-viral transfection reagent that contains a high density of positive charges due to amine groups. It self assembles with plasmid to generate condensed structures that facilitate cellular uptake and intracellular trafficking. Given its ability to efficiently bind DNA via an electrostatic interaction, PEI has also been used to modify the surface of microspheres to promote DNA adsorption.¹²⁴

PEI was incorporated in PLG microspheres by directly dissolving it in the organic phase prior to the emulsion procedure (rather than using it as a surfactant in the aqueous phase which was the case for CTAB). PEI/PLG microspheres were fabricated using a previously described double emulsion procedure.¹²⁴ PLG (75/25 mole ratio of D,L-lactide-to-glycolide, i.v. = 0.6-0.8 dl/g) was dissolved in dichloromethane to make a 5% (w/w) solution. PEI (25 kDa, branched) was co-dissolved in the polymer solution at different concentrations (1%, 2.5%, 5%, or 10% wt. PEI/wt. PLG). The first emulsion was formed by adding 500 μ L of phosphate-buffered saline (PBS) to 5 mL of the organic PEI/PLG solution, and sonicating for 30 sec. at 70 W. The first emulsion was then injected into 25 mL of an aqueous solution containing surfactant (i.e. 0.5% (w/v) CTAB or PVA), and homogenized at 10,000 rpm for 30 sec. The second emulsion was then stirred for 3 hours to allow evaporation of the organic solvent. Microspheres were washed with water or 0.1% (w/v) CTAB, and centrifuged at 4000 rpm for 10 min (repeated twice).

For all PEI concentrations tested, microspheres exhibited a normal morphology (i.e. discrete spheres with no aggregation) (**Fig. 6-7**). Notably, a decrease in microsphere size was apparent for higher PEI concentrations, likely due to higher positive surface charges and increased particle repulsion (**Fig. 6-7**). A Malvern Zetasizer was used to measure the zeta

potential of the microparticles. All PEI concentrations resulted in highly positive zeta potentials of > 40 mV (**Fig. 6-8**). Additionally, the 5% and 10% PEI microspheres promoted efficient DNA adsorption, with loadings of up to $50 \mu\text{g DNA/mg microspheres}$. However, scaffolds fabricated from the 5% PEI microspheres exhibited better structural integrity relative to those fabricated with 10% PEI microspheres. To evaluate *in vivo* gene delivery, $185 \mu\text{g}$ of luciferase plasmid was adsorbed to 3.7 mg of 5% PEI/PLG microspheres, and the mixed with 100 mg of sucrose particles ($250 \mu\text{m} < d < 425 \mu\text{m}$) to make scaffolds. Notably, none of the adsorbed DNA was lost during the leaching process, presumably due to strong electrostatic interactions. The scaffolds were implanted subcutaneously and gene expression was monitored by bioluminescence imaging. However, at day 7, no luciferase expression was detected. It is likely that the electrostatic interaction between the PEI and DNA is too strong to allow for DNA release. This highlights the important balance between adsorption and release. In an effort to decrease the positive surface charge, the molecular weight of PEI was decreased to 1.8 kDa . The resulting microspheres still exhibited positive zeta potentials of $> +20 \text{ mV}$, although they were no longer able to support DNA adsorption. Overall, more studies are needed to identify an appropriate cationic molecule that balances the competing processes of adsorption and release.

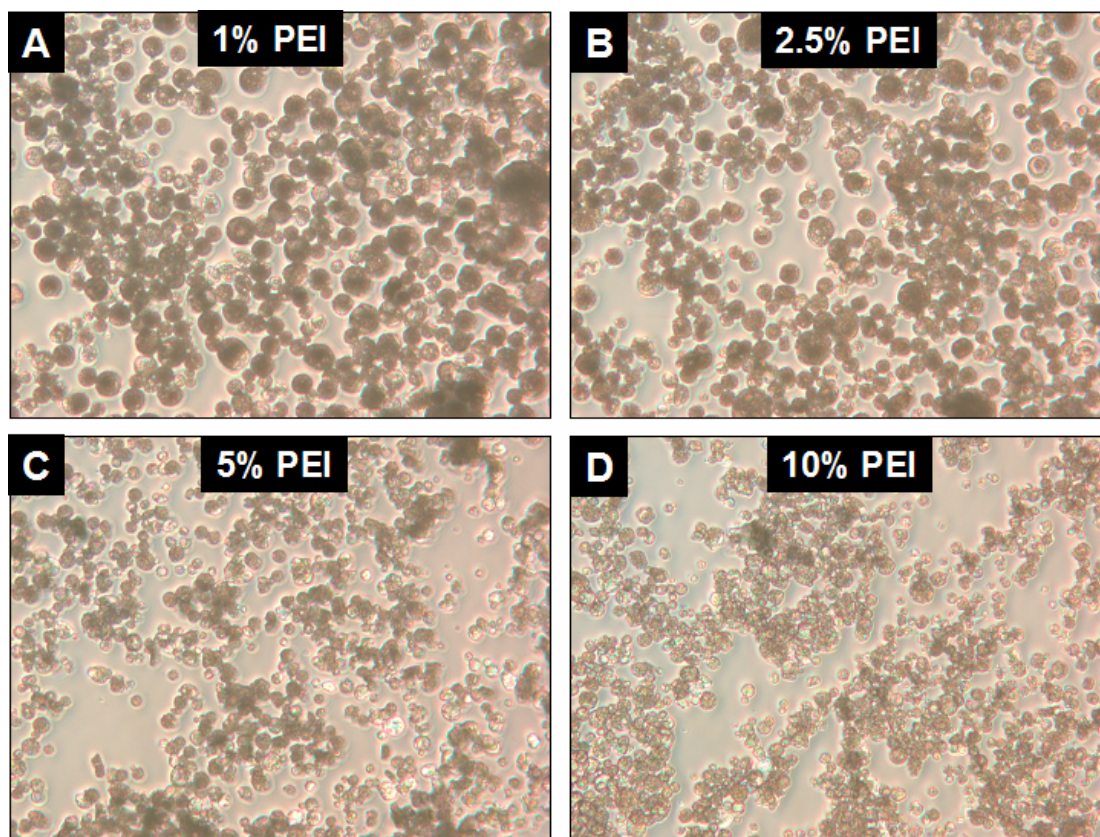


Figure 6-7. Images of PEI/PLG microspheres fabricated with different concentrations of PEI. (A) 1% PEI, (B) 2.5% PEI, (C) 5% PEI, and (D) 10% PEI. All images are the same magnification, 400x.

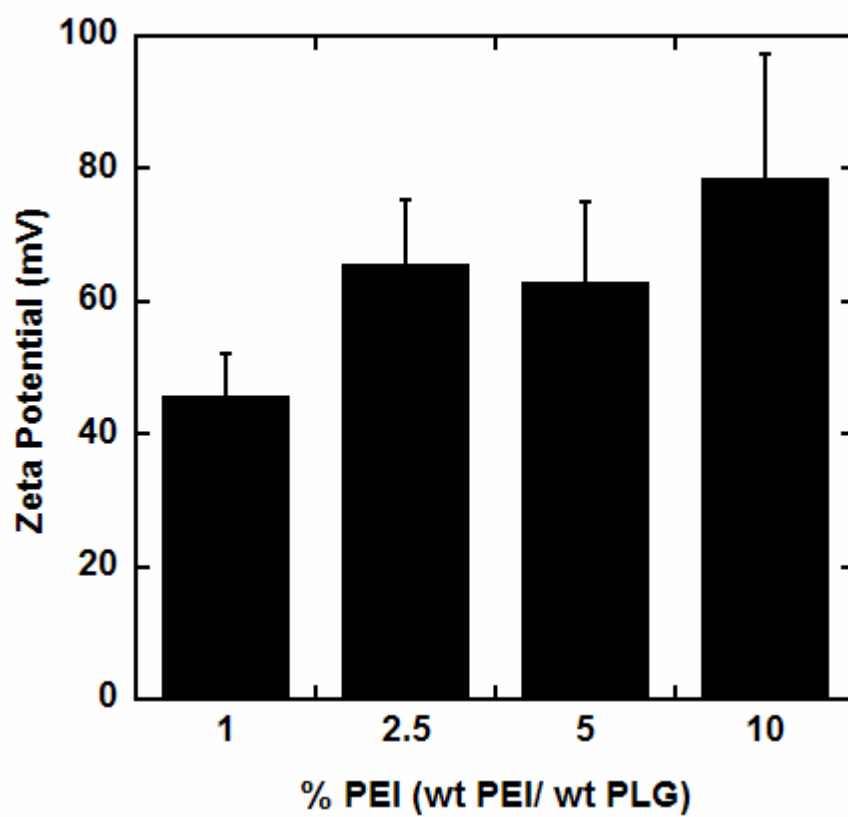


Figure 6-8. Zeta potential measurements of PEI/PLG microspheres.

6.4. Flow cytometric analysis to determine the cellular composition of tissue forming within scaffolds at the intraperitoneal fat site

Introduction

Identifying cell types that can be readily transfected, and characterizing their abundance over time at different implant sites will likely be important for developing strategies for effective gene transfer *in vivo*. In Chapter 3, immunohistochemical analysis revealed that a large number of macrophages were transfected at the intraperitoneal fat site. Additionally, a previous report examining plasmid delivery from scaffolds at a subcutaneous site indicated that endothelial cells were the primary cell type transfected.⁸¹ Thus, using flow cytometry, we sought to determine the percentages of both macrophages and endothelial cells present within scaffolds following implantation into intraperitoneal fat.

Materials and Methods

Layered PLG scaffolds loaded with 800 μ g of GFP plasmid or no DNA were implanted into the intraperitoneal fat of mice (as described in chapter 3), and then retrieved after 3, 7, and 14 days for analysis by flow cytometry. The retrieved tissue samples were cut into small pieces and digested in 3 mL of 200 U/mL type 2 collagenase (Worthington, Lakewood, NJ) in PAB buffer (i.e. PBS supplemented with 0.5% BSA and 0.1% sodium azide) for 45 minutes at 37°C, as previously described.⁸¹ The digested tissue was then filtered through a 43 μ m sieve, and the cell suspension was washed twice with PAB buffer. Cells were incubated with allophycocyanin-conjugated (APC) anti-mouse F4/80 antibody (eBiosciences) and phycoerythrin-Cy7-conjugated (PE-Cy7) anti-mouse CD-31 antibody (eBiosciences) for 30 minutes at room temperature (0.5 μ g antibody/500,000 cells), and then analyzed on a Becton Dickinson LSRII flow cytometer using

FACSDiva software (Becton Dickinson). At least 75,000 events were collected for each sample. CD-31 and F4/80 are surface markers for endothelial cells and macrophages, respectively.

Results

Forward/side scatter gating was used to distinguish the cell population from debris (**Fig. 6-9**). The percentage of F4/80⁺ macrophages ranged from 10% to 40%, and was similar for scaffolds with DNA or without DNA at all time points (**Fig. 6-10**). This suggests that the released plasmid does not induce an increase in macrophage recruitment to the implant site; however, given the small n value and large variance, it is difficult to make conclusions. Additionally, a general trend was observed for both conditions, in which the percentage of macrophages increased with time (**Fig. 6-10**). An increase in macrophage presence after day 3 is expected as part of the normal inflammatory response. Staining with anti-CD-31 antibody was similar to background fluorescence, indicating either a lack of intact endothelial cells or a problem with the antibody. As a result, the percentage of endothelial cells could not be determined.

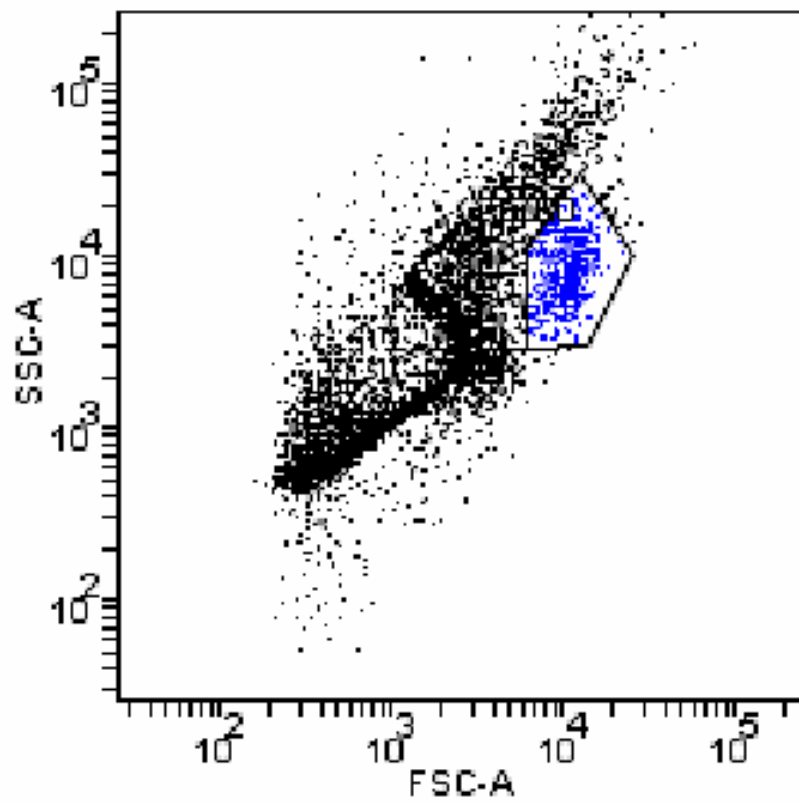


Figure 6-9. Forward scatter vs. side scatter plot showing the gated cell population.

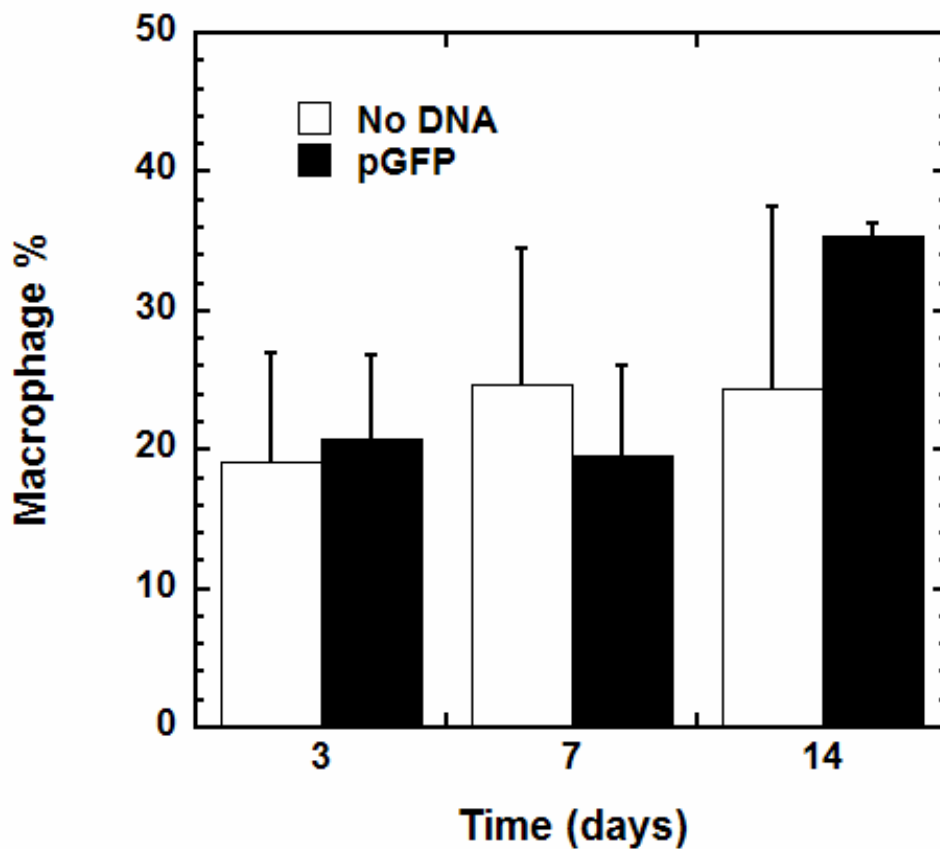


Figure 6-10. Percentage of F4/80⁺ macrophages present within scaffolds as a function of time. Empty bars represent control scaffolds without DNA and black bars represent scaffolds loaded with 800 μ g of GFP plasmid. Values represent averages \pm standard deviations (n=3 per condition per time point).

6.5. VEGF-releasing scaffolds: evaluation of angiogenesis by microcomputed tomography

Introduction

PLG scaffolds capable of delivering VEGF protein were fabricated using an established method¹²⁹⁻¹³² and employed in initial studies to develop methods for evaluating angiogenesis by microcomputed tomography (μ CT).⁸⁸ μ CT is a substantially more advanced method for vascular analysis than traditional histology. The quantitative information obtained by histology is relatively limited, only 2-D, and not necessarily representative of the vascularity throughout the entire sample.⁸⁸ In contrast, μ CT can provide detailed quantitative analyses as well as visualization of the 3-D vascular networks, which is not possible with histology.

Materials and Methods

To incorporate VEGF into scaffolds, PLG microspheres (3.7 mg) were reconstituted in a solution containing 1 μ g of recombinant VEGF (Millipore) and 5% alginate (wt. alginate/wt. PLG), frozen in liquid nitrogen, and lyophilized overnight to form a powder. The inclusion of alginate has been shown to substantially increase VEGF incorporation efficiency via an electrostatic interaction with the protein.¹²⁹ The lyophilized powder was mixed with NaCl particles (100 mg, 250 μ m < d < 425 μ m) and compressed in a 5 mm Kbr die (International Crystal Labs, Garfield, NJ) at 1500 psi using a Carver press. The resulting construct was processed by gas foaming. To remove the salt, scaffolds were immersed in 2 mL of water for 2 hours. Radiolabeled VEGF (¹²⁵I-VEGF) was used to determine protein incorporation and *in vitro* release kinetics from scaffolds. For the release assay, scaffolds were immersed in 1 mL of PBS

and incubated in a 37°C water bath. At desired time points, scaffolds were transferred to fresh PBS and the activity of the release buffer was measured with a gamma counter.

As an alternative method for incorporating VEGF into scaffolds, the protein was encapsulated inside PLG microspheres using a double emulsion process,¹³³ and scaffolds were fabricated from the protein-loaded microspheres. Briefly, PLG (75/25 mole ratio of lactide-to-glycolide, i.v. = 0.6-0.8 dl/g) was dissolved in dichloromethane to make a 3% (w/w) solution. Separately, an aqueous protein solution (total volume = 62 µL) was prepared containing 2 mg of BSA, 50 mg/mL sucrose, 3% wt. MgCO₃/wt. BSA,²³ 1 µg of non-radiolabeled VEGF, and ~3.5 µCi of radiolabeled VEGF. The protein solution was added to 1.5 mL of the PLG solution and sonicated at 40 W for 15 sec. to create the first emulsion. Next, the emulsion was poured into a 100 mL flat bottom beaker, and immersed in liquid nitrogen for 6 sec. to selectively freeze the aqueous phase.^{87, 99, 133} Then, 50 mL of 5% poly(vinyl alcohol) (PVA) (with 50 mg/mL sucrose) was added, and the solution was homogenized for 15 sec. at 7000 rpm to form the second emulsion. Lastly, the solution was poured into 30 mL of 1% PVA (with 50 mg/mL sucrose) and stirred for 3 hours allow evaporation of dichloromethane. The microspheres were washed 3 times in water, frozen in liquid nitrogen, and lyophilized overnight.

To evaluate the ability of VEGF-releasing scaffolds to stimulate angiogenesis *in vivo*, scaffolds were implanted subcutaneously into male CD-1 mice (20-22 g). At 1 and 3 weeks post-implantation, animals were transcardially perfused with Microfil® (Flow Tech, Carver, MA) in preparation for imaging by µCT, as described in Chapter 3. Microfil® is a yellow silicone rubber injection compound that polymerizes in the presence of a curing agent, creating a cast of the animal's vascular system (**Fig. 6-11**). The lead chromate contained in this compound serves as a

contrast agent for μ CT imaging. Samples were scanned in a 16.4 mm diameter sample holder at high resolution, creating a 2,048 x 2,048 pixel image matrix and an isotropic voxel (volume element) size of $\sim 8 \mu\text{m}$. Each scan consisted of 360 slices ($\sim 3 \text{ mm}$), which included almost the entire tissue sample (**Fig. 6-12**). Reconstructed serial slices were globally thresholded based on X-ray attenuation and used to create 3-D renderings of the vascular networks. The distribution of vessel diameters was calculated using a model-independent method for assessing thickness in 3-D images.⁸⁹



Figure 6-11. Image of a subcutaneous vascular network that has been completely perfused with Microfil® injection compound.

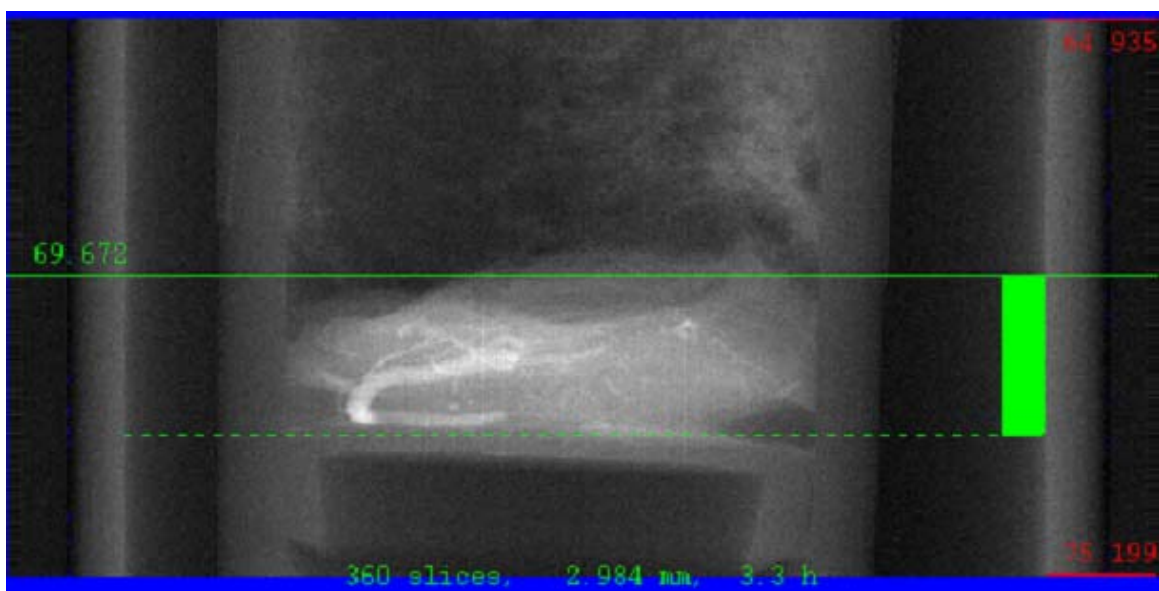


Figure 6-12. Scout view of a tissue sample defining the measurement area for μ CT imaging. The green reference line determines the position of the first slice, and the total thickness measured is determined by the number of slices and slice thickness.

Results

When VEGF was incorporated into scaffolds by mixing with alginate, the protein incorporation efficiency was found to be $48.3 \pm 13.8\%$ (n=3 scaffolds). This value is consistent with previous studies, which have reported incorporation efficiencies ranging from 40-70%.^{129,}
¹³¹ In characterizing the *in vitro* release kinetics, a large initial burst ($67.3 \pm 8.3\%$) was observed within the first 5 days, followed by a slower release of $\sim 0.5\%/day$ that was sustained through 4 weeks (**Fig. 6-13**). In comparison, when VEGF was incorporated into scaffolds by encapsulation inside polymer microspheres, the initial burst was decreased by more than 2-fold to $30.1 \pm 5\%$, and the subsequent rate of release was doubled ($\sim 1\%/day$ sustained through 4 weeks) (**Fig. 6-13**). However, the total extent of protein release through 4 weeks was substantially lower ($51.9 \pm 7.8\%$ for the encapsulation method vs. $79.1 \pm 5.5\%$ for the mixing method) (**Fig. 6-13**). The microsphere encapsulation efficiency was approximately 20%. Given this poor encapsulation efficiency, the encapsulation method was not used to fabricate VEGF-releasing scaffolds for evaluation *in vivo*; instead, VEGF was incorporated into scaffolds by mixing with alginate. Scaffolds with or without VEGF were implanted subcutaneously in mice, and angiogenesis was examined using microcomputed tomography. Three-dimensional renderings of the vascular networks within scaffolds were created to visually assess the extent of blood vessel formation. An increased angiogenic response was apparent for the VEGF-releasing scaffolds at both 1 and 3 weeks, although the effect was more pronounced at 3 weeks (**Fig. 6-14**). Visual representation of the blood vessel size distribution was produced by mapping a color-coded scale to the object surface (**Fig. 6-15**).

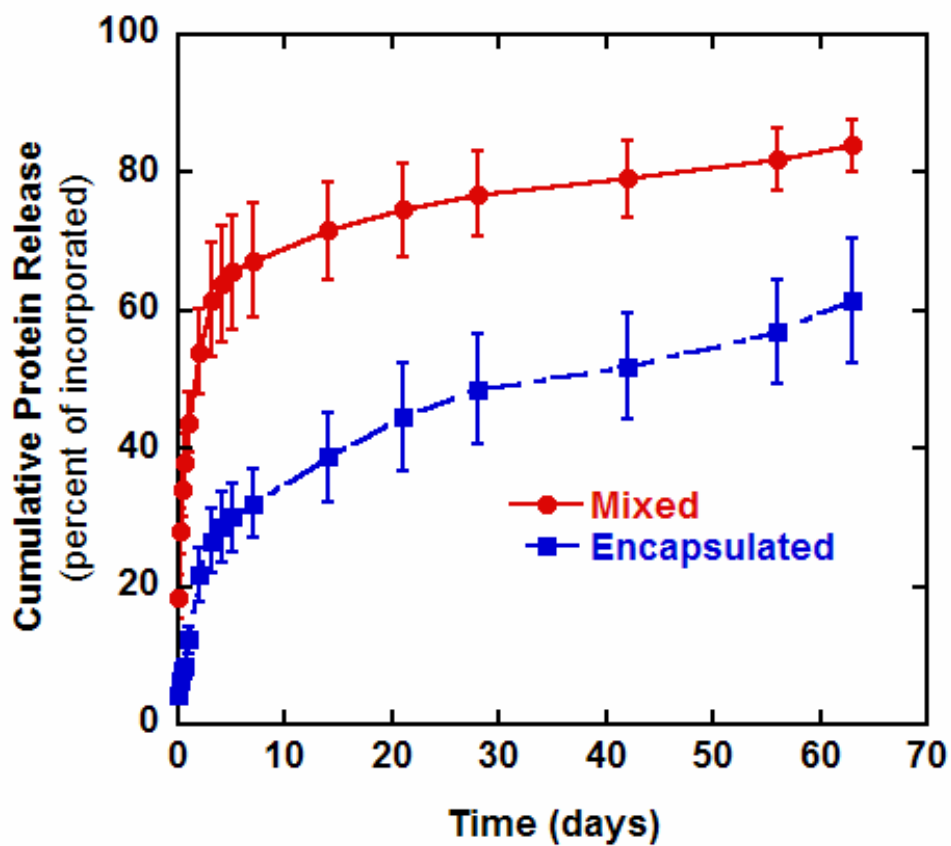


Figure 6-13. *In vitro* VEGF release kinetics from scaffolds. VEGF was incorporated into scaffolds by mixing with alginate (red circles) or encapsulation inside microspheres (blue squares). Values represent averages \pm standard deviations (n=3 scaffolds per condition).

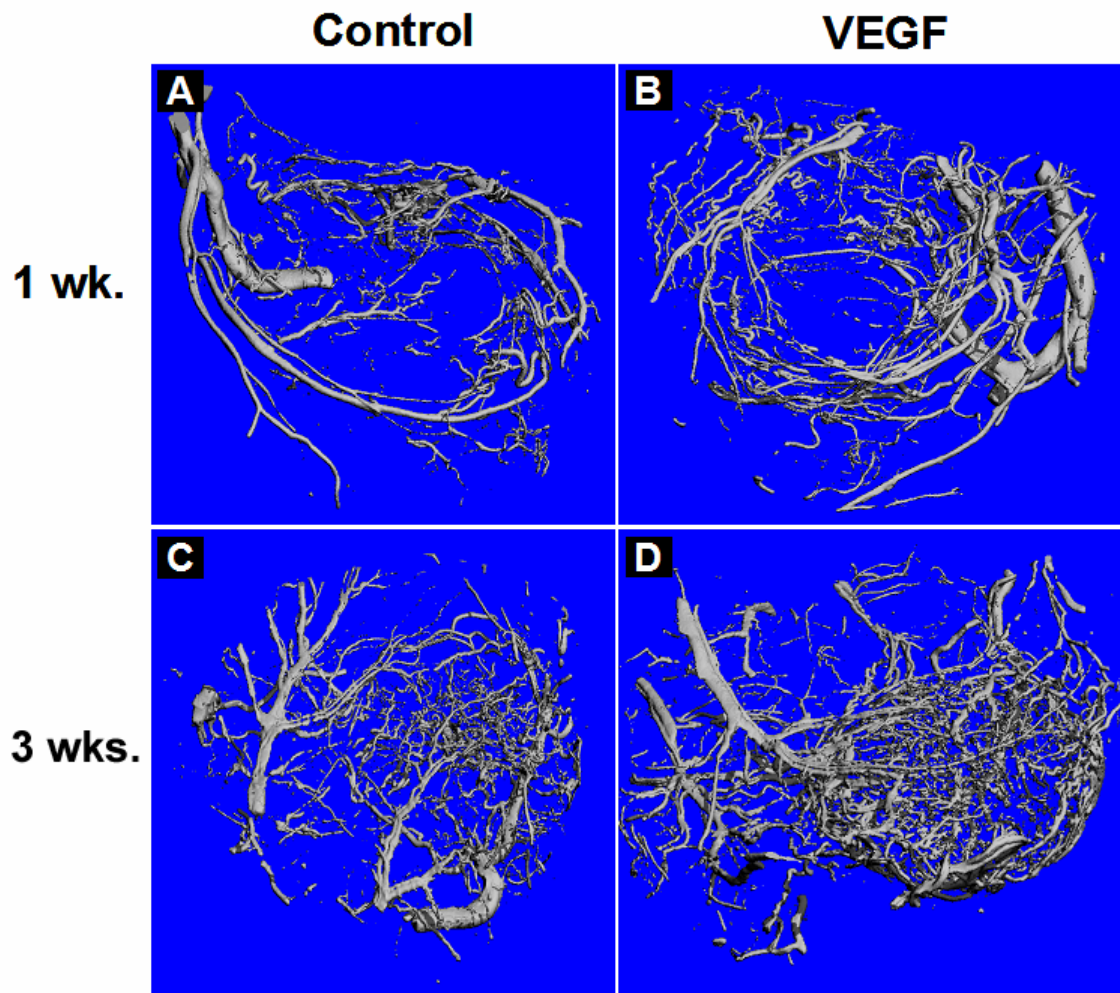


Figure 6-14. Microcomputed tomography 3-D renderings of vascular networks within scaffolds. Control scaffolds at (A) 1 week and (C) 3 weeks post-implantation. VEGF-releasing scaffolds at (B) 1 week and (D) 3 weeks post-implantation. Images are composed of 360 serial slices, and represent a total measurement thickness of ~3 mm.

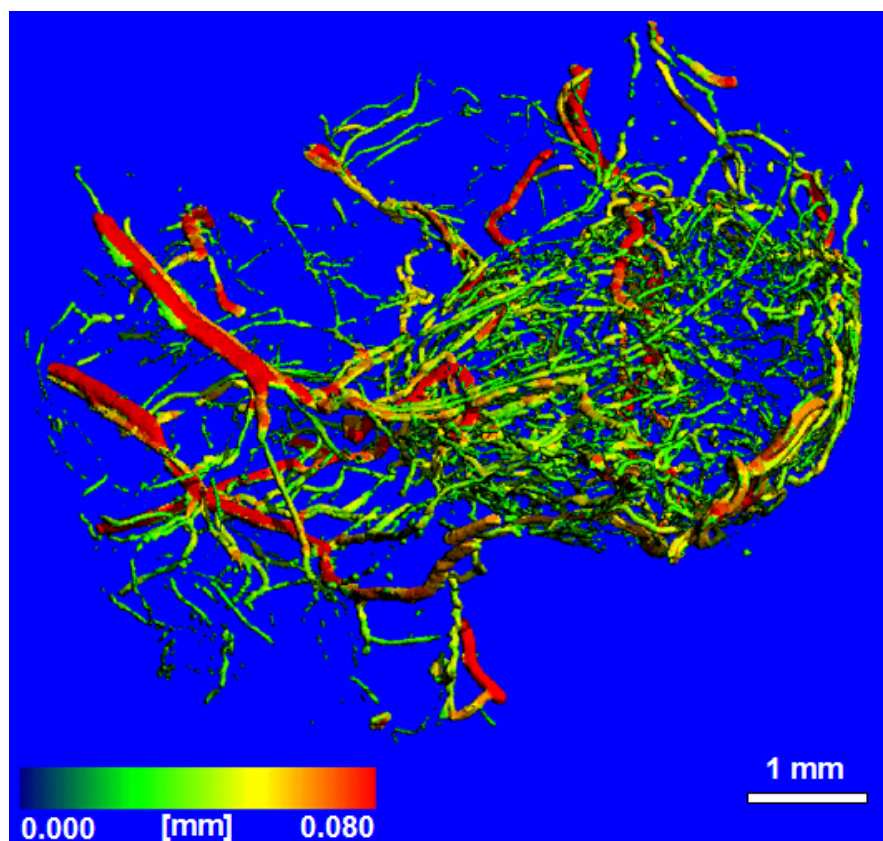


Figure 6-15. Microcomputed tomography 3-D rendering of the vascular network within a VEGF-releasing scaffold at 3 weeks post-implantation, with a color-coded vessel diameter scale mapped to the 3-D image surface.

6.6. *In vitro* plasmid release kinetics from layered scaffolds: increasing the amount of polymer in the center layer

Increasing the mass of polymer microspheres contained within the scaffold's center layer was investigated as a means for slowing the rate of plasmid release. When the amount of polymer in the center layer was increased from 2 mg to 3 mg (using the same DNA dose of 800 μg), there was no decrease in the initial burst of plasmid released within the first 3 days ($89.9 \pm 2.5\%$ for 2 mg vs. $88.1 \pm 3.3\%$ for 3 mg) (**Fig. 6-16**). Additionally, there was no improvement in the plasmid incorporation efficiency ($86.8 \pm 6.3\%$ for 2mg vs. $77.4 \pm 6.9\%$ for 3 mg). Since DNA is mixed throughout the entire center layer, there is likely a large quantity of DNA near the surface of the center layer that can be rapidly released. Thus, the next idea was to include two additional solid polymer layers flanking (i.e. one above and one below) the center layer containing the DNA. The extra polymer layers were intended to create barriers that would slow DNA release from the innermost layer. In this experiment, the amount of polymer contained in the center layer was kept constant at 1 mg, while the amount of polymer used for the flanking layers was varied (1 mg, 1.5 mg, or 2 mg). The three polymer layers were sequentially packed together in one of the following ways: (i) 1mg / 1mg+DNA / 1mg, (ii) 1.5mg / 1mg+DNA / 1.5mg, or (iii) 2mg / 1mg+DNA / 2mg. In measuring the *in vitro* DNA release kinetics for these three conditions, it was apparent that increasing the amount of polymer had no effect on the DNA release rate (**Fig. 6-17**).

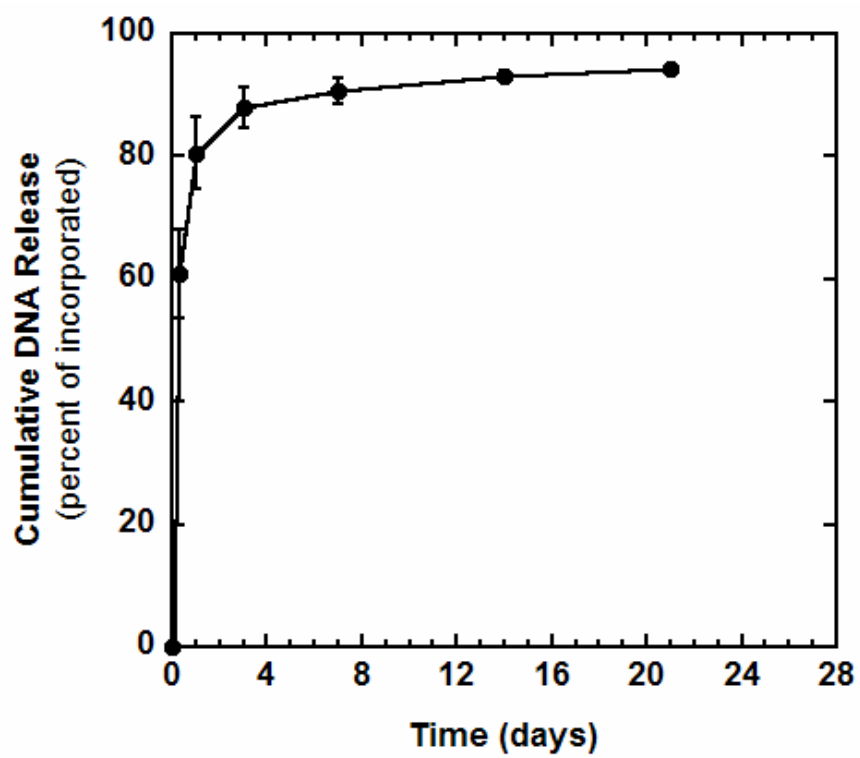


Figure 6-16. *In vitro* DNA release kinetics for a layered scaffold containing 3 mg of polymer microspheres in the center layer. Values represent averages \pm standard deviations (n=3).

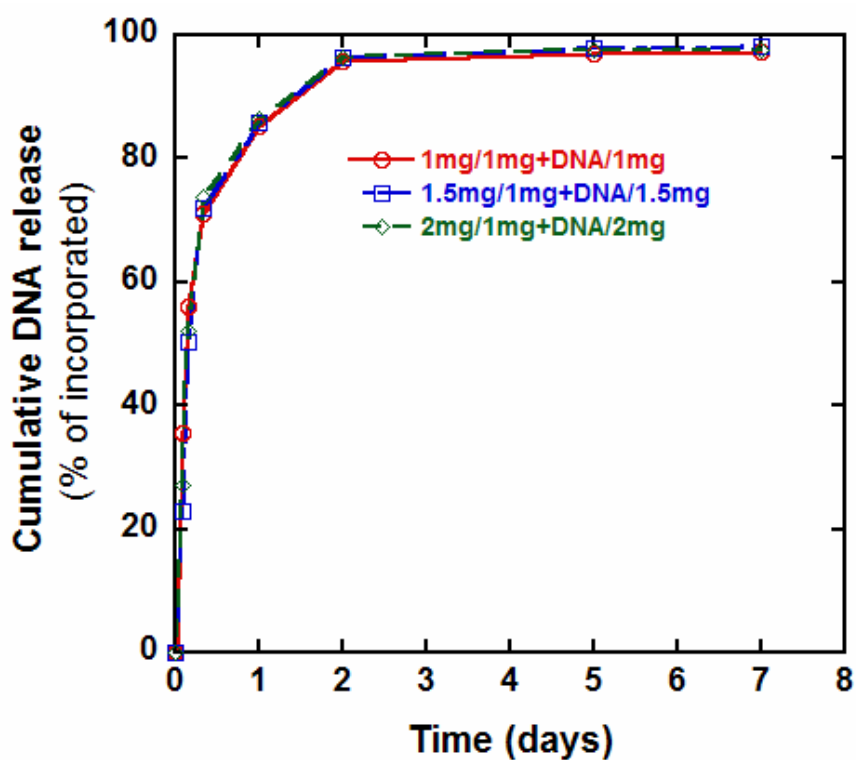


Figure 6-17. *In vitro* DNA release kinetics for layered scaffolds containing different masses of polymer within the center layer. Scaffolds were loaded with 500 μ g of DNA. Values represent measurements from a single scaffold (n=1 per condition).

6.7. *In vivo* transgene expression at the intraperitoneal fat site for traditional scaffolds

Traditional (i.e. non-layered) scaffolds described in chapter 2 were evaluated for their ability to promote gene transfer at the intraperitoneal fat site. Scaffolds loaded with 800 μg of pLuc were implanted into the intraperitoneal fat of mice, and luciferase transgene expression was monitored using bioluminescence imaging. Transgene expression levels peaked near day 1, and then quickly declined to background within 1 week (Fig. 6-18). This rapid drop in expression is consistent with the expression profile obtained for layered scaffolds at the intraperitoneal fat site, as described in chapter 3.

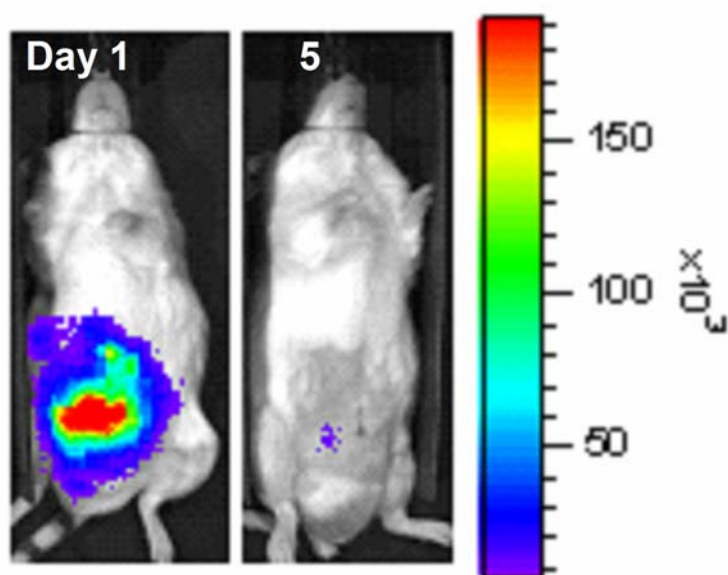


Figure 6-18. Bioluminescence imaging of luciferase transgene expression at the intraperitoneal fat site following implantation of a non-layered scaffold loaded with 800 μg of pLuc. The images are of a single mouse at different time points.

7. References

1. Langer, R. & Vacanti, J.P. Tissue engineering. *Science* **260**, 920-926 (1993).
2. Lavik, E. & Langer, R. Tissue engineering: current state and perspectives. *Appl Microbiol Biotechnol* **65**, 1-8 (2004).
3. Putnam, A.J. & Mooney, D.J. Tissue engineering using synthetic extracellular matrices. *Nat Med* **2**, 824-826 (1996).
4. Kim, B.S. & Mooney, D.J. Development of biocompatible synthetic extracellular matrices for tissue engineering. *Trends Biotechnol* **16**, 224-230 (1998).
5. Lutolf, M.P. & Hubbell, J.A. Synthetic biomaterials as instructive extracellular microenvironments for morphogenesis in tissue engineering. *Nat Biotechnol* **23**, 47-55 (2005).
6. Saltzman, W.M. & Olbricht, W.L. Building drug delivery into tissue engineering. *Nat Rev Drug Discov* **1**, 177-186 (2002).
7. Chen, R.R. & Mooney, D.J. Polymeric growth factor delivery strategies for tissue engineering. *Pharm Res* **20**, 1103-1112 (2003).
8. Richardson, T.P., Murphy, W.L. & Mooney, D.J. Polymeric delivery of proteins and plasmid DNA for tissue engineering and gene therapy. *Crit Rev Eukaryot Gene Expr* **11**, 47-58 (2001).
9. Babensee, J.E., McIntire, L.V. & Mikos, A.G. Growth factor delivery for tissue engineering. *Pharm Res* **17**, 497-504 (2000).
10. Murphy, W.L. & Mooney, D.J. Controlled delivery of inductive proteins, plasmid DNA and cells from tissue engineering matrices. *J Periodontal Res* **34**, 413-419 (1999).
11. Jang, J.H., Houchin, T.L. & Shea, L.D. Gene delivery from polymer scaffolds for tissue engineering. *Expert Rev Med Devices* **1**, 127-138 (2004).
12. De Laporte, L. & Shea, L.D. Matrices and scaffolds for DNA delivery in tissue engineering. *Adv Drug Deliv Rev* **59**, 292-307 (2007).
13. Ryan, E.A. et al. Successful islet transplantation: continued insulin reserve provides long-term glycemic control. *Diabetes* **51**, 2148-2157 (2002).
14. Shapiro, A.M. et al. Islet transplantation in seven patients with type 1 diabetes mellitus using a glucocorticoid-free immunosuppressive regimen. *N Engl J Med* **343**, 230-238 (2000).

15. Shapiro, A.M., Nanji, S.A. & Lakey, J.R. Clinical islet transplant: current and future directions towards tolerance. *Immunol Rev* **196**, 219-236 (2003).
16. Ryan, E.A. et al. Five-year follow-up after clinical islet transplantation. *Diabetes* **54**, 2060-2069 (2005).
17. Rowley, J.A., Madlambayan, G. & Mooney, D.J. Alginate hydrogels as synthetic extracellular matrix materials. *Biomaterials* **20**, 45-53 (1999).
18. Hubbell, J.A. Bioactive biomaterials. *Curr Opin Biotechnol* **10**, 123-129 (1999).
19. Sakiyama-Elbert, S.E. & Hubbell, J.A. Functional biomaterials: Design of novel biomaterials. *Annual Review of Materials Research* **31**, 183-201 (2001).
20. Saltzman, W.M. & Olbricht, W.L. Building drug delivery into tissue engineering. *Nature Reviews Drug Discovery* **1**, 177-186 (2002).
21. Madsen, S. & Mooney, D.J. Delivering DNA with polymer matrices: applications in tissue engineering and gene therapy. **3**, 381-384 (2000).
22. Bonadio, J. Tissue engineering via local gene delivery. *J Mol Med* **78**, 303-311 (2000).
23. Zhu, G., Mallery, S.R. & Schwendeman, S.P. Stabilization of proteins encapsulated in injectable poly (lactide- co-glycolide). *Nat Biotechnol* **18**, 52-57 (2000).
24. Ledley, F.D. Pharmaceutical approach to somatic gene therapy. *Pharm Res* **13**, 1595-1614 (1996).
25. Wolff, J.A. The "grand" problem of synthetic delivery. *Nature Biotechnology* **20**, 768-769 (2002).
26. Glover, D.J., Lipps, H.J. & Jans, D.A. Towards safe, non-viral therapeutic gene expression in humans. *Nat Rev Genet* **6**, 299-310 (2005).
27. Tomlinson, E. & Rolland, A.P. Controllable gene therapy pharmaceuticals of non-viral gene delivery systems. *Journal of Controlled Release* **39**, 357-372 (1996).
28. Pouton, C.W. & Seymour, L.W. Key issues in non-viral gene delivery. *Adv Drug Deliv Rev* **34**, 3-19 (1998).
29. Pannier, A.K. & Shea, L.D. Controlled release systems for DNA delivery. *Mol Ther* **10**, 19-26 (2004).
30. Bonadio, J., Smiley, E., Patil, P. & Goldstein, S. Localized, direct plasmid gene delivery in vivo: prolonged therapy results in reproducible tissue regeneration. *Nat Med* **5**, 753-759 (1999).

31. Fang, J. et al. Stimulation of new bone formation by direct transfer of osteogenic plasmid genes. *Proc Natl Acad Sci U S A* **93**, 5753-5758 (1996).
32. Shea, L.D., Smiley, E., Bonadio, J. & Mooney, D.J. DNA delivery from polymer matrices for tissue engineering. *Nat Biotechnol* **17**, 551-554 (1999).
33. Jang, J.H., Rives, C.B. & Shea, L.D. Plasmid delivery in vivo from porous tissue-engineering scaffolds: transgene expression and cellular transfection. *Mol Ther* **12**, 475-483 (2005).
34. Robertson, R.P. Islet transplantation as a treatment for diabetes - a work in progress. *N Engl J Med* **350**, 694-705 (2004).
35. Kulkarni, R.N. The islet beta-cell. *Int J Biochem Cell Biol* **36**, 365-371 (2004).
36. Brissova, M. et al. Assessment of human pancreatic islet architecture and composition by laser scanning confocal microscopy. *J Histochem Cytochem* **53**, 1087-1097 (2005).
37. Jansson, L. & Carlsson, P.O. Graft vascular function after transplantation of pancreatic islets. *Diabetologia* **45**, 749-763 (2002).
38. Carlsson, P.O., Palm, F., Andersson, A. & Liss, P. Markedly decreased oxygen tension in transplanted rat pancreatic islets irrespective of the implantation site. *Diabetes* **50**, 489-495 (2001).
39. The effect of intensive treatment of diabetes on the development and progression of long-term complications in insulin-dependent diabetes mellitus. The Diabetes Control and Complications Trial Research Group. *N Engl J Med* **329**, 977-986 (1993).
40. Ryan, E.A. et al. Clinical outcomes and insulin secretion after islet transplantation with the Edmonton protocol. *Diabetes* **50**, 710-719 (2001).
41. Wang, R.N. & Rosenberg, L. Maintenance of beta-cell function and survival following islet isolation requires re-establishment of the islet-matrix relationship. *J Endocrinol* **163**, 181-190 (1999).
42. Rosenberg, L., Wang, R., Paraskevas, S. & Maysinger, D. Structural and functional changes resulting from islet isolation lead to islet cell death. *Surgery* **126**, 393-398 (1999).
43. Thomas, F.T. et al. Anoikis, extracellular matrix, and apoptosis factors in isolated cell transplantation. *Surgery* **126**, 299-304 (1999).
44. Paraskevas, S. et al. Modulation of JNK and p38 stress activated protein kinases in isolated islets of Langerhans: insulin as an autocrine survival signal. *Ann Surg* **233**, 124-133 (2001).

45. Thomas, F. et al. A tripartite anoikis-like mechanism causes early isolated islet apoptosis. *Surgery* **130**, 333-338 (2001).
46. Wang, R.N., Paraskevas, S. & Rosenberg, L. Characterization of integrin expression in islets isolated from hamster, canine, porcine, and human pancreas. *J Histochem Cytochem* **47**, 499-506 (1999).
47. Lucas-Clerc, C., Massart, C., Campion, J.P., Launois, B. & Nicol, M. Long-term culture of human pancreatic islets in an extracellular matrix: morphological and metabolic effects. *Mol Cell Endocrinol* **94**, 9-20 (1993).
48. Brendel, M.D., Kong, S.S., Alejandro, R. & Mintz, D.H. Improved functional survival of human islets of Langerhans in three-dimensional matrix culture. *Cell Transplant* **3**, 427-435 (1994).
49. Davalli, A.M. et al. Vulnerability of islets in the immediate posttransplantation period. Dynamic changes in structure and function. *Diabetes* **45**, 1161-1167 (1996).
50. Dionne, K.E., Colton, C.K. & Yarmush, M.L. Effect of hypoxia on insulin secretion by isolated rat and canine islets of Langerhans. *Diabetes* **42**, 12-21 (1993).
51. Zhang, N. et al. Elevated vascular endothelial growth factor production in islets improves islet graft vascularization. *Diabetes* **53**, 963-970 (2004).
52. Carlsson, P.O., Palm, F., Andersson, A. & Liss, P. Chronically decreased oxygen tension in rat pancreatic islets transplanted under the kidney capsule. *Transplantation* **69**, 761-766 (2000).
53. Mattsson, G., Jansson, L. & Carlsson, P.O. Decreased vascular density in mouse pancreatic islets after transplantation. *Diabetes* **51**, 1362-1366 (2002).
54. Azrin, M. Angiogenesis, protein and gene delivery. *Br Med Bull* **59**, 211-225 (2001).
55. Ennett, A.B. & Mooney, D.J. Tissue engineering strategies for in vivo neovascularisation. *Expert Opin Biol Ther* **2**, 805-818 (2002).
56. Ferrara, N., Gerber, H.P. & LeCouter, J. The biology of VEGF and its receptors. *Nat Med* **9**, 669-676 (2003).
57. Keyt, B.A. et al. The carboxyl-terminal domain (111-165) of vascular endothelial growth factor is critical for its mitogenic potency. *J Biol Chem* **271**, 7788-7795 (1996).
58. Ferrara, N. Vascular endothelial growth factor: basic science and clinical progress. *Endocr Rev* **25**, 581-611 (2004).

59. Ozawa, C.R. et al. Microenvironmental VEGF concentration, not total dose, determines a threshold between normal and aberrant angiogenesis. *J Clin Invest* **113**, 516-527 (2004).
60. Springer, M.L., Chen, A.S., Kraft, P.E., Bednarski, M. & Blau, H.M. VEGF gene delivery to muscle: potential role for vasculogenesis in adults. *Mol Cell* **2**, 549-558 (1998).
61. Schwarz, E.R. et al. Evaluation of the effects of intramyocardial injection of DNA expressing vascular endothelial growth factor (VEGF) in a myocardial infarction model in the rat--angiogenesis and angioma formation. *J Am Coll Cardiol* **35**, 1323-1330 (2000).
62. Sundberg, C. et al. Glomeruloid microvascular proliferation follows adenoviral vascular permeability factor/vascular endothelial growth factor-164 gene delivery. *Am J Pathol* **158**, 1145-1160 (2001).
63. Dor, Y. et al. Conditional switching of VEGF provides new insights into adult neovascularization and pro-angiogenic therapy. *Embo J* **21**, 1939-1947 (2002).
64. Slavin, J. Fibroblast growth factors: at the heart of angiogenesis. *Cell Biol Int* **19**, 431-444 (1995).
65. Florkiewicz, R.Z., Majack, R.A., Buechler, R.D. & Florkiewicz, E. Quantitative export of FGF-2 occurs through an alternative, energy-dependent, non-ER/Golgi pathway. *J Cell Physiol* **162**, 388-399 (1995).
66. Pugh, C.W. & Ratcliffe, P.J. Regulation of angiogenesis by hypoxia: role of the HIF system. *Nat Med* **9**, 677-684 (2003).
67. Ke, Q. & Costa, M. Hypoxia-inducible factor-1 (HIF-1). *Mol Pharmacol* **70**, 1469-1480 (2006).
68. Vaupel, P. The role of hypoxia-induced factors in tumor progression. *Oncologist* **9 Suppl 5**, 10-17 (2004).
69. Trentin, D., Hall, H., Wechsler, S. & Hubbell, J.A. Peptide-matrix-mediated gene transfer of an oxygen-insensitive hypoxia-inducible factor-1alpha variant for local induction of angiogenesis. *Proc Natl Acad Sci U S A* **103**, 2506-2511 (2006).
70. Middaugh, C.R., Evans, R.K., Montgomery, D.L. & Casimiro, D.R. Analysis of plasmid DNA from a pharmaceutical perspective. *J Pharm Sci* **87**, 130-146 (1998).
71. Mooney, D.J., Baldwin, D.F., Suh, N.P., Vacanti, J.P. & Langer, R. Novel approach to fabricate porous sponges of poly(D,L-lactic-co-glycolic acid) without the use of organic solvents. *Biomaterials* **17**, 1417-1422 (1996).

72. Harris, L.D., Kim, B.S. & Mooney, D.J. Open pore biodegradable matrices formed with gas foaming. *J Biomed Mater Res* **42**, 396-402 (1998).
73. Carstensen, J.T. *Pharmaceutical principles of solid dosage forms.* (Technomic Pub., Lancaster, Pa.; 1993).
74. Okada, H. & Toguchi, H. Biodegradable microspheres in drug delivery. *Crit Rev Ther Drug Carrier Syst* **12**, 1-99 (1995).
75. Yla-Herttuala, S. & Alitalo, K. Gene transfer as a tool to induce therapeutic vascular growth. *Nat Med* **9**, 694-701 (2003).
76. Herweijer, H. & Wolff, J.A. Progress and prospects: naked DNA gene transfer and therapy. *Gene Ther* **10**, 453-458 (2003).
77. Herweijer, H. et al. Time course of gene expression after plasmid DNA gene transfer to the liver. *J Gene Med* **3**, 280-291 (2001).
78. Wolff, J.A., Ludtke, J.J., Acsadi, G., Williams, P. & Jani, A. Long-term persistence of plasmid DNA and foreign gene expression in mouse muscle. *Hum Mol Genet* **1**, 363-369 (1992).
79. Wells, D.J. Intramuscular injection of plasmid DNA. *Mol Cell Biol Hum Dis Ser* **5**, 83-103 (1995).
80. Storrie, H. & Mooney, D.J. Sustained delivery of plasmid DNA from polymeric scaffolds for tissue engineering. *Adv Drug Deliv Rev* **58**, 500-514 (2006).
81. Riddle, K.W. et al. Modifying the proliferative state of target cells to control DNA expression and identifying cell types transfected in vivo. *Mol Ther* **15**, 361-368 (2007).
82. Blomeier, H. et al. Polymer scaffolds as synthetic microenvironments for extrahepatic islet transplantation. *Transplantation* **82**, 452-459 (2006).
83. Heilmann, C. et al. Comparison of protein with DNA therapy for chronic myocardial ischemia using fibroblast growth factor-2. *Eur J Cardiothorac Surg* **22**, 957-964 (2002).
84. Ivan, M. et al. HIF α targeted for VHL-mediated destruction by proline hydroxylation: implications for O₂ sensing. *Science* **292**, 464-468 (2001).
85. Jaakkola, P. et al. Targeting of HIF- α to the von Hippel-Lindau ubiquitylation complex by O₂-regulated prolyl hydroxylation. *Science* **292**, 468-472 (2001).
86. Yu, F., White, S.B., Zhao, Q. & Lee, F.S. HIF-1 α binding to VHL is regulated by stimulus-sensitive proline hydroxylation. *Proc Natl Acad Sci U S A* **98**, 9630-9635 (2001).

87. Ando, S., Putnam, D., Pack, D.W. & Langer, R. PLGA microspheres containing plasmid DNA: preservation of supercoiled DNA via cryopreparation and carbohydrate stabilization. *J Pharm Sci* **88**, 126-130 (1999).
88. Duvall, C.L., Taylor, W.R., Weiss, D. & Guldberg, R.E. Quantitative microcomputed tomography analysis of collateral vessel development after ischemic injury. *Am J Physiol Heart Circ Physiol* **287**, H302-310 (2004).
89. Hildebrand, T. & Ruegsegger, P. A new method for the model-independent assessment of thickness in three-dimensional images. *J Microsc-Oxford* **185**, 67-75 (1997).
90. Hyon, S.H., Tracey, K.J. & Kaufman, D.B. Specific inhibition of macrophage-derived proinflammatory cytokine synthesis with a tetravalent guanylhydrazone CNI-1493 accelerates early islet graft function posttransplant. *Transplant P* **30**, 409-410 (1998).
91. Kaufman, D.B. et al. Effect of 15-Deoxyspergualin on Immediate Function and Long-Term Survival of Transplanted Islets in Murine Recipients of a Marginal Islet Mass. *Diabetes* **43**, 778-783 (1994).
92. Yew, N.S. Controlling the kinetics of transgene expression by plasmid design. *Adv Drug Deliv Rev* **57**, 769-780 (2005).
93. Qin, L. et al. Promoter attenuation in gene therapy: interferon-gamma and tumor necrosis factor-alpha inhibit transgene expression. *Hum Gene Ther* **8**, 2019-2029 (1997).
94. Zhang, X.Y. et al. Increasing binding of a transcription factor immediately downstream of the cap site of a cytomegalovirus gene represses expression. *Nucleic Acids Res* **23**, 3026-3033 (1995).
95. Prosch, S. et al. Inactivation of the very strong HCMV immediate early promoter by DNA CpG methylation in vitro. *Biol Chem Hoppe Seyler* **377**, 195-201 (1996).
96. Loser, P., Jennings, G.S., Strauss, M. & Sandig, V. Reactivation of the previously silenced cytomegalovirus major immediate-early promoter in the mouse liver: involvement of NFkappaB. *J Virol* **72**, 180-190 (1998).
97. Yew, N.S. et al. CpG-depleted plasmid DNA vectors with enhanced safety and long-term gene expression in vivo. *Mol Ther* **5**, 731-738 (2002).
98. Nof, M. & Shea, L.D. Drug-releasing scaffolds fabricated from drug-loaded microspheres. *J Biomed Mater Res* **59**, 349-356 (2002).
99. Jang, J.H. & Shea, L.D. Controllable delivery of non-viral DNA from porous scaffolds. *J Control Release* **86**, 157-168 (2003).

100. Takakura, Y. et al. Characterization of plasmid DNA binding and uptake by peritoneal macrophages from class A scavenger receptor knockout mice. *Pharm Res* **16**, 503-508 (1999).
101. Takagi, T. et al. Involvement of specific mechanism in plasmid DNA uptake by mouse peritoneal macrophages. *Biochem Biophys Res Commun* **245**, 729-733 (1998).
102. Stacey, K.J., Sweet, M.J. & Hume, D.A. Macrophages ingest and are activated by bacterial DNA. *J Immunol* **157**, 2116-2122 (1996).
103. Takahashi, A., Palmer-Opolski, M., Smith, R.C. & Walsh, K. Transgene delivery of plasmid DNA to smooth muscle cells and macrophages from a biostable polymer-coated stent. *Gene Ther* **10**, 1471-1478 (2003).
104. Fukuyama, N. et al. Intravenous injection of phagocytes transfected ex vivo with FGF4 DNA/biodegradable gelatin complex promotes angiogenesis in a rat myocardial ischemia/reperfusion injury model. *Basic Res Cardiol* **102**, 209-216 (2007).
105. Thomas, E.D., Ramberg, R.E., Sale, G.E., Sparkes, R.S. & Golde, D.W. Direct evidence for a bone marrow origin of the alveolar macrophage in man. *Science* **192**, 1016-1018 (1976).
106. Anderson, J.M. Inflammatory response to implants. *ASAIO Trans* **34**, 101-107 (1988).
107. Lakey, J.R., Mirbolooki, M. & Shapiro, A.M. Current status of clinical islet cell transplantation. *Methods Mol Biol* **333**, 47-104 (2006).
108. Boyle, J.P. et al. Projection of diabetes burden through 2050: impact of changing demography and disease prevalence in the U.S. *Diabetes Care* **24**, 1936-1940 (2001).
109. Biarnes, M. et al. Beta-cell death and mass in syngeneically transplanted islets exposed to short- and long-term hyperglycemia. *Diabetes* **51**, 66-72 (2002).
110. Robertson, R.P. Intrahepatically transplanted islets--strangers in a strange land. *J Clin Endocrinol Metab* **87**, 5416-5417 (2002).
111. Eng, J., Kleinman, W.A., Singh, L., Singh, G. & Raufman, J.P. Isolation and characterization of exendin-4, an exendin-3 analogue, from *Heloderma suspectum* venom. Further evidence for an exendin receptor on dispersed acini from guinea pig pancreas. *J Biol Chem* **267**, 7402-7405 (1992).
112. Goke, R. et al. Exendin-4 is a high potency agonist and truncated exendin-(9-39)-amide an antagonist at the glucagon-like peptide 1-(7-36)-amide receptor of insulin-secreting beta-cells. *J Biol Chem* **268**, 19650-19655 (1993).
113. Barnett, A. Exenatide. *Expert Opin Pharmacother* **8**, 2593-2608 (2007).

114. Xu, G., Stoffers, D.A., Habener, J.F. & Bonner-Weir, S. Exendin-4 stimulates both beta-cell replication and neogenesis, resulting in increased beta-cell mass and improved glucose tolerance in diabetic rats. *Diabetes* **48**, 2270-2276 (1999).
115. Urusova, I.A., Farilla, L., Hui, H., D'Amico, E. & Perfetti, R. GLP-1 inhibition of pancreatic islet cell apoptosis. *Trends Endocrinol Metab* **15**, 27-33 (2004).
116. Parkes, D.G., Pittner, R., Jodka, C., Smith, P. & Young, A. Insulinotropic actions of exendin-4 and glucagon-like peptide-1 in vivo and in vitro. *Metabolism* **50**, 583-589 (2001).
117. Sharma, A. et al. Exendin-4 treatment improves metabolic control after rat islet transplantation to athymic mice with streptozotocin-induced diabetes. *Diabetologia* **49**, 1247-1253 (2006).
118. Varde, N.K. & Pack, D.W. Microspheres for controlled release drug delivery. *Expert Opin Biol Ther* **4**, 35-51 (2004).
119. Cleland, J.L. Protein delivery from biodegradable microspheres. *Pharm Biotechnol* **10**, 1-43 (1997).
120. Singh, M., Briones, M., Ott, G. & O'Hagan, D. Cationic microparticles: A potent delivery system for DNA vaccines. *Proc Natl Acad Sci U S A* **97**, 811-816 (2000).
121. Singh, M. et al. The effect of CTAB concentration in cationic PLG microparticles on DNA adsorption and in vivo performance. *Pharm Res* **20**, 247-251 (2003).
122. Briones, M. et al. The preparation, characterization, and evaluation of cationic microparticles for DNA vaccine delivery. *Pharm Res* **18**, 709-712 (2001).
123. Singh, M. et al. A modified process for preparing cationic polylactide-co-glycolide microparticles with adsorbed DNA. *Int J Pharm* **327**, 1-5 (2006).
124. Oster, C.G. et al. Cationic microparticles consisting of poly(lactide-co-glycolide) and polyethylenimine as carriers systems for parental DNA vaccination. *J Control Release* **104**, 359-377 (2005).
125. Munier, S., Messai, I., Delair, T., Verrier, B. & Ataman-Onal, Y. Cationic PLA nanoparticles for DNA delivery: comparison of three surface polycations for DNA binding, protection and transfection properties. *Colloids Surf B Biointerfaces* **43**, 163-173 (2005).
126. Kasturi, S.P., Sachaphibulkij, K. & Roy, K. Covalent conjugation of polyethyleneimine on biodegradable microparticles for delivery of plasmid DNA vaccines. *Biomaterials* **26**, 6375-6385 (2005).

127. Ravi Kumar, M.N., Bakowsky, U. & Lehr, C.M. Preparation and characterization of cationic PLGA nanospheres as DNA carriers. *Biomaterials* **25**, 1771-1777 (2004).
128. Wischke, C., Borchert, H.H., Zimmermann, J., Siebenbrodt, I. & Lorenzen, D.R. Stable cationic microparticles for enhanced model antigen delivery to dendritic cells. *J Control Release* **114**, 359-368 (2006).
129. Peters, M.C., Polverini, P.J. & Mooney, D.J. Engineering vascular networks in porous polymer matrices. *J Biomed Mater Res* **60**, 668-678 (2002).
130. Richardson, T.P., Peters, M.C., Ennett, A.B. & Mooney, D.J. Polymeric system for dual growth factor delivery. *Nat Biotechnol* **19**, 1029-1034 (2001).
131. Smith, M.K., Peters, M.C., Richardson, T.P., Garbern, J.C. & Mooney, D.J. Locally enhanced angiogenesis promotes transplanted cell survival. *Tissue Eng* **10**, 63-71 (2004).
132. Ennett, A.B., Kaigler, D. & Mooney, D.J. Temporally regulated delivery of VEGF in vitro and in vivo. *J Biomed Mater Res A* **79**, 176-184 (2006).
133. Yang, Y. et al. Neurotrophin releasing single and multiple lumen nerve conduits. *J Control Release* **104**, 433-446 (2005).